Fermi National Accelerator Laboratory

FERMILAB-TM-1907

Proceedings of the Workshop on Future Hadron Facilities in the U.S.

Indiana University Cyclotron Facility,
Indiana University
Bloomington, Indiana

July 6-10, 1994

Operated by Universities Research Association Inc. under Contract No. DE-AC02-76CHO3000 with the United States Department of Energy

Disclaimer

This report was prepared as an account of work sponsored by an agency of the United States Government. Neither the United States Government nor any agency thereof, nor any of their employees, makes any warranty, express or implied, or assumes any legal liability or responsibility for the accuracy, completeness, or usefulness of any information, apparatus, product, or process disclosed, or represents that its use would not infringe privately owned rights. Reference herein to any specific commercial product, process, or service by trade name, trademark, manufacturer, or otherwise, does not necessarily constitute or imply its endorsement, recommendation, or favoring by the United States Government or any agency thereof. The views and opinions of authors expressed herein do not necessarily state or reflect those of the United States Government or any agency thereof.

TABLE OF CONTENTS

Proceeding of the Workshop on Future Hadron Facilities in the U.S.

FERMILAB-TM-1907

Workshop Summary

Workshop on Future Hadron Facilities in the U.S. — Page 1
S. D. Holmes

Facilities Summary Reports

30 x 30 TeV-Summary Report — Page 9
A. Chao, G. Dugan and M. Harrison

A High Luminosity, 2 x 2 TeV Collider in the Tevatron Tunnel — Page 17
G. P. Jackson and R. H. Siemann

Working Group Summaries

Magnets Working Group — Page 23
J. Tompkins

Cryogenics Discussion — Page 45
T. Peterson

Vacuum Report — Page 53
W. Turner and G. Chapman

Antiproton Source Production — Page 65
J. Marriner

Injector Working Group — Page 81
R. York

Interaction Region Working Group — Page 85
S. Peggs

Lattice/Beam Dynamics Working Group — Page 91
M. Syphers

Contributed papers

LEBT for High-Luminosity Colliders — Page 99
S.K. Guharay and M. Reiser

Some Notes on Long-Range Beam-Beam Effects for the 2TeV Collider — Page 107
M. J. Syphers

Synchrotron Radiation Masks for High Energy Proton Accelerators — Page 113
R. Talman

Emittance Preservation in a Proton Synchrotron — Page 123
Y. Huang

Beam-Beam Interaction Effects on Betatron Tunes — Page 129
J. Y. Liu and L. Wang

Analytic Solutions for Phase Trombone Modules — Page 133
D. Li, L. Wang and S. Y. Lee

Chromatic Corrections of RHIC When One or Two Insertions is at $\beta^* = 0.5$m — Page 141
W. Scandale and S. Tepikian

List of Participants — Page 146

Fermi National Accelerator Laboratory

Workshop Summary: Workshop on Future Hadron Facilities in the U.S.

S.D. Holmes

Fermi National Accelerator Laboratory
P.O. Box 500, Batavia, Illinois 60510

Operated by Universities Research Association Inc. under Contract No. DE-AC02-76CHO3000 with the United States Department of Energy

Workshop Summary:
Workshop on Future Hadron Facilities in the U. S.

S. D. Holmes
Fermi National Accelerator Laboratory
Batavia, IL 60510

I. Introduction

A workshop on "Future Hadron Facilities in the U.S." was held at the Indiana University Cyclotron Facility over the period July 6-10, 1994. Workshop participation included 52 registrants from 17 institutions in the United States and from CERN in Europe. This workshop was held under the auspices of the Accelerator Physics, Technologies, and Facilities Working Group of the DPF Long Term Planning Study. This working group operated under the following general charge:

"The Accelerator Physics, Technologies, and Facilities Working Group will undertake an assessment of the current state-of-the-art and foreseeable advances in accelerator facilities utilized to support High Energy Physics research into the 21st century. The group will attempt to identify fundamental performance limitations in existing and proposed facilities, to identify avenues for advancement in the implementing technologies, to assess the promise and prospects of new accelerator directions, and to construct realistic timetables for achievement of specific performance milestones."

The specific goals of the Indiana workshop were three-fold:

1. To develop defensible parameter lists for a luminosity and/or energy upgrade, to 2×10^{33} cm^{-2}sec^{-1} and/or 2 x 2 TeV, of the $\bar{p}$ - p collider at Fermilab.

2. To develop a defensible parameter list for a 1×10^{34} cm^{-2}sec^{-1}, 30 x 30 TeV p - p collider.

3. To identify R&D requirements for achieving the stated parameters.

The two facilities examined were chosen because they were felt to span the potential needs of the U.S. HEP community following the completion of the Main Injector upgrade at Fermilab, and through and beyond the period of utilization of the LHC in Europe. It was felt that the necessary R&D required to realize either of these facilities would likely provide a strong basis for nearly any direction that the community wished to move in the realm of hadron facilities over the next twenty years or so. The work of this meeting rests upon and extends previous studies of higher energy options in the Tevatron tunnel, as chronicled in the 1988 Snowmass Proceedings, and the extensive design and development work completed at the SSC Laboratory.

Six working groups were charged with identifying the technology issues related to each of the potential facilities. The working groups and their leaders were:

Magnets	J. Tompkins	(Fermilab)
Cryogenics & Vacuum	T. Peterson	(Fermilab)
	W. Turner	(Lawrence Berkeley Lab)
Antiproton Sources	J. Marriner	(Fermilab)
Injectors	R. York	(Michigan State)
Interaction Regions	S. Peggs	(Brookhaven National Lab)
Lattice & Beam Dynamics	M. Syphers	(Brookhaven National Lab)

These groups were assisted by two teams with overall responsibility for coordinating study and evaluating parameters for each of the two facilities mentioned above. These two teams were:

2 x 2 TeV $\bar{p}$ - p collider at Fermilab	G. Jackson	(Fermilab)
	R. Siemann	(Stanford Linear Accelerator Center)
30 x 30 TeV p - p collider	A. Chao	(Stanford Linear Accelerator Center)
	G. Dugan	(SSC Laboratory)
	M. Harrison	(Brookhaven National Lab)

These proceedings describe a study of options for future hadron facilities in the United States and identification of the R&D programs that need to be supported if such facilities are to be realized. The main body of this proceedings is composed of the reports from each of the coordinating teams and working groups. Individual contributions to the workshop are included as Appendices.

II. Historical Perspective

Hadron accelerators and storage rings have provided the U.S. HEP program with research opportunities at the high energy frontier for nearly forty years. Following the invention of the strong focusing concept in the early 1950's a series of proton accelerators of ever increasing energy has been constructed in the United States and Europe. Included in this group are the Brookhaven Alternating Gradient Synchrotron (AGS); the Proton Synchrotron (PS), the Intersecting Storage Rings (ISR), and Super Proton Synchrotron (SPS) at CERN; the proton ring in the HERA facility at DESY; and the Main Ring and Tevatron accelerators at Fermilab. While the basic accelerator design has largely changed only in scale, advances in the underlying technology have allowed a nearly 250-fold increase in the center-of-mass energy achieved in these facilities. The advent of superconducting magnets and the invention of stochastic cooling have spurred the latest advances.

The highest energy accelerator facility in the world today is the Tevatron at Fermilab. This facility, the first high energy accelerator ever constructed utilizing superconducting magnets, provides proton-antiproton collisions at 1.8 TeV in the center-of-mass, with a luminosity currently exceeding 1×10^{31} $cm^{-2}sec^{-1}$. The construction and operation of the Tevatron made possible development of the concepts of the Superconducting Super Collider (SSC) and the Large Hadron Collider (LHC).

The construction of the SSC has been the highest priority construction project in the U.S. HEP program over the preceding decade. The construction in Waxahachie, Texas of this project, a superconducting proton-proton collider operating at a center-of-mass energy of 40 TeV, was canceled by the U.S. government in the fall of 1993. The cancellation of the SSC has prompted a complete reexamination of future options in both the United States and abroad, most notably in Europe. It now appears likely that the construction of the LHC will proceed in Europe over the next ten or so years. This facility, when completed, will provide proton-proton collisions at 14 TeV in the center-or-mass, eclipsing the energy reach of the Fermilab Tevatron early in the next century.

III. Current State of the Art in Hadron Colliders

The Fermilab Tevatron is the highest energy collider operational in the world today. Protons and antiprotons counter-circulate within the Tevatron superconducting accelerator, colliding in two interaction regions. Collisions at 1.8 TeV in the center-of-mass are observed by the "CDF" and "D0" detectors. The Tevatron was completed in 1983 and represents the first high energy accelerator constructed utilizing superconducting magnet technology. The Tevatron is currently operating with a luminosity in the range 1-1.5x10^{31} $cm^{-2}sec^{-1}$. Completion of the Fermilab Main Injector (FMI) project, currently under construction, is expected to yield a luminosity in the range 5-10x10^{31} $cm^{-2}sec^{-1}$ in the year 1999. The increase in luminosity is primarily related to an increase in the antiproton production rate achievable with the newly constructed Main Injector accelerator. It is anticipated that improvements to the Tevatron refrigeration system will allow operation at 2.0 TeV in the center-of-mass during this period. However, further energy enhancements are dependent on construction of either higher field dipole magnets (presently 4.4 T), or of a larger circumference tunnel (presently 6280 m), or both. Completion of the FMI will also afford the opportunity for a 120 GeV fixed target program concurrent with collider operations at Fermilab.

The design of the SSC was based on the technology developed in the Fermilab Tevatron. Proton-proton collisions were to be produced by colliding protons counter-circulating in separate rings utilizing dipole magnets operating at 6.6 T. The total circumference was to have been 87 km. A total energy of 40 TeV in the center-of-mass with a luminosity of 1x10^{33} $cm^{-2}sec^{-1}$ was anticipated. The magnetic dipole field of 6.6 T represented a 50% improvement over the Tevatron design. This improvement was primarily derived from improved performance in superconducting cable over the period 1978-1988. The design of the magnets also showed significant advances over the Tevatron in the area of reduced heat leak through advanced cryostat design. The new significant design issues in the SSC were largely related to the enhanced level of synchrotron radiation and to the achievement of significantly smaller transverse emittances in the SSC relative to the Tevatron. The superconducting magnet design for the SSC was fully developed with technology transfer to industry underway at the time of cancellation of the project.

The LHC complex, as currently proposed, is very similar to the SSC except for the smaller scale. The design energy is 14 TeV in the center-of-mass with a luminosity of 1x10^{34} $cm^{-2}sec^{-1}$. The LHC is proposed to be constructed in the existing, 27 km, LEP tunnel. The magnet, a two-in-one design operating at 8.7 T, represents a significant extension of the SSC design. Models of this magnet have been successfully built and tested. If this project proceeds as currently proposed it is anticipated that operations will commence around the year 2005.

IV. Summary and Recommendations

IV.1 Design Issues: 2 x 2 TeV $\bar{p}$ - p Collider at Fermilab

Design issues in the construction at Fermilab of a 2 x 2 TeV $\bar{p}$ - p collider, operating at $2x10^{33}$ $cm^{-2}sec^{-1}$ were studied. Such a facility represents a factor of twenty improvement in luminosity, and a factor of two energy enhancement over performance expected following the Main Injector upgrade. It should be noted that the energy and luminosity upgrades can be considered separately. Implementation of the luminosity enhancements alone would result in the same beam parameters but one half the luminosity of the full upgrade.

The primary design issue for this facility is the antiproton production/accumulation rate. An accumulation rate of $9x10^{11}$ $\bar{p}$/hour is required to support a luminosity of $2x10^{33}$ $cm^{-2}sec^{-1}$. This represents nearly a factor of twenty beyond the present performance of the Antiproton Source at Fermilab, and a factor of six beyond the performance expected in the Main Injector era. In addition a new facility is required in which up to 10^{13} antiprotons can be stored prior to injection into the collider. The current accumulation capability of the Antiproton Accumulator is about $2\text{-}3x10^{12}$ antiprotons. Potential solutions to these issues are related to an increase in the number of protons targeted per hour and increased cooling bandwidth. At least one, and perhaps two, new rings are required. Details may be found in the report from the Antiproton Working Group.

Secondary design issues are related to providing the required magnetic fields and gradients, and understanding beam stability and dynamics with large numbers of bunches in each beam. The achievement of 2 TeV in the existing Tevatron tunnel requires dipole magnets operating at 8.8 T and quadrupoles in the interaction regions with gradients of 210 T/m. The dipole field required is a factor of 33% beyond that achieved in the SSC development program and is comparable to current achievements in the LHC program. The achievement of this field is not considered a major challenge. Development of the large aperture, 210 T/m quadrupole represents a greater challenge. The development of such a magnet would probably closely parallel the development of the interaction region quadrupoles required for the LHC program. It should be noted that the magnet design is strongly impacted by the potential need to support a slow extracted beam program at 2 TeV. The decision of whether to include such a performance specification would have to be made fairly early in the development program

A number of potential issues relating to operations with a large number of bunches deserve further study. These include the long range beam-beam interaction, intrabeam scattering, issues related to the production and preservation of low emittance, and single beam instabilities. Many of these issues could be addressed through beam studies in the Tevatron.

Many of the beam dynamics issues referred to above could be ameliorated through reduction of the number of bunches. The motivation for operating with large numbers of bunches is reduction of the number of interactions per crossing at the detectors. For example, with a luminosity of $2x10^{33}$ $cm^{-2}sec^{-1}$ the number of interactions/crossing seen in the detectors ranges from 2.5 to 17 as the number of bunches is varied between 750 and 108. It is obvious that a dialog between

accelerator and detector designers will have to take place early within the developmental period of such a facility in order to select the appropriate number of bunches.

For a luminosity upgrade of the Tevatron unaccompanied by an energy upgrade essentially all the above issues remain with the exception of those related to magnet development.

IV.2 Design Issues: 30 x 30 TeV p - p Collider

Design concepts for a collider operating at an energy a factor of four beyond LHC and a factor of one-and-a-half beyond the SSC were investigated. While the energy of such a facility is only 50% higher than that planned for the SSC, it was recognized fairly quickly that the design and operational issues of such a machine would be quite different due to the enhanced role of synchrotron radiation. A proton collider operating at 30 TeV per beam, with dipole fields of 10 T or greater would represent the first hadron facility in which the role of synchrotron radiation went beyond being irrelevant, as at the Tevatron, or a nuisance, as at LHC and SSC. Radiation damping in a 30x30 TeV collider has a significant impact on the operating characteristics. Every effort must be taken to understand how best to utilize synchrotron radiation as an aid for simplifying the design of the facility.

The number one design issue in such a facility is clearly the dipole magnets. Fields of 10-15 T are required to keep the size of the ring manageable (where manageable means equal to the SSC). Quadrupoles with gradients of 250 T/m are required for the interaction regions. Achieving fields above 10 T will not be easy. It is felt that 10 T is achievable but probably represents the maximum reach of the currently employed NbTi/cosθ technology. Going past 10 T will require new technology. It is difficult to predict at the moment a rate of development for such technologies.

Synchrotron radiation damping, with damping times of 4-5 hours, is shown to have a substantial positive impact on the performance of a 30x30 TeV collider. However, one must remove the heat generated within the cold magnets. The linear heat load for the parameters described below is three times that being planned for in the LHC. As in the case of the Tevatron upgrade there is a strong coupling between relaxing the challenges to the accelerator builders at the expense of interactions per crossing seen by the experimenters. In this case fewer bunches reduces the magnitude of the synchrotron radiation heat load problems. For the example given in the 30x30 TeV report, a luminosity of 1×10^{34} cm^{-2}sec^{-1} is obtained with a bunch spacing of 100 nsec accompanied by 60 interactions/crossing.

Options for staging such a facility, e.g. starting out with lower energy or with a single ring and proton-antiproton collisions, were not examined in this study. In general one would expect the luminosity achievable to scale with energy as the energy is lowered (at a fixed circumference), and the proton-antiproton luminosity to be approximately a factor of ten lower than the proton-proton case.

IV.3 Conclusions

Upgrading the Fermilab $\bar{p}$ - p collider complex to either 1×10^{33} cm^{-2}sec^{-1} at 1x1 TeV, or to 2×10^{33} cm^{-2}sec^{-1} at 2 x 2 TeV is an aggressive goal. Increasing the antiproton production rate by a factor of 6 beyond that anticipated following completion of the Main Injector is the key. Several

ideas exist for accomplishing this, but none are mature at this stage. Further design and development work are required to generate assurance of achieving this performance. Long range beam-beam effects are likely to be important if the Tevatron were configured to run with many (>100) bunches at high ($>1\times10^{33}$) luminosity. Machine studies in the Tevatron could shed much light on this issue.

A proton-proton collider operating at $\geq$ 60 TeV in the center-of-mass, and with a luminosity of 1×10^{34} $cm^{-2}sec^{-1}$, is a reasonable goal for the next hadron facility following the LHC. The possibility of utilizing synchrotron radiation emittance damping to enhance the performance, and simplify the construction, of a next generation hadron collider looks promising enough to warrant further attention. An operating energy in the range of 25 - 40 TeV/beam would require 12.5 $\pm$ 3 T dipoles. As in all high energy hadron facilities, magnets are the key. A reinvigorated U.S. superconducting magnet R&D program will be needed to support these aims. Facility cost will clearly be a significant design consideration and needs to be integrated into thinking on even the most preliminary designs. Cost minimization through simplification of injector performance specifications, utilization of existing facilities and infrastructure, optimization of fabrication and procurement strategies, and staging all deserve considerable thought.

There is a real trade off between relaxation of accelerator parameters and increasing the number of interactions per crossing in each of these facilities. There must be a close interaction between accelerator and detector designers to identify an optimum bunch spacing.

IV.4 R&D Priorities and Recommendations

Superconducting magnets are the enabling technology for high energy hadron colliders. As such the highest priority for the future of hadron facilities in the U.S. is the reassembly of a U.S. superconducting magnet R&D program. This effort should be broad based, utilizing the considerable expertise still resident in a number of the high energy labs, with an emphasis on conductor development and new magnet designs. The goals of such a program might be: 1)the development of a 9-10 T dipole magnet based on NbTi technology; 2)the development of high quality quadrupoles with gradients in the range 250-300 T/m; and 3)initiation of R&D activities aimed at moving beyond the existing technology as appears to be required for the development of a magnet operating at 12-15 T.

The key to increasing the luminosity of the Tevatron proton-antiproton collider has been, and will continue to be, increasing the antiproton production rate. Development of this capability deserves continuing support. Issues that need to be addressed include: 1)targeting of up to 3×10^{13} 120 GeV protons every 1.5 seconds; 2)the development of 8-16 GHz stochastic cooling systems; 3)development of new concepts for storing large numbers (at least 10^{13}) of antiprotons.

Significant participation in the LHC project could be a valuable and important component of a U.S. program for hadron collider R&D. Such participation would be most valuable if targeted toward those areas which represent the greatest challenges in moving toward the future, for example superconducting magnet and beam tube vacuum technology. In addition to making a worthwhile contribution to the LHC and world wide high energy physics effort, such participation would be an important ingredient in maintaining the vitality of the U.S. accelerator scientific and engineering community.

New ideas for overall systems designs of energy/luminosity upgrades of the Tevatron complex and of construction of a 60 TeV collider facility, sometime following completion of the LHC, need to be pursued. These facilities represent the future of hadron facilities in the U.S. While the accelerator physics community anticipates that final decisions on specific directions will be determined within the wider U.S. HEP community based on physics considerations, vigorous activity on the fronts listed above will provide the most effective mechanism for assuring that our community is given the opportunity to pursue hadron physics in the future.

Fermi National Accelerator Laboratory

30 x 30 TeV - Summary Report

A. Chao

SLAC
Stanford, California 94309

G. Dugan

SSC Laboratory
2550 Beckleymeade Avenue, Dallas, Texas 75237

M. Harrison

Brookhaven National Laboratory
Upton, Long Island, New York 11973

Operated by Universities Research Association Inc. under Contract No. DE-AC02-76CHO3000 with the United States Department of Energy

30 x 30 TeV - Summary Report

Alex Chao, Gerry Dugan, Mike Harrison
SLAC SSCL BNL

Introduction

In this report we summarize the basic conceptual ideas that were developed during the workshop. Using 30 TeV as an example we looked at the potential consequences of a hadron collider where synchrotron radiation was sufficient to produce significant emittance damping. The machine footprint was "SSC -like" and consisted of two interaction regions and two arc sections. The desired luminosity regime was ~10^{34} cm^{-2} s^{-1} in a proton-proton, 2-in-1 magnet environment. No detailed parameter adjustment was made to achieve any exact performance goals however, interest was focused more on the consequences of parametric variations.

Optimizations

Synchrotron radiation, broadly speaking, produces two main issues. Emittance damping which results in enhanced beam phase space density and is a positive attribute, and radiated power into the bore tube producing vacuum and cooling complications. The conceptual goal of this study involved utilizing the former while mitigating the latter in what we perceive to be a reasonable fashion.

The synchrotron radiation damping rate is determined by the collision energy and the dipole field, thus for a fixed set of these parameters the factor linking the damping rate to the radiated power is the number of circulating protons in the machine. Minimizing the circulating current for a fixed luminosity argues for lower beta-star at the IP and increased bunch spacing/intensities. The maximum luminosity for a fixed circulating current is obtained by increasing the bunch intensity and bunch spacing. This can be accomplished by a bunch coalescing in the injector chain. The practical limits to this exercise are determined by the experimental consequences of the increased number of events per bunch crossing. Another issue which becomes important for low beam currents, is particle burn-off at the IR's. Significant particle burn-off results in short luminosity lifetimes which pushes the machine operation in the direction of short store lengths. This in turn requires a relatively rapid cycling injector.

On the positive side, significant emittance damping provides luminosity enhancement and may also result in less sensitivity to emittance growth arising from the beam-beam interaction i.e. increase the tolerable tune shift limit. Insensitivity to many of the traditional sources of emittance growth in hadron colliders can be expected to result in slackening of tolerances in many areas and thus a simpler, cheaper and more robust machine. Integrated luminosity is not strongly correlated to the initial beam size which simplifies the injector complex. Since significant emittance growth can be accepted during the injection cycle, field quality requirements on the arc magnets (invariably defined by low energy criteria) can be relaxed. Likewise, less sensitivity to persistent and eddy current phenomena, can be used to increase the dynamic range of the machine energy to simplify the injector specifications. Similarly, beam transfer issues are less complicated with a lack of stringent emittance growth requirements. Matching, kicker specifications and damping systems will all benefit. Instrumentation is helped by (relatively speaking) large beam sizes at injection and significant photon emission at high energies. Emittance growth due to vibration effects and power supply noise in the arcs will be ameliorated by the emittance damping, maintaining beam collisions must still be assured however. Reduced circulating beam currents also result in less stored energy in the beams,

which, while still a very difficult issue, is less of a challenge than might have been expected from a straightforward scaling of LHC/SSC parameters.

Parameters

A partial parameter list for a 30 x 30 TeV machine is shown below :-

Collision Energy	30 TeV
Injection Energy	1 TeV
# of IR's	2
Dipole field	12.5 T (10 T)
Circumference	~60 km (~80 km)
# of dipoles	3335
initial transverse emittance - collisions	1.5 π mm-mrad rms (x&y)
initial transverse emittance - injection	1.0 π mm-mrad rms (x&y)
initial longitudinal emittance	0.5 eV-s rms
rf frequency	360 MHz
rf voltage	25 MV
bunch length	4 cm rms
bunch intensity	2.4 E10
# bunches	2030
bunch spacing	30 m (100 ns)
number of events / crossing	90 (60 mb tot. inel. X-section)
revolution frequency	5 kHz
initial beam lifetime - burn off	16 hr
initial $\Delta\nu$ beam-beam head-on / IR	0.002
crossing angle	50 μrad
initial $\Delta\nu$ long-range / IR	0.0039
beta-star	20 cm
syn. radiation power / length / ring	0.56 W/m
total syn. radiation power / ring	29 kW
syn. radiation damping time initial	4.7 hr (FODO lattice) transverse
	2.3 hr longitudinal
stored energy / beam	230 MJ
Filling time / ring	~ 10 min
Injector cycle time	~ 1 min
Acceleration time	~ 5 min
Injection dipole field	0.4 T

The collision energy of 30 TeV was chosen purely to illustrate the potential consequences of operating a hadron machine in a radiation damping regime. It should be emphasized that there is an energy window where this behavior applies and is correlated to the assumed dipole field. If the machine energy is too low then the damping is insufficient to be useful. If the energy is too high then the radiated power becomes prohibitive for the cryogenic magnets. The injection energy is defined by the somewhat arbitrary choice of collision energy together with a choice of 30:1 for the dynamic range which seems reasonable with an allowance for 50% emittance growth at flat bottom. The dipole field of 12.5 T was chosen as a representation of next generation superconducting magnets, though as we demonstrate, a range of dipole fields can be accommodated in this approach. A marginal parameter remix can produce similar machine

characteristics with lower dipole fields as can non - FODO lattices. The desired injector beam emittance of 1 π mm-mrad rms was taken from the SSC injector chain specifications somewhat arbitrarily. As alluded to in the next section, the luminosity evolution is relatively insensitive to initial emittance values. The criteria for injected beam parameters would appear to be set by the somewhat less demanding requirement that beam should stay in the machine for the ~ 30 minute filling time rather than any emittance specifications. Since this is difficult to quantify in the short time period of a workshop we chose the SSC - like parameters. The 20 cm beta-star was picked to be the lowest value that the IR working group deemed realistic. The rf parameters were picked to deliver a bunch length consistent with the beta-star value.

The total beam current was loosely defined by the desire to produce an ~ 8 hr optimum store length. The bunch intensity, bunch spacing and hence number of bunches was influenced by stability considerations and the projected 90 events per bunch crossing at maximum luminosity. It would appear that the LHC with 16 events per crossing has removed the option of event by event vertex reconstruction from the detectors. We have pushed this harder. Since this is one of the more controversial aspects of this design we expect further discussion on this point. Every cloud is reputed to have a silver lining, and the increased beam granularity does provide much more time between crossings for trigger processing than the LHC, for example.

The initial beam-beam tune shift is relatively benign but does increase during the store. We assumed a tolerable tune shift limit of ~ 0.03 which is a modest increase on the 0.02-0.025 achieved today.

A crucial parameter in this conceptual exercise is the radiated beam power per unit length. We chose a value of 0.6W/m which is approximately a threefold increase over the LHC. At this level a bore tube liner is necessary but vacuum issues arising from the desorbed gases are certainly tractable as are cryogenic problems associated with the heat removal. As discussed in the vacuum/cryogenic section of this workshop report power densities as high as 3 W/m could be handled with increased complexity in the various systems and beam conditioning scenarios. Since there is almost a straight trade-off between events per crossing and radiated power, and the situation with respect to either issue is complicated we imagine further discussions on this point.

The injector cycle time and the machine acceleration time are determined by the short store regime and correspond to the present Tevatron cycle time and a ramp rate of about 20% that of the Tevatron.

Operating Characteristics

The operating characteristics of this machine show, not surprisingly, more dynamic variation than present day hadron colliders i.e. more electron like behavior. Figures 1 a -> d show an analytic estimate of the time evolution of the transverse emittance, bunch intensity, luminosity, and head-on beam-beam tune shift. In obtaining these results we have assumed no emittance growth mechanisms. The luminosity rises from an initial value of ~ 5 x 10^{33} to ~ 10^{34} over a period of ~ 4 hr and then slowly falls again in a more or less symmetric fashion. The peak to average luminosity is a healthy 70% across this time span. During the 8 hr storage period the bunch intensity falls by a factor of 5 and the transverse emittance shrinks by an order of magnitude. The head-on tune shift increases with bunch density to ~ 0.01/IR but this is partially compensated by the reduction in long range tune shift which is not shown. The quite rapid fall in initial emittance intuitively leads one to suspect that the integrated luminosity is not strongly correlated to the assumed value for initial transverse emittance and other runs, not shown here, confirmed this. One interesting fact did emerge from this superficial exercise; initial emittances significantly less the 1 π result in a rapid saturation of the relaxed beam-beam tune shift limit i.e. this machine does not like very dense beams !

Other runs were performed with the same parameters using a 10T dipole field (80 km circumference) and the results are shown in figures 2 a ->d. With the reduced damping rate the luminosity peaks at a lower value and the optimum store length is longer but the same basic features are evident albeit at a ~40% loss of performance. The lack of sensitivity to the dipole operating field is a healthy attribute given that we chose to use a "dipole" that is beyond the state of the art today. While these simulations were performed using a straight forward FODO lattice in the arc sections, the lattice working group demonstrated during the workshop enhanced damping lattices by manipulating the partition functions through the use of combined function magnets. Changing the partition functions from a FODO-like $J_x = J_y = 1.0$, $J_z = 2.0$, to a more desirable $J_x = J_y = 1.5$, $J_z = 1.0$, then the performance of the 10T machine is virtually identical to a 12T one. Other techniques to enhance the damping rate such as operating with a small momentum offset are also potentially attractive from this point of view.

Since we are relying for luminosity on the increased phase space density to counter balance the loss of bunch intensity, it is natural to be concerned about the effect of emittance dilution mechanisms. It is evident from the figures that a beam emittance which asymptotically approaches zero is non physical in the limit, and a more rational simulation would include beam heating mechanisms where the equilibrium beam emittance is defined by the balance between heating and cooling. Intra-beam scattering (IBS) is such a heating term which increases with increasing beam density. A first estimate of the impact of IBS was made by including a parameterised IBS heating term in a self-consistent way. These results can be compared to those of figure 1 (a different calculation). As expected, there is little effect at the beginning of the store when the beam size is large, but it becomes progressively more important as the beam shrinks. The peak luminosity is reduced by ~20% and instantaneous luminosity falls off faster after the peak value with the transverse emittance approaching an asymptotic value of ~ 0.15π . This results in a 20% decrease in integrated luminosity over a 10 hr period. Maintaining the longitudinal emittance at it's initial value of 0.5 eV-s by beam heating halves this decrease. While the effect of IBS is significant the overall features of the store evolution are similar.

Observations

Since magnets are a crucial and dominant feature of any accelerator in this energy regime it is appropriate to include some observations on this topic which are not strictly related to machine performance. While our basic machine model assumed a 12.5 T dipole it became apparent during the workshop that there is no threshold field necessary to enter the regime of usable emittance damping. All things being equal, the biggest impact on synchrotron radiation emission is operating energy, which produces the somewhat interesting observation that for a constant damping rate, the lower the dipole field the higher the operating energy, and vice versa. Alternatively, for a desired operating energy there is a maximum dipole field beyond which radiated power becomes prohibitive. These factors together with fiscal realities would indicate that optimistic but otherwise reasonable people would conclude that dipoles in the range of 9 - 15 T and a machine energy of 25 - 40 TeV can be made to fit into the basic conceptual framework outlined here. Beyond this regime a different approach is called for.

Magnet aperture and field quality are related quantities. As discussed in the other workshop reports, at the back-of-an-envelope level, a 5 cm magnet aperture would appear to suffice, including the needs of bore tube liners. Since field quality in the arc regions is invariably defined by the low energy performance of the magnets, the short dwell time (20 min) and 50% allowance for emittance growth in this model should permit a relaxation of SSC-like field quality specifications (factor of 3 ?) which in turn will reduce magnet costs. A 2-in-1 magnet style is also preferred for both cost implications and simplifications in the IR regions when the beams are brought into collision.

The use of high T_c superconductors for the magnets does not appear to be necessary to achieve the magnet performance alluded to here. An elevated operating temperature (10 - 15K say) while not necessary is still highly desirable. The bore tube liner could become passive with no dedicated cooling circuits, a greater allowable temperature fluctuation across the magnet strings greatly simplifies the cryogenic system, as does the removal of radiated power at the higher temperature. Cryogenic operating costs are also reduced. High T_c materials also raise the possibility of permitting an increase in the tolerable synchrotron radiation power density in the magnets i.e. a potential increase in luminosity. Since these items are, in principle, quantifiable, the basic elements for a cost/benefit study of a high T_c magnet R&D program are available.

Conclusions

The possibility of utilizing synchrotron radiation emittance damping to enhance the performance, and simplify the construction, of a next generation hadron collider looks promising enough to warrant further attention. An operating energy in the range of 25 - 40 TeV would require 12.5 ± 3 T dipoles. Some form of magnet R&D program will be needed to support these aims.

The authors would like to thank the workshop organizers, the host institution, and the other working groups, for providing the impetus and facilities to embark on a speculative venture like this. This was a fun workshop.

Figure 1. Time Evolution of the Store Parameters
Dipole Field 12.5 T

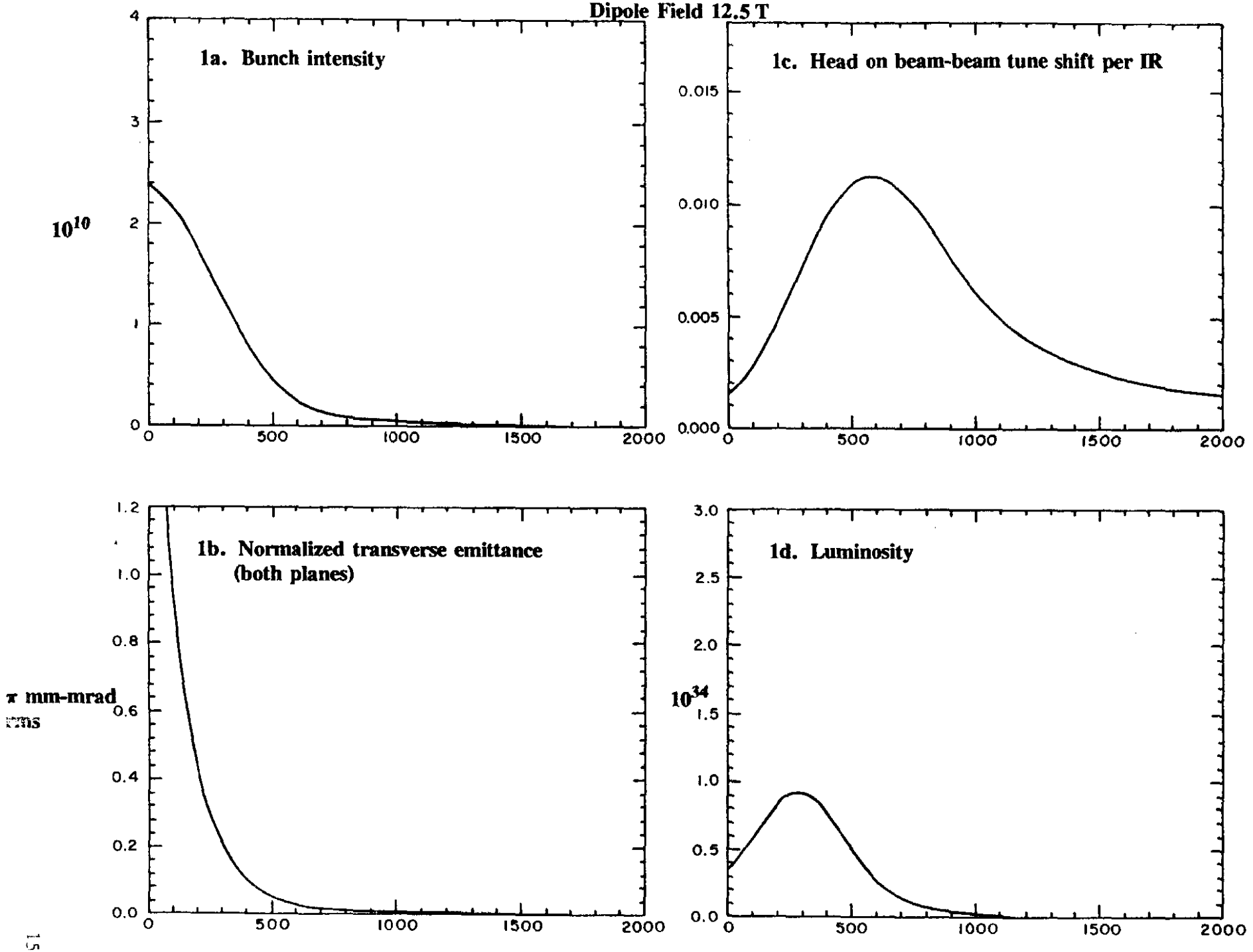

Figure 2. Time Evolution of the Store Parameters
Dipole Field 10 T

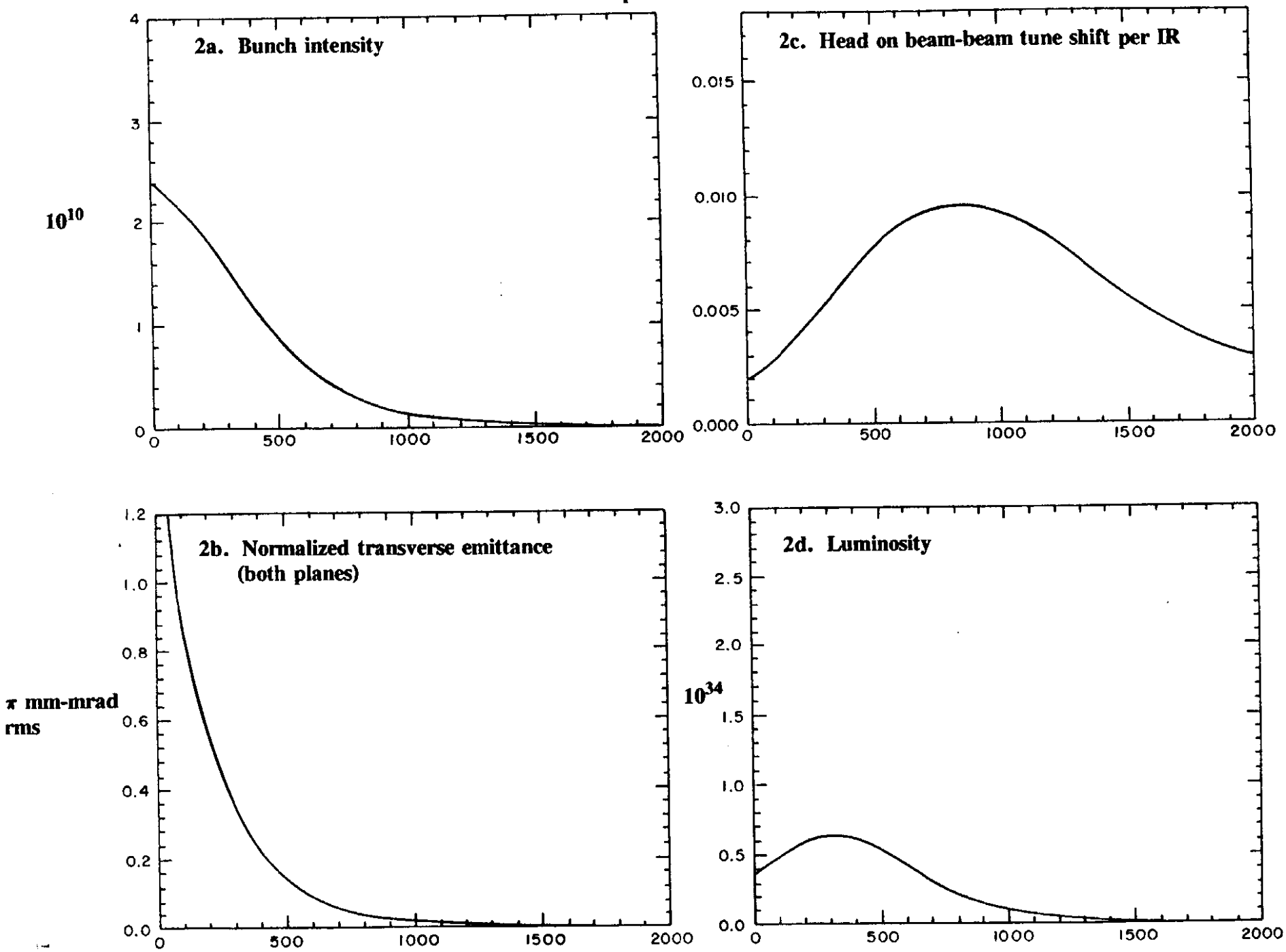

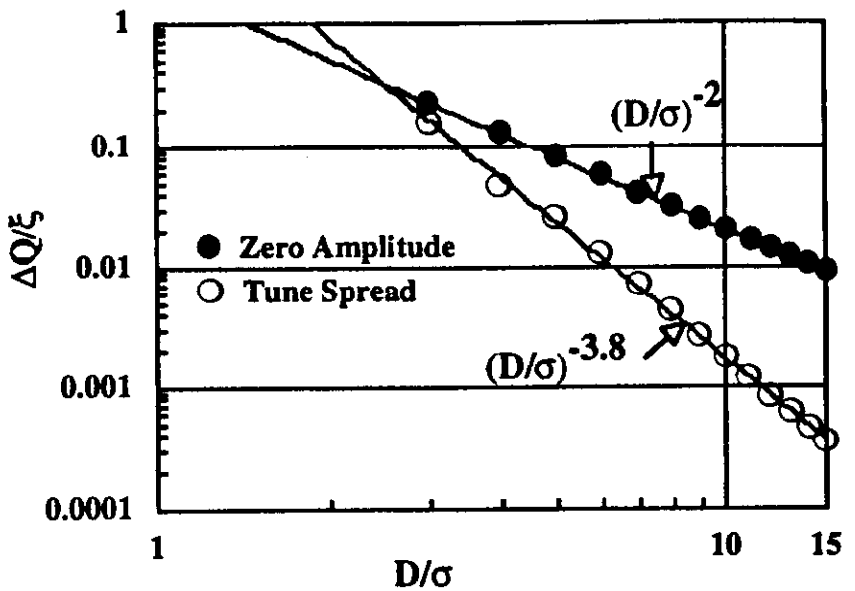

Figure 1: Parasitic beam-beam interaction. The tune shift of a zero amplitude particle and the tune spread for particles with 2σ amplitudes of oscillation. These are normalized to the head-on beam-beam tune shift. D is the center-to-center separation and σ is the RMS beam size.

The major elements of an upgrade to the 2×2 TeV collider are some additional accelerators to substantially increase the anti-proton production rate and a new superconducting ring replacing the existing Tevatron. The improvements of the anti-proton production rate could be done without replacing the Tevatron giving a high luminosity 1×1 TeV collider.

Original DiTevatron Parameters

Tevatron Lattice: A crossing angle of 120 μrad is used to separate the beams at the interaction regions. After that, electrostatic separators are needed to establish spiral orbits in the arcs to avoid other unwanted conditions. These separators must be placed where the appropriate β-function is large and points are needed with 90° phase advance between horizontal and vertical. A lattice needs to be developed that satisfies these criteria with a footprint consistent with the Tevatron tunnel, possibly with minor modifications.

Beam Intensity: There are 1500 parasitic collisions. The tune shift of a zero amplitude particle and the tune spread for particles with oscillation amplitudes up to 2σ are plotted in Figure 1. These are normalized to the head-on tune-shift, and the approximation has been made that the beams are round at the parasitic crossing point. Bunches are separated by $D/\sigma = 4 - 5$ in present Tevatron operation where there are 10 parasitic collisions and no significant problems observed from them. Keeping the same ratio of parasitic to head-on tune spread, the separation should become $D/\sigma \sim 15 - 20$. Since the emittance and energy spread are smaller in the DiTevatron, the beam size is smaller, and roughly the same center-to-center separation as used at present should be adequate for this consideration.

The average tune shift is more of a problem because there are a number of effects that cannot be compensated by changing the lattice tune. These include the difference in proton and $\bar{p}$ tunes, approximately $0.014\ \sigma^2/D^2$ per parasitic collision, and rapidly changing tunes

Fermi National Accelerator Laboratory

A High Luminosity, 2 x 2 TeV Collider in the Tevatron Tunnel

G.P. Jackson

Fermi National Accelerator Laboratory
P.O. Box 500, Batavia, Illinois 60510

R.H. Siemann

Stanford Linear Accelerator Center
Stanford, California 94309

Operated by Universities Research Association Inc. under Contract No. DE-AC02-76CHO3000 with the United States Department of Energy

A High Luminosity, 2 × 2 TeV Collider in the Tevatron Tunnel

R. H. Siemann, Stanford Linear Accelerator Center, Stanford, CA 94309†
G. P. Jackson, Fermi National Accelerator Laboratory, Batavia, IL 60510*

A goal of this workshop was preliminary evaluation of a high luminosity 2×2 TeV collider in the Tevatron tunnel. The parameters that were distributed at the beginning of the workshop and were the focus of much of the discussion are given in Table I in the "Original DiTevatron" column. The peak luminosity would be L ~ 2×10^{33} $cm^{-2}s^{-1}$ achieved with 750 bunches spaced 19 nsec apart. There would be 2.5 interactions per crossing in the particle physics detectors assuming a 45 mb cross section. Some of the problems with the original parameters discovered during the workshop could be solved by reducing the number of bunches at the cost of increasing the interactions per crossing to 17. These are given in the "Modified DiTevatron" column. The parameters for the 1992/93 Tevatron run and the first run planned with the Main Injector are given in Table I for comparison.

Table I: TEVATRON PARAMETERS

Parameter	1992/93 Actual	Main Injector	Original DiTevatron	Modified DiTevatron
Beam energy (GeV)	900	1000	2000	2000
Peak luminosity ($\times10^{30}$ cm^{-2} s^{-1})	5.4	123	1980	1980
Protons/bunch ($\times10^{9}$)	120	380	60	238
$\bar{p}$'s/bunch	31	36	16.5	90
Proton emitt (95%, π mm-mrad)	20	30	5	18
$\bar{p}$ emitt (95%, π mm-mrad)	12	15	5	18
β^* (cm)	35	25	25	25
Bunches/beam	6	36	750	108
Bunch spacing (nsec)	3493	395	18.9	132
Total number of protons ($\times10^{12}$)	0.72	13.7	45.0	25.7
Total number of $\bar{p}$'s ($\times10^{12}$)	0.19	1.30	12.38	9.8
Interaction regions	2	2	2	2
Fract momentum spread ($\times10^{-4}$)	6.0	5.0	0.9	2.4
Rms bunch length (cm)	55	45	8	22
Crossing half angle (mr)	0	0	0.12	0
Luminosity form factor due to hourglass and crossing angle	0.62	0.58	0.69	0.79
Integrated luminosity (pb^{-1}/wk, 33% duty factor)	1.1	25	400	400
Interactions/crossing (45 mb)	0.9	3.2	2.5	17
Total $\bar{p}$ tune shift (2 IR's)	0.009	0.020	0.019	0.019
Total proton tune shift	0.004	0.004	0.005	0.005
Peak $\bar{p}$ loss rate (10^{10}/hr, 90 mb)	0.35	8.0	130	130
Stacking rate (10^{10}/hr)	4.0	15	100	100

Future Hadron Facilities Workshop, Bloomington, Indiana, July 6 - 10, 1994

† Work supported by the Department of Energy, contract DE-AC03-76SF00515.
* Work supported by the Universities Research Association, Inc. under contract DE-AC02-76CH03000 from the Department of Energy.

during injection of the opposing beam. A theoretical analysis is needed, and the effects of parasitic collisions should be studied experimentally by looking at the behavior of an anti-proton bunch in the presence of a fixed target proton beam .

The average proton current is comparable to the beam used in fixed target operation. Coupled bunch instabilities have been observed there, and they have been cured by careful tuning of cavity higher mode frequencies. In addition, reducing the higher mode Q's could be used as a cure also, and the average current does not present a problem.

The single bunch longitudinal and transverse instability limits have been estimated, and the longitudinal microwave instability sets the impedance limit. The high frequency impedance limit is $Z / n \leq 2\Omega$ which is be compared with the estimated Tevatron impedance, $Z / n \approx 5\Omega$. The new collider ring will have to have a lower impedance, and the microwave instability seems to be a performance limit for upgrades that do not replace the Tevatron. Of course, this can be studied experimentally.

The emittance growth rate due to intrabeam scattering has been estimated in two ways. A 2 hour horizontal emittance growth time was calculated by scaling from the SSC,[1] and a growth time an order of magnitude longer was found using approximations in the original Piwinski reference.[2] If the first result was correct, intrabeam scattering would dominate the luminosity lifetime and it would be unacceptably short. The disagreement between the calculations is due to strong dependence on lattice functions which are not known, and a better calculation must be performed when they are.

Magnets: The 8.8 T dipole magnet technology that is needed for the DiTevatron remains to be proved, but this should be done soon as part of LHC development. The good field aperture may have to be comparable to that of the present Tevatron, 4.5 cm dia., to allow adequate separation at parasitic crossing points. SSC magnets could be run at low temperature to test the feasibility of those magnets for producing 8.8 T, but they do not have sufficient good field aperture. A design iteration addressing field quality had been planned as part of SSC development.

A gradient of 150 T/m is required for the lattice quadrupoles is comparable to the present Fermilab IR quad gradient of 140 T/m and the SSC lattice quadrupole gradient of 220 T/m. Scaling of present Tevatron lattice would require IR quadrupole gradients of 280 T/m. This is not feasible, but this is not a problem since the design $\beta^* = 25$ cm has been reached in lattice designs with a lower gradient of 210 T/m. Accommodating the electrostatic separators is a more serious issue.

Vacuum: The critical energy for a 2 TeV proton beam in an 8.8 T magnetic field is 3.8 eV which is close to the work function of many metals. Desorption rates have not been measured for these energies, so the impact on the vacuum system is not clear.

Low Emittance Proton Source: The present performance of the Fermilab Booster is that it accelerates batches of 84 bunches with a single bunch intensity of 4×10^{10} and longitudinal and transverse emittances of 0.08 eV-sec and 10 π mm-mrad, respectively. The intensity must be higher and the transverse emittance lower for the DiTevatron, and the space charge tune shift in the Booster would be a factor of 2 - 3 times higher. This cannot be achieved with the present linac, and the linac energy would have to be raised to roughly 0.8 - 1 GeV to avoid emittance degradation from space charge. The space charge tune shift at injection to the Main Injector is low, and that should not present a problem.

Modifications to the Fermilab ion source and low energy beam optics are needed for the low transverse emittance. The requirements are within the ranges of developments for the SSC.

Anti-Proton Production

The $\bar{p}$ stacking rate is 5×10^{10}/hour at the present time, and this must be increased to 10^{12}/hour for high luminosity. The consensus of the anti-proton source group was that at least two additional accelerators for manipulating the $\bar{p}$ phase space, cooling and accumulating $\bar{p}$'s would be required. Common features of the sources considered are: i) stochastic cooling in the present Accumulator ring, ii) followed by additional stacking in a new, high energy accumulator ring; iii) $\bar{p}$ recovery from the previous collider store which gives some flexibility in store length; and iv) an 8 - 16 GHz cooling system. The differences between approaches were: i) the role of the present Debuncher ring in a new $\bar{p}$ source, ii) whether one or six 84-bunch Booster batches of Main Injector beam were targeted, iii) proton beam manipulations before targeting, iv) targeting, and v) anti-proton manipulations after targeting.

The different approaches are detailed in the report from the anti-proton source group. All of them have advantages and drawbacks, and none is developed sufficiently to judge feasibility, reliability and cost. The viability of a high luminosity collider in the Tevatron tunnel depends on developing an adequate $\bar{p}$ source, and the research and development associated with that is crucial.

Modified DiTevatron Parameters

The original parameters had 750 bunches to get a small number of interactions per crossing. With a limit on $\bar{p}$ production, the transverse emittance must be small for high luminosity and the longitudinal emittance must be small for the short bunch needed for crossing at an angle. These considerations lead to a high proton phase space density and the dominant problems of the original parameter list: space charge tune shift at injection into the Booster and intrabeam scattering (which needs to be checked as discussed above).

The modified parameters are for 108 bunches. Longitudinal coalescing could be used, as it is now, to reduce the space charge tune shift in the Booster, and the larger emittances make intrabeam scattering unimportant.

The situation with parasitic beam-beam collisions does not change substantially. While the number of parasitic collisions is reduced by a factor of 7, the beam sizes are larger, and the required separation could be larger although D/σ is smaller.

Conclusions

This workshop was helpful for identifying potential problems and suggesting areas of research. The most important ones are:

I. Anti-proton production is the key to high luminosity in the Tevatron. No fatal flaws were found in the approaches considered, but because of their preliminary nature, the trade-offs, costs, and potential impact on the Main Injector fixed target program, they need to be evaluated carefully.

II. Parasitic beam-beam interactions would produce substantial tune shifts and tune spreads because of the large number of bunches in either case. The parasitic beam-beam interaction needs to be studied theoretically and experimentally to evaluate the impact.

The required separation will determine the required good field aperture and magnet costs.

III. The two DiTevatron parameter lists are contrasted by the number of interactions per crossing and phase space density of the proton beam. If the intrabeam scattering lifetime is as short as calculated by scaling from the SSC, the original list is flawed. If that is not the case, a linac energy increase and modifications to the low energy portion of the linac would be required for the phase space density in the original list. The modified list does not have these accelerator physics problems, but does have 17 interactions per crossing. That needs to be considered by experimenters.

Finally, a comparison of the DiTevatron parameters with the actual performance in 1992/1993 shows that a 2×2 TeV high luminosity collider in the Tevatron tunnel would be a substantial extension of the 1992/1993 performance. Fortunately, experiments are possible to test many aspects of the design, clarify the issues we have raised, and provide an opportunity to see unexpected ones. A concerted experimental effort would be a wise investment.

---

1 SSC Central Design Group, Conceptual Design of the Superconducting Super Collider, SSC-SR-2020 (1986).
2 A. Piwinski, Proc. 9th Int. Conf. High Energy Part Accel, 405 (1974).

Fermi National Accelerator Laboratory

Summary of the Magnets Working Group

J. Tompkins

Fermi National Accelerator Laboratory
P.O. Box 500, Batavia, Illinois 60510

Operated by Universities Research Association Inc. under Contract No. DE-AC02-76CHO3000 with the United States Department of Energy

Summary of the Magnets Working Group

DPF Workshop on Future Hadron Colliders
Indiana University Cyclotron Facility

July 6-10, 1994

DPF IUCF Workshop Attendees:

M. Coles (former SSCL)
R. Meinke (former SSCL)
S. Mendelsohn (Grumman)
G. Snitchler (Amer. Super.)
P. McIntyre (TAMU)
T. Ogitsu (KEK)
R. Schermer (Fermilab)
J. Tompkins (Fermilab)

Overview

Prior to the IU meeting, a one and one half day workshop, organized by J. Strait (FNAL), was held at Fermilab on June 6 and 7, 1994. Thirty to forty people attended the various sessions and were joined at times via teleconference, by participants at the University of Wisconsin, BNL, LBL, KEK, and American Superconductor Corp. Members of the 'magnet community', who were not able to attend the IU meeting due to schedule conflicts, were able to attend the earlier Fermilab session. The meeting was organized around discussion groups typically begun with presentations by the group leaders. Particularly useful talks on the status of various conductor materials were given by Prof. D. Larbalestier (U. Wisc.), and R. Scanlan (LBL). In addition to magnet design and conductor issues, talks on cryogenics and machine physics issues were presented by Fermilab staff. A copy of the agenda is attached to this report.

At the IUCF workshop, a smaller group concentrated on further developing approaches to the two conceptual colliders: the 2X2 TeV $p\bar{p}$ collider and the 30X30 TeV pp collider. Interaction with the synthesizers and accelerator physics subgroups for the two machines was considerable. Joint sessions were held with both the cryogenics and IR subgroups; a talk was given by P. McIntyre (Texas A&M University) presenting a novel design for a high field, Nb_3Sn 'pipe magnet' for use in accelerators.

The first day of the workshop was spent discussing details of the 2X2 TeV machine. The 8.8 Tesla field strength for the arc dipoles listed in the parameters could be achieved by an SSC-like dipole with some modifications for field quality (cross section iteration, additional iron to reduce saturation effects, etc.) at 1.8K. A summary of issues and the R&D necessary to resolve them was developed.

The workshop's second day finished up consideration of the 2X2 TeV machine and proceeded to discuss the 30X30 TeV collider; these discussions continued through the third day of the workshop. A critical concern was the nominal time of ten years allotted before construction of the machine was to begin. Based on Tevatron and SSC experience with NbTi conductor-based magnets, it was felt that the goal of a production ready, 12.5 Tesla field strength dipole could not be met within that time period. To achieve field strengths in the range of 12.5 Tesla or higher, it would be necessary to employ a different conductor, most likely Nb_3Sn or even extrapolate to the use of high temperature superconductors (HTS). Conductors made of these materials have yet to demonstrate the properties necessary for accelerator magnets, such as low losses, low harmonic content, high J_c, and ductility. At present, the cost (by weight) of these materials is estimated to be from three to ten times that of the NbTi alloy. *It is clear that there are too many technical uncertainties to be able to reliably predict success within the 10 year period.* However, a significant investment in conductor development must begin now to determine if it is possible to meet requirements for high field accelerator magnets.

Based on the daunting conductor issues raised, the group decided to separate the 30X30 TeV collider discussions into two models: a 'low field' version employing ≈10 Tesla dipoles which could be made of 'conventional' NbTi (or NbTiTa) superconductor, and a 'high field' (≥12.5 Tesla) version - favored by our accelerator physics colleagues - postulating magnets employing 'non-conventional' conductors such as Nb_3Sn or HTS. For the high field hypothesis, we assume an extended development time of more than ten years with early emphasis on conductor R&D. We note that it had been suggested in the preliminary workshop (P. Mantsch, FNAL) that the cost effective solution to a 30X30 TeV machine might lie with designs utilizing an even lower central field value than the 10 Tesla option when the latest cost information is

used[†] . We did not explicitly pursue this option during the workshop, but it is consistent with our low field approach.

The design of the intersection region (IR) quadrupoles poses special problems for all of the colliders: they require gradients on the order of 250 T/m, have high heat loads from energy deposited by interaction products, and must withstand high radiation loads. Consideration of the issues for IR quadrupoles took place on the fourth day of the workshop.

While not an explicit goal of this workshop, we attempted to list areas of cost tradeoff for an overall minimization of the machine cost. A partial list of quasi-'design independent' magnet features was developed to be studied for cost impact and reduction as well as tradeoffs between magnet performance parameters and cryogenic system costs, including synchrotron radiation liner (or 'beam screen') design and operating temperature. The liner and cryogenic issues will be discussed by the Cryogenics working group.

Finally, a few sage words were written to express general concerns and principles for proceeding with any significant superconducting magnet program as part of a new machine. These general principles should be viewed as a part of a framework in which to develop a detailed design and proceed with its implementation.

This summary is organized as follows: the first section presents the general overview statements concerning magnet R&D, followed by a relatively detailed discussion of the 2X2 TeV $p\bar{p}$ collider in the second section. The third section discusses the 30X30 TeV pp collider, with 'low' and 'high' field magnet versions, while 'generic R&D' for superconducting magnets is discussed in the fourth section. A brief discussion of the R&D challenges facing quadrupoles is presented in section five and a brief discussion of overall cost saving approaches is given in the last section.

I. GENERAL PRINCIPLES

Superconducting magnets are the most costly subsystem of the hadron colliders being considered and any design effort must address the cost issue from its onset. The cost derives from many significant areas, including materials, design choices, requirements, and tradeoffs among various subsystems. We attempt, in this brief section, to discussing general approaches to magnet (and collider) development. We consciously use a series of terms that are somewhat worn by overuse and/or applied without intelligence: it is our intent to use the approaches suggested by these terms as tools not ends in themselves.

A 'concurrent engineering' approach must be employed which actively considers quality, production, reliability, and maintainability issues - in addition to complex technical requirements - early in the design process. Specifically, 'production engineering' should be involved in the design effort at the earliest practical juncture. By this we mean that the design should be developed with manufacturability as one of the requirements: efforts should be made to reduce cost and complexity while meeting technical constraints. We must avoid the situation where a technically successful design is turned over to a production organization that then must make design changes to reduce cost.

Tradeoffs between different systems and cost phases of a collider must be considered. The cost goal of the entire project - magnets for the superconducting machines, cryogenic systems,

---

[†] We allude to the reported significant cost savings realized in the SSC tunnel construction.

accelerator systems, conventional construction, etc. - should be to minimize the total LIFETIME costs of the machine. I.e., one cannot minimize projects costs to the detriment of operating costs, nor create local subsystem cost minima independent of cost impact in other systems.

'Value engineering' methodologies should be employed early in the overall machine design process to provide a framework for constant focus on cost saving and cooperative design efforts.

Industry should be involved early in the design process. We must determine how to encourage industrial partnership, while controlling cost, near the beginning of the magnet program to develop a design jointly. This would avoid the difficulty of simultaneously transferring technology while building facilities, tooling, etc. under severe schedule and cost constraints. Given the complicated set of restrictions that govern procurements, this approach requires careful, creative thinking with support and encouragement both from industry and our funding agencies.

The R&D required for the 2X2 TeV machine is relatively small and narrowly focused for the magnets and conductor. A program could be laid out almost immediately and pursued with a relatively small amount of funding,

The 30X30 TeV machine is a different situation. Development efforts with modest funding must begin early to resolve the many R&D issues that have been identified. The relevant time scale is determined by when significant R&D funding becomes available; this is vital to the conductor development where a host of issues must be resolved for the high field magnet designs. Magnet R&D must begin immediately and it should be broadly based but coordinated among the participating institutions: a detailed R&D plan should be developed as an outcome of this workshop. Too often in the past magnet R&D has been strictly tied to the needs of a particular machine, dictated by early, limited design choices, and constrained by tight schedules. Development of new materials for accelerator magnet applications and new and innovative magnet designs should be part of a broader, ongoing research program.

II. THE 2X2 TEV MACHINE

The 2X2 TeV $p\bar{p}$ collider requires single aperture dipoles with a field strength of 8.8 Tesla. The dipoles must provide a 'good field region' of between 20 and 40mm depending on assumptions about potential fixed target operation and machine physics issues. We assert that the superconducting dipoles built for the SSC, with relatively minor design modifications could be the basis for the dipoles required for this collider operating at 1.8K. We discuss the status of the SSC dipoles and the development needed for application to the 2X2 collider in some detail below.

The SSC Dipoles:

During 1991 and 1992, twenty three, 5-cm bore, 15-m long dipoles were constructed and tested at BNL and FNAL. This set of magnets is generically referred to as "ASST magnets", because a subset were used in the ASST string test at SSCL. The successful test program demonstrated that acceptable Collider magnets could be built, using several different construction options.

These dipoles were designed to produce a central field of 6.6 T at 4.35 K with a comfortable engineering margin. One magnet, DCA322, was also tested in superfluid helium at

1.8 K, with a first training quench at 9780A and a plateau above 9900A[†]. While this gives us confidence in the basic soundness of the design, engineering modifications are nevertheless needed before 400 such magnets would be expected to reach 8.8 T reliably and reproducibly. We would also expect modifications to be required before the field quality at 8.8 T is acceptable. Finally, we would re-examine engineering decisions taken some years ago that might now be resolved differently in the light of more recent information, resulting in a net saving to the project.

We did not prepare an estimate of time, manpower or money to accomplish these tasks. Although most of the necessary resources existed at SSCL a year ago, these are dissipating rapidly. An immediate task, then, would be to locate the necessary resources. If these exist, and if the initial development steps discussed below are conducted in parallel, it is not unreasonable to expect that prototype dipoles could be in test within two years.

Development Issues:

Mechanics - quench stability.

An operating field of 8.8 T with a margin requirement similar to that of the SSC, roughly ten per cent, translates to quench limit of nearly 10T. We must investigate the mechanics of the two variants (FNAL & BNL) of the SSC ASST dipole design to determine suitability for the nearly doubled forces at the higher operating field. To achieve the roughly 10T field level, the conductor should be examined to see if a small amount of additional development can translate into higher J_c.

Finite element models of the dipole exist and have been used for detailed studies of various mechanical options. These results, together with existing experimental data, should be used to select a collar material, yoke split direction, collar/yoke interference. The same inputs should be used as a basis for any necessary engineering modifications to the cold mass cross section, e.g. changing the thickness of the helium shell. Thus it should not be necessary to build or test new model magnets prior to settling these issues, although it will eventually be necessary to build magnets to verify the decisions.

Several existing long magnets should be tested at 1.8 K. These tests will increase our confidence in the soundness of the basic design, provide data to be used in quench protection studies, and provide data on the field quality of the present design at high field.

It is likely that magnet performance at 1.8 K, 8.8 T will be enhanced if a conductor is used that has higher critical current than at present. Thus, developmental quantities of NbTiTa, and APC-NbTi should be acquired, and tested in model magnets. These conductors would be scheduled to replace the present conductor during prototype testing.

We recommend a 42-mm inner diameter for the copper plated bore tube. Wall thickness and material need to be specified from a consideration of magnetic properties and of loads applied during a quench.

Field Quality.

[†] We note that DCA322 did not reach quench plateaus at 3.0K and 2.5K; however, its quench current increased nearly 1000A when operated at superfluid temperatures. Two current ramps exceeded 9900A without quenching.

The field quality discussion includes the following topics: systematic values of allowed and un-allowed multipoles, random variation (σ_{rms}) of multipoles, persistent current effects at injection fields, and saturation effects at the operating field level. Also, AC loss and ramp rate performance need to be considered. The systematic values of multipoles are largely determined by coil cross section design; random variation is influenced by fabrication processes and materials. The persistent current effects are dominated by the conductor design and J_c, while saturation is governed by the iron yoke and cold mass position within the cryostat. We discuss these field quality issues below.

The SSC magnet multipoles are quoted at a reference radius of 10 mm, which is 2/5 of the bore radius while the Tevatron multipoles are evaluated at a reference radius of 25 mm, which is 2/3 the bore radius. We assume that the SSC dipoles would be acceptable if they produce field quality at 2/3 of their radius, or 16 mm, at least equal to that of the Tevatron dipoles. (Our understanding is that such a situation would be possible given scheduled improvements to the main injector and $\bar{p}$ source at FNAL.) An SSC multipole coefficient (a_n, b_n) can be expressed at 2/3 radius by multiplying by $(2/3)^n$. The following SSC-to-Tevatron comparisons assume that both are given at 2/3 the bore radius.

The average (or 'systematic') value of an allowed harmonic for a set of magnets depends upon details of mechanical design, construction and insulation system. The ASST dipoles had some non-zero systematic values for allowed multipoles: e.g., b_8 was designed to be non-zero for measurement reasons, other non-zero values occurred due to changes in the cable dimensions that were not corrected for in the collar design due to schedule constraints. To meet field quality requirements, a design iteration of the cross section is necessary. This process involves changes to mechanical dimensions of order 50 microns, or less. Changes are calculated using existing computer models, but must be verified by magnetic measurement on short model magnets. Use of any previously untried option requires additional iterations, and should be avoided if time is of the essence.

The RMS spread of allowed harmonics is already considerably better than the Tevatron. With one or two exceptions, both the average value and RMS spread of unallowed harmonics are smaller than those in the Tevatron.

Ramesh Gupta (BNL) has performed computations on a variety of methods to control values of quadrupole and sextupole moments, either on a magnet-to-magnet basis, or on an ensemble of magnets. The schemes employ the use of iron shims at the collar-iron boundary, or variations in the top/bottom distribution of yoke iron. Several of these methods have been verified experimentally, and could be employed to further improve field quality.

Persistent current multipoles at 1.8 K should be computed, and later verified by experiment. Three options can be pursued if this value is unacceptably large. First, the SSC program to produce wire with 2.5 micron filaments can be restarted. Second, serious consideration can be given to the use of passive superconductor within the magnet bore, or nickel coating on the conductor. Both these latter schemes have already been the subject of theoretical analysis and limited experimental verification.

Computations should be performed to specify the outer diameter and construction details for the iron yoke (and details of the cold mass - cryostat relationship that affect field quality) that will produce satisfactory saturation multipoles at 8.8 T.

The ASST magnets showed unexpectedly large ramp rate dependence; quench currents were sharply depressed at elevated ramp rates and eddy current multipoles were seen. In their

present state, the magnets might have been acceptable for the collider but not for the HEB. Similarly, the magnets might be acceptable for the 2X2 TeV machine in collider mode, but would probably not be adequate in fixed target mode.

We believe that the source of the ramp rate dependence is related to the interstrand resistance and that the cure involves either a change in strand/cable processing or the addition of a coating to the strand. In collider mode, the use of Zebra cable might be all that is required. A ramp rate should be specified and loss computations performed to compare the expected heat load with projected cryogenic capacity. Eventually, long magnets would have to be constructed and tested. This appears to be the critical path development item for the 2X2 TeV machine.

The problem is, presumably, more difficult if fixed target operation is to be accommodated. A cable with higher transverse resistivity than Zebra might be required; if so, this would involve additional R&D time. Strand with 2.5 micron filaments might also be necessary to reduce losses at high ramp rates.

Quench protection issues need to be investigated. Computations should be performed to verify that there are no serious protection issues in using the SSC magnets under 2X2 TeV machine operating conditions. Cold diodes were rejected for SSC use because of radiation problems that do not exist in the 2X2 TeV machine. Given the use of cold diodes in HERA, RHIC, and their projected use at LHC, the use of cold diodes in the 2X2 TeV machine should be given serious consideration.

Quadrupoles.

If the 2x2 machine has the Tevatron lattice, the arc quadrupoles would require a gradient of 140 T/m. SSC quadrupoles with 5-cm bore should reliably produce about 220 T/m at 1.8 K. We recommend that one of the two (collider and HEB) SSC designs be adopted and that the magnet length be shortened appropriately.

A choice must be made between the two designs. The HQM, arc quadrupoles for the HEB, were designed by Saclay and are similar to HERA quads. Complete drawing packages exist, but specific "contact" tooling was not built and models were not constructed. So called 'QSE' magnets, intended for use in the IR region of the Collider, were designed at the SSCL; several short models have been tested at 4.3 K.

Computations should be performed to see if the iron yoke is adequate to provide required field quality at 220 T/m. In any case, it is necessary to test models at 1.8 K to verify that the mechanical structure and field quality are adequate.

Scaling from the Tevatron lattice, it appears that an IR quad is required with a gradient of 280 T/m. Such a magnet cannot be built using current technology, and would require a long development time. A lattice must be designed that requires magnets with maximum gradient of order 230 T/m. If the aperture is determined solely by field quality requirements, the field quality of IR quadrupoles can be adjusted via tuning shims (as mentioned above) to reduce the aperture to obtain a high gradient.

Correction System

The corrector system represents a significant cost in any accelerator. Value Engineering studies at SSC showed that it might be worthwhile to reconsider correcting certain low-order errors by use of trim power supplies on the main magnets, rather than by separately wound corrector magnets.

III. 30X30 TEV PP COLLIDER

The parameter list for the 30X30 TeV pp collider includes an arc dipole central field value of B_0=12.5 Tesla; subsequent discussions with the synthesizers (Harrison, Chao, Dugan) indicated that this would be the lowest desirable field. The prospects of a synchrotron radiation damped beam led the machine physicists to push for as high a field as possible. Promises of reduction in field quality requirements and relaxation of operating temperature ΔT restrictions were made in attempt to persuade the magnet group to adopt an extremely aggressive, (overly-?) optimistic view of magnet evolution. While enticed by the siren song of our accelerator theorist colleagues, we did not feel it appropriate to base a future machine solely on conductors that either had yet to be used in accelerator applications (or had not been developed to the point where they had many of the properties necessary for accelerator magnets). Instead, we decided that if the time allotted for development of a magnet to production readiness was ten years, we would restrict ourselves to 'conventional' superconducting magnet technology and a maximum field of roughly 10 Tesla. This is designated as our 'low field' magnet option. If the time constraint were to be relaxed significantly, higher field magnets (≥12.5 Tesla) could be considered with early emphasis on conductor development. We have named this our 'high field' magnet option.

In pursuing either option, it is clear that a two-in-one design should be pursued for significant cost savings. Less iron is used and the number of cryostats is halved, although the size is increased somewhat. Importantly, the number of interconnects, bellows, flanges, cryogenic lines, buses, etc. is reduced by nearly a factor of two from that of individual ('one-in-one') magnets.

While the cosθ coil configuration is economical in its use of conductor, it was generally held that cosθ coil designs are not practical much above 10 Tesla: the conductor geometry required results in high force levels and stress concentrations. In addition, the angle of the field with respect to the cable leads to large eddy current and persistent current effects. The cost of a magnet rises rapidly as the field is increased: more conductor is required at larger radii from the beam center and thus their differential contribution is less. Conductors with considerable higher J_c at high field are required for the high field option.

The materials being considered for the high field option are cost-prohibitive at this time, even if the large number of technical issues did not exist. As previously stated, the costs of these materials would have to be reduced by a factor of three to ten to make them competitive with NbTi alloys. Cost reduction can only result from improvements in processing and in increase in capacity due to increased demand. This can take place only if a conductor development program is proposed and funded.

The requirements for accelerator magnets are stringent; including:

- field strength in the range of 10T and greater
- field uniformity to better than 1 part in 10^4
- minimized persistent current effects (e.g., sextupole at injection)
- low AC losses and small ramp rate dependence
- mechanical/quench stability to minimize the amount of conductor required to attain a suitable operating margin
- high reliability and long lifetime

all in a manufacturable configuration that minimizes costs. In the final analysis, cost must be

the most heavily weighted factor in the machine design. Both of the proposed options must be studied in terms of total project cost: the resultant machines look quite different depending on the choice of dipole field strength. It is clear that there is not enough information available at this time to make meaningful cost comparisons between the two options: the newer materials are not sufficiently mature to estimate volume production rates even if we were to make the highly optimistic assumption that technical issues would be satisfactorily resolved.

Finally, an important consideration in either the low or high field option is beginning the development necessary at the earliest possible time. Funding must be made available to resolve R&D issues early in the development phase to avoid schedule determined decisions which incur significant technical risk. The early funding for magnet and conductor development needs to be at modest but not insubstantial levels. In the case of newer conductor materials, the basic R&D - preceding larger scale conductor procurement - should begin as soon as possible: the development of Nb_3Sn and HTS materials is not presently driven by accelerator magnet applications.

We discuss the two different magnet options for the 30X30 TeV collider in the next two sections.

III. A. The 'Low Field' Option

The low field magnet design would follow that employed by the LHC: a two-in-one magnet with an operating field strength of 10 Tesla. To attain an operating field of this strength, margin requirements dictate a maximum field strength (corresponding to the short sample limit) in the range of 11 Tesla; the operating temperature would be 1.8K. The list of development issues parallels that of the 8.8Tesla dipole discussed in the 2X2 TeV collider section above, complicated by the 2-in-1 structure and the higher force levels at 10 Tesla. The conductor would most likely be NbTiTa with APC and fine (2.5μm) filaments.

The 30X30 TeV machine creates a large synchrotron radiation heat load, calculated to be 3W/m in the initial parameter list, which must be removed to maintain the magnet temperature. A liner (or 'beam screen') must be inserted to intercept the synchrotron radiation at a higher temperature than the 1.8K bore tube surface. for both magnet temperarture and vacuum reasons. While liner issues are being considered in the cryogenics group, the liner interacts directly with the magnet design in terms of the aperture, support, and cooling penetrations required.

Radiation damage. especially in the IR regions, is a major concern for high energy machines. Studies of materials for coil parts, insulation, etc. such as undertaken at the SSC, will need to be performed, or previous work extended.

Field quality issues include saturation effects at full field and persistent current effects at the injection field level. Overall cost savings might be obtained by reducing the energy of the next lower accelerator in the collider chain (the High Energy Booster, or HEB in SSC terminology). A lower injection energy increases the persistent current multipole contribution and would require active or passive correction. Saturation effects can be reduced by increasing the yoke iron for flux containment at the expense of increased mass and size (hence cost) of the cryostat. Other schemes of flux containment, such as passive shields, should be investigated.

Persistent current effects, as discussed in the 2X2 TeV collider section above, can be reduced by using smaller filaments (2.5μm) in the strand and by either passive correction with superconductor around the bore tube or by strand coating with a magnetic material such as nickel.

III. B. The 'High Field' Option

The high field magnet option requires use of new materials and, most likely, new magnet designs. The agressive thrust of this machine, with ≥12.5T dipoles, was to utilize synchrotron radiation damping of the beams to reduce beam size and maintain high luminosity with short re-fill times. In a such a regime, the number of beam bunches is reduced and the stored beam energy and synchrotron radiation heat load is decreased. A beam store would last roughly 4-8 hours in this mode so that overall efficiency requires a much faster re-fill time, and hence faster ramp rates for the magnets.

To attain fields of 12.5T or greater, materials such as Nb_3Sn or even HTS must be considered. While Nb_3Sn has been studied as a superconductor for a long time, it has not been amenable to accelerator magnet applications†. Nb_3Sn poses many problems: its processing is difficult requiring reacting materials at high temperatures; it is brittle; its J_c decreases rapidly with strain. (At the FNAL workshop, Alvin Tollestrup described Nb_3Sn as "horrible stuff" - its handling and fabrication difficulties are considerable). Coupling and insulation are additional problems with this material. The HTS picture is even more difficult to evaluate: the material is new, J_c's are still too low for accelerator magnets, details of processing are complicated, and bulk quantities in high current conductor form have never been made. In the face of these significant technical difficulties, research directed at accelerator applications must be promoted. For while these materials are problematic at present, they represent the only choices for going to significantly higher fields in future colliders.

In discussing either a Nb_3Sn or HTS based magnet, there are important advantages in raising the operating temperature to the 4-5K range (Nb_3Sn) or 10-15K (HTS): reduction in cryogenic system costs and complexity and simplification of the synchrotron radiation intercept. These are potentially significant savings and, along with the accelerator physics issues which depend on the high field magnets, they provide a strong impetus to pursue the first steps toward this longer term, less certain approach.

The list of R&D issues for the high field magnet option includes those discussed in previous sections - field quality, quench stability, synchrotron radiation, etc. - in addition to the overriding issue of conductor development. We discuss the generic magnet R&D that needs to precede development of new magnets that operate at the 10 Tesla level or higher in the next section. In the following section, we include a short discussion of the two conductor materials mentioned as candidates for a high field dipole. In the remainder of this section we discuss aspects of magnet design.

Magnet Design Considerations

While conductor development is the key issue, high priority should be placed on the exploration of new magnet design concepts. The accelerator magnet field has been dominated by $\cos\theta$ designs: the Tevatron, Isabelle/CBA, HERA, SSC, RHIC, and the LHC all used this conductor geometry. Emphasis should now be placed on new geometries. One recent effort was reported at the workshop: the 'pipe magnet' design being developed at Texas A&M by P.

---

† There is a short model high field Nb_3Sn dipole under construction at LBL which will begin to investigate the use of this conductor in high field applications. In the past, a few short models were constructed at CERN in an early phase of the LHC program. At present, the demand for Nb_3Sn superconductor is dominated by the ITER project which uses it in a 'conductor in conduit' configuration.

McIntyre and collaborators. While many aspects of this design remain to be resolved, it is a sufficiently innovative approach to merit further support and encouragement.

Higher fields present many design issues to be resolved: mechanical support of the forces on conductors, flux containment, and geometries to reduce eddy current effects are among the major concerns. Mechanical issues, such as the reaction of the Lorentz force by the magnet structure and stress concentrations due the non uniform cross section of the cable are crucial to the success of a high field design. In non-cosθ designs, it may be possible to achieve the necessary field quality and reduce stress concentration in the cable.

Conductor orientation with repect to the field is an important consideration for eddy current and persistent current effects; this is certainly not optimized in cosθ designs. Again, designs with new conductor geometries need to place greater emphasis on controlling the eddy current effects. To achieve a less costly high field design it may be necessary to use hybrid conductors where the conductor in the highest field region uses a different material from that in the low field region of the magnet cross section.

Active shielding should be studied as a means of containing the flux and reducing the magnet size. (E.g., increasing the dimensions of the iron in the yoke to contain the flux at 12.5T adds additional mass to be supported, aligned, and cooled, and increases the diameter and cost of the cryostat.) It may be possible to realistically consider iron-less designs that rely on superconductor geometry alone to confine the flux. Superconducting tapes and sheets are being developed that could be of use in these designs.

Finally, combined function magnets, such as a dipole with a small quadrupole gradient might be considered as further means of cost reduction. Such a design had been proposed for the LHC.

IV. GENERIC R&D FOR MAGNET DEVELOPMENT

There are several issues common to superconducting magnets for either a 2X2 TeV or 30X30 TeV collider, especially if 'conventional' (NbTi-based) superconducting magnet technology is employed. These issues include field quality issues due to iron saturation, and persistent current effects, and field quality, AC losses, and quench stability issues associated with ramp rate dependent phenomena. We discuss these more general issues here rather than repeat the details in each of the magnet subsections.

Field Quality - Iron Yoke Saturation.

Saturation of the yoke iron in current, cold-iron magnet designs can cause large field distortions at high fields. A short term approach would concentrate on modification of the yoke cross section, e.g., a larger yoke inner radius (further from the superconductor), and shaping of the yoke specific to the peak field requirements. Flux leakage from the yoke can be reduced or eliminated by increasing the yoke volume. It is also possible to control saturation distortions by appropriate placement of small iron shims for a fixed operating current.

However, at very high fields, the tradeoff between additional iron and the attendant increase in cryostat system costs (larger diameters, increased mass to support, etc.) may limit the extent to which adding iron is an effective method of field shaping. Designs using active and passive superconductor shielding as well as fully 'iron-less' designs should be pursued to evaluate their practicality and cost effectiveness for high field magnets.

Field Quality - Persistent Current Multipoles.

With a large dynamic range (lower injection energy) and/or operation at 1.8K, the harmonics due to superconductor magnetization may be more problematic at injection fields. Development of thinner (e.g. 2.5 micron dia.) filament strand should be pursued to reduce the effect of persistent current multipoles. Conductors developed during SSC R&D proved fine filament strand to be feasible. The strands with 2.5 micron filaments used a CuMn matrix to avoid proximity coupling, and this matrix material also reduces intra-strand eddy current losses.

A complementary correction scheme uses passive superconductor within the magnet bore. Another method of correcting for the persistent current field distortions employs a nickel coating on the conductor. Both these latter schemes have already been the subject of theoretical analysis and limited experimental verification. These schemes should be investigated in greater depth with additional experimental effort.

Ramp Rate Dependent Effects

With higher ramp rate operation (i.e. the fixed target operation for the 2X2 TeV machine, >100 A/s), eddy currents can contribute a significant amount of field distortion. There are two kinds of eddy currents considered: *intra* -strand eddy currents, and *inter* strand eddy currents. Harmonics and AC-losses due to intra-strand eddy currents may not be neglected if ramp rates are higher than 100 A/s. The influence of intra-strand eddy currents is proportional to the intra-strand time constant. The time constant of SSC type strands is expected to be less than 10 msec.

Very large AC-losses and excessive field harmonics due to interstrand eddy currents were observed in some of the SSC dipole magnets. Those phenomena seem to be related to interstrand resistances which were not controlled and that varied widely from magnet to magnet. Control of interstrand resistance is definitely required for the future magnets. Although suitable values for interstrand resistances are well not known, a resistance of 100 micro ohm may be a lower limit of the values to operate the magnet at 100 A/s.

As described previously, several SSC magnets displayed an excessively large sensitivity of the quench current on ramp rates at low ramp rate but were generally much less sensitive at ramp rates above 50 A/s. These magnets had low eddy current losses indicating less interstrand eddy current. Although the exact cause of this behavior has not been identified, it is widely believed that the lack of current redistribution between strands due to the high interstrand resistances is a prime suspect. This indicates that insulating each individual strand to prevent interstrand eddy currents may not be acceptable because it might introduce the low ramp rate sensitivity.

Thus we are forced us to better understand the correlation between the various types of ramp sensitivity, interstrand resistance, and the loss mechanisms to develop strand surface processes which control interstrand resistances to a suitable value. Further R&D is necessary to determine the best solution to the problem and the solution most certainly depend on the specifics of the application - ramp rate requirements, cable geometry, and strand composition. We discuss this further in the next section on Conductor R&D.

Conductor R&D

As described before, use of a new kind of material such as NbTiTa or a new technology such as APC maybe required for a high field, e.g. 10 Tesla, magnets. The AC characteristics of these conductors should be measured prior to a magnet development. Especially for APC conductors: there are possibilities to tune the pinning force such that one can reduce the

magnetization at low field. Such possibilities should also be investigated if APC conductors are in consideration.

In order to reduce superconductor magnetization, strands having 2.5 micron filaments will most likely be necessary. These conductors were developed during SSC R&D, and proved to be feasible. Reduction of intra-strand eddy currents will be required if high ramp rate operation is considered. The use of strand cross sections which are developed for AC applications, e.g. CuNi or CuMn matrix, should be considered. (Strands with 2.5 micron filaments use CuMn matrix to avoid proximity couplings.)

We also note that the cable development at the SSC did not resolve issues of conductor RRR value. It had been decided to remove the final anneal of the strand and the cable produced was essentially 100% cold worked with a low (~30-40) RRR value. During the coil curing process - at temperatures on the order of 135 °C and pressures near 10kpsi - the conductor anneals and reaches 'as built' RRR values in the range of 160-200. The contact area between strands in the cross over regions can be increased as the Cu softens. This effect also contribute to a decrease in interstrand resistance. The annealing schedule for the strand needs to be incorporated into the overall R&D program to understand the AC behavior of the cable.

As discussed in the previous section, a technology which can control interstrand resistances to a desirable value has not been established. Changes in the strand composition, e.g. CuMn or CuNi sheaths, Ni coating, etc, should be studied to establish a reliable technology. Strand coatings, such as ebanol, stabrite, or the 'zebra' pattern have been employed in the past. Coatings appear to be a simpler solution since they do not change the details of the strand processing but they add additional steps and handling problems as well as concerns over long term stability. R&D in both areas is clearly needed. Model magnets need to be constructed to test the conductor and finally, full length magnets need to be built and tested to verify the results.

Nb_3Sn

It is important to determine if it is possible to develop processes and wire designs which would enable us to use Nb_3Sn conductors for accelerator magnets. The high critical termperature and critical field values for Nb_3Sn make it an attractive candidate for high field magnets but considerable work is needed to attain the conductor J_c required (J_c is usually quoted in the superconducting fraction of the wire). Nb_3Sn conductor is made by reacting the niobium and tin at temperatures on the order of 600-700°C. The resultant material is very hard and brittle and it is difficult to handle.

There are two methods of processing the material: the 'internal tin' method which yields higher J_c but suffers from filament growth to relatively large effective diameters, on the order of 50μm; and the 'internal bronze' method which yields less superconductor and hence lower strand J_c but controls filament size. And there are presently two approaches to fabricating the material into coils: 'react and wind' and 'wind and react'. The first method suffers from the fact that forming a coil introduces strain in the cable and the J_c of Nb_3Sn decreases rapidly with strain. The second method, 'wind and react', has been used in most of the model magnets developed to date. The wind and react method suffers from difficulties in insulation and strand to strand coupling.

The AC performance of Nb_3Sn conductors is being studied extensively in fusion programs. Although the conductors used in these programs are very different from that of accelerator magnets, some of the technologies may be applied to accelerator magnet conductors.

While long term development of the conductor is needed to bring it to the stage where it might be suitable for large scale magnet production, there are specific niches in which Nb_3Sn may have applicablility now. Magnets with special requirements such as high gradient IR quadrupoles could be fabricated from Nb_3Sn; the increase in AC loss and magnetization effects can be tolerated in a few specialty magnets. The higher cost of the conductor does not play too great a role in the development of a small number of magnets, since the total cost is typically dominated by other costs such as design and tooling.

The use of APC conductor designs for Nb_3Sn could help increase the critical current density. Work is needed to determine suitable strand coatings to control AC loss effects. Additional studies of cable magnetization effects are needed. Reduction in cost due to volume production needs to be demonstrated.

High Temperature Superconductor (HTS)

High temperature superconductors (HTS) potentially offer key performance benefits which could be useful for the next generation of accelerator magnets. HTS current densities (J_e- the current density in the superconducting portion of the material, not the cable) vary slowly with field above 6 Tesla at 4 K which provides a design path for >15T dipole magnets. In contrast, low temperature superconductor (LTS) current densities vary dramatically with field which places design constraints on peak field. If it were possible to develop HTS for accelerator magnets, operation might take place at 10-15K and greatly simplify the cryogenics and synchrotron radiation intercept systems.

Cryostability is the ability to withstand large heat input to the superconductor while maintaining a superconducting state. Conventional LTS accelerator magnets demonstrated significant training performance problems associated with quenches initiated by small mechanical disturbances. HTS magnets are nearly cryostable, which represents a key technological improvement over the LTS magnets. In addition, J_e in HTS materials vary slowly with changes in temperature providing design opportunities in regions where significant heat loads are present and a significant thermal gradients are anticipated. For example, large heat loads are generated in the final focus quadrupole magnets near the beam collision point. A change in temperature of 5K from a nominal 4 K cooling path would be acceptable for removing the heat in a HTS magnet.

The present technology is based on Bi-Sr-Ca-Cu-O (BSCCO). There are many drawbacks to the technology at this time which pose serious questions as to its eventual suitability for high field, high current applications. It has not been manufactured in geometries and quantities suitable for magnet production. While its potential J_c looks promising, the J_c realized is tests in magnet fields is low since only a small fraction of the cross section carries current. Progress is being made with BSCCO tapes, but the material is typically brittle and difficult to form. There is siginifcant investment in HTS development but very little of it is directed at applications with demands similar to accelerator magnets. The time scale associated with HTS is much longer than the other classes of conductors and has a much larger uncertainty in the outcome.

HTS development for the next generation of accelerator magnets will require a focus on several key issues. The primary issue is the need for increased critical current density to develop high field accelerator magnets. In parallel, a development effort must address control of the persistent current effects and dynamic effects (eddy currents in strand and cable) which give rise to field harmonic perturbation and AC losses. An HTS cable development program is needed to address magnet construction requirements, the high Lorentz forces experienced in high field magnets, and cable AC losses.

Test Facilities

Research and development activities relating to the investigations of suitable magnet technologies for a 30 x 30 TeV collider are likely to occur over a very long time (ten or more years). The tests are likely, therefore, to span a broad range of possible magnet and conductor types. The test facility must have sufficient generality to be useful in all of these circumstances. At this point, it appears that superfluid liquid helium cooled magnets operating at 1.8K may hold the greatest promise. Early R&D activities will therefore probably be mostly concerned with this operating environment. The test facilities must allow superfluid operation at 1.8K for dewar testing of conductor and short cold masses. Testing of high field magnets (B> 12.5 T) will require well regulated power supplies with operating currents of approximately 15 KAmps and appropriate power leads. Additionally, an external magnetic field near this intensity must be available for conductor tests. Measurements of magnetic field quality, especially persistent currents at injection, and dynamic multipoles at ramp rates that range from injection to full field in about five minutes, will be major activities.

Developments in high temperature superconductivity may yield advances which facilitate their use in a future accelerator magnet program. It was the consensus of the study group that a small scale, long term effort in this direction be supported as a partnership with interested industrial partners. Specialized test facilities to support this program are unlikely to be available within industry and therefore must also be included in the overall considerations of what should be available at a national lab participating in this effort. Unique considerations relating to the characteristics of HTSC's which influence needed features of a test facility are:

- Quench detection. The current sharing characteristics of BSCCO are such that quenches may not propagate, making their detection difficult. A test facility must be equipped to conduct extensive MIIT's studies of conductor. This may require a very large number of voltage taps per magnet, very low noise isolation amplifiers, and excellent control of the magnet power supply. An energy extraction system well matched to the magnet and test bed characteristics must also be available.

- Operating temperature. HTSC's exhibit quite flat J_c versus applied magnetic field at temperatures in the 5-20K range. It is likely that investigations of the suitability for accelerator magnet use of presently available HTSC's would be conducted within or near this temperature range. The test facility must be able to supply sufficient cryogens to operate in this range for both conductor and model magnet testing. Specially designed power leads may be required for this operating regime.

The testing of full scale cryostated prototypes also requires special consideration. Given the emphasis of this workshop on a rapid cycling accelerator, power supply voltages somewhat higher than the approximately 40 V typical of most supplies presently available may be required (perhaps by bussing two supplies in series). Also, understanding of the effects of possible high heat loads on IR magnets and larger temperature differences across magnets in general (driven by cost considerations) will require testing. Full scale setups that allow accurate measurement of an externally applied heat load on a cold mass will be required. It will be useful to simultaneously measure the axial distribution of magnetic multipoles during these tests. Consideration must be given to the feed can, end can, and warm bore instrumentation used for these studies.

Finally, reliability testing is certain to be a big issue in a long term R&D program. There is very little reliability data existing at present other than that obtained from installed magnets in actual operation. It is important that such tests on new magnet designs be conducted economically and with sufficient sensitivity to be able to detect possible trends in magnet performance. Refrigeration capacity at temperatures to 1.8K sufficient to support this in parallel with shorter duration tests will be required.

Multi-function magnets, which include a substantial gradient in addition to the dipole field, are likely to be very difficult to measure magnetically. In particular, the determination of the quadrupole field center (the location which has the average dipole value over the aperture) could be very tough if uncertainties in x and y at the 50 micron level (the SSC requirement) are needed. Stretched wire techniques may be impossible if there is considerable sagitta in the magnet and rotating coils may not provide sufficient accuracy. Additionally, integral field measurements may not be possible because NMR sensors cannot be used when a significant field gradient is present. The measurement of relative field angle in a two-in-one magnet of this design may also be very difficult. If this design approach is pursued, effort must be allocated to develop the appropriate tools for magnetic field measurement.

It is worthwhile to note that some of the presently available resources of the SSC may be usefully applied to this program. In particular, the three helium refrigerators at the N-15 site could each supply 500-1000 W of refrigeration at 1.8K. (Some modification of the existing facilities is required in order to accomplish this and the capacity is determined by the level of modification undertaken.) The short magnet test facility has 10 ppm power supplies rated at 10 KAmps and 15 KAmps. Also, 240 channels of very low noise voltage tap data loggers are available. The model magnet test dewars have been designed for superfluid operation with lambda plates already installed. Also, the large number of magnetic field measurement devices available there should be useful to a future program.

V. HIGH GRADIENT QUADRUPOLES

The intersection regions of all of the colliders being considered place stringent requirements on the 'low beta' quadrupole magnets. These magnets are located close to the intersection region and typically are surrounded by detector components making support and access difficult. To achieve high luminosity, these quadrupoles typically require gradients of 250T/m and higher. Being intimate to the intersection region, these magnets receive high radiation doses from collision products and large heat loads that must be removed. For example, the first low beta quadrupole in the LHC will have a roughly 70-80 Watt heat load at maximum luminosity; the numbers for the 30X30 TeV collider will be significantly larger. The aperture of the quadrupoles tends to be larger than the arc magnets to accomodate two beams in one beam tube.

The high gradients require designs with additional superconductor and/or new materials such as Nb_3Sn. The high heat load demands a magnet with additional margin as well as special cooling schemes. It will be necessary to study methods of shielding the quadrupole to reduce the energy deposition. Short, small aperture iron quadrupoles in front of the first full length superconducting quad may be one method of 'active' shielding.

The large interaction loading of the IR quadrupoles places stringent requirements on the radiation hardness of materials used in their fabrication. It is not reasonable to expect that the components will last for the lifetime of the collider, hence plans must be made to periodically replace the IR quads.

The alignment of IR quadrupoles is critical to achieve the desired luminosity. Since these magnets are most likely to be cantilevered into the detectors in the IR regions, alignment and replacement are difficult requirements to be met. Early design must go into systems that actively align the quadrupoles while installed and running in the machine. New support methods and reference systems must be investigated. The design of the magnet system must incorporate the alignment requirements at a very high priority.

VI. OTHER GENERAL CONSIDERATIONS

This sections contains brief comments on various aspects of collider development that affect cost and performance. Similar to the 'generic R&D' section above, these comments are largely 'collider-independent': they do not depend heavily on the details of the specific machine being considered.

The HEB.

The HEB (High Energy Booster) is the second highest energy accelerator in the collider chain. It is typically rapid cycling and places stringent demands on the magnet performance. The magnet challenge for the HEB may equal or surpass that of the collider dipoles themselves. The design of the HEB should begin as early as the collider and the full impact of operating regime should be evaluated. Lower injection energies, with a larger dynamic range for the collider, may result in cost savings.

Correctors.

Correction elements become a costly, complicated sub-systems added to the arc magnets in the superconducting machines. Studies at the SSC indicated that trim power supplies or shunt supplies could be used with the arc dipoles to obtain the correction strengths necessary for dipole and sextupole correctors. Intergration of correction into the arc magnets should be carefully considered.

Magnet Interconnects and Ends.

The ends of superconducting magnets tend to be expensive - specially shaped parts are required and special support pieces must be made. The interconnects - the connections between adjacent magnets - also are expensive being comprised of bellows, shields, connectors, etc. Cost savings can be obtained by making longer magnets (consistent with practicalities of fabrication and transportation) and simplifying the interconnect design.

Field Quality.

The field quality requirements drive the aperture size, tooling and fabrication costs, measurement costs, etc. If it is possible to relax these requirements (as in the case of a synchrotron radiation damped collider), the magnet costs might be significantly decreased. Additionally, if field quality requirements are loosened, then restrictions on ΔTcan be relaxed and the cost and complexity of the cryogenic system can be reduced.

New Magnet Designs.

While most of the new magnet designs increased cost by requiring more exotic conductor, it is still possible to consider designs that help reduce costs. For example, if a 'no iron' design were feasible, the mass of the system would be reduced, the cryostat size could shrink, and the

requirements on the support posts would be lessened. Finally, combined function magnets such as a dipole-quadrupole could reduce the number of quadrupoles required in the ring. Such a magnet was proposed for the LHC but was not adopted since it was too late for consideration. Further study of combined function magnets should be undertaken to understand the issues of field quality, measurement, and alignment.

Appendix I

Agenda for the Magnet Workshop held at Fermilab
June 6-7, 1994

DPF Workshop on Superconducting Magnets
for Future Hadron Facilities in the US

Monday June 6

Session I	location: "Black Hole" (Wilson Hall, 2nd floor, NW corner) with video link to the University of Wisconsin and audio link to American Superconductor Corp.	
9:00	Introduction - Objectives of the workshop - Magnet issues in the context of 2+2 and 30+30 TeV colliders	Jim Strait
9:30	Prospects for superconductor development over the next decade: NbTi, Nb3Sn, high Tc, etc.	David Larbalestier
9:45	Hybrid magnet for B>13T using high Tc conductor	Greg Snitchler
10:30	Break	
Session II	location: "Snake Pit" (Wilson Hall, 2nd floor, NE corner)	
10:45	Field quality: how to maximize the good field region over the full dynamic range	Shlomo Caspi Ramesh Gupta
12:00	Passive correction methods - Passive superconductor - Magnetic material	 Bruce Brown Arup Ghosh
12:30	Lunch	
	Alternative magnet designs for high field	
1:30	- The pipe magnet	Peter McIntyre
2:00	- LBL plans for 16 T	Al McInturff
2:30	Ultra-high field magnets: what is the limit?	Paul Mantsch
3:00	Manufacturing issues	J. Carson, E. Willen
3:30	Break	
4:00	Quench Antennas	Toru Ogitsu
5:00	Break	
Session II	Location: Wilson Hall, 12th floor, NW with video links to BNL, KEK, and LBL	
5:30	Vacuum issues (beam tube liners, etc.)	Bill Turner
6:00	Superconducting Wire and Cable	R. Scanlan, A. Ghosh
6:30	AC Losses	M. Wake, V. Yarba

7:30	Discussion: How do we lay the basis for collaboration on future hadron colliers (among US Labs or internationally)?	All
8:00	Adjourn	

Tuesday June 7

Session IV Location: Theory Conference Room (Wilson Hall, 3rd floor, NE corner)

8:30	Accelerator Issues and requirements	David Finley
9:00	Cryogenics/refrigeration issues	Joel Fuerst Peter Mazur
9:30	Closing Discussion - What magnet technology could be applied to a 2+2 TeV collider -What is the optimal field for a 30+30 TeV (or higher) collider - If high intensity pbar sources can be developed, why use twin aperture magnets? - What R&D is needed to answer these questions? - What R&D is needed to develop magnets for the two benchmark machines? - What do we report to the Indiana University accelerator workshop? - etc.	All
11:30	End	

Fermi National Accelerator Laboratory

Cryogenics Discussion Summary Report

T. Peterson

Fermi National Accelerator Laboratory
P.O. Box 500, Batavia, Illinois 60510

Operated by Universities Research Association Inc. under Contract No. DE-AC02-76CHO3000 with the United States Department of Energy

Future Hadron Facilities Workshop, Bloomington, 6 - 10 July 1994

Cryogenics Discussion Summary Report

(Cryogenics participants: Mike McAshan, Tom Peterson, Claus Rode, Jay Theilacker, K.C. Wu)

Introduction.

Reports for background information included a presentation about the Tevatron cryogenic system from Jay Theilacker and a report on the CEBAF 2 Kelvin system from Claus Rode. We reviewed the LHC cryogenic system design using information from CERN which had been provided to members of our working group at previous meetings.

Specific concepts for cooling systems for a 2x2 TeV machine in the Tevatron tunnel and a 30 x 30 TeV machine were discussed in order to highlight possible problems and topics for research and development.

Some Specific Ideas for Systems.

1. 2x2 TeV collider using 8.8 Tesla magnets in the Tevatron tunnel.

A magnet cooling system operating at 1.8 K (keeping magnets about 2 K or slightly less) similar to LHC is envisioned. One could use Fermilab's existing central helium liquefier (CHL) plus two new refrigerators located on opposite sides of the accelerator ring (Figure 1). The existing satellite refrigerators would not be used. The CHL would provide current lead flow plus some liquid helium which could be used by the two 2 K plants as large "satellite" refrigerators.

One should include the option of operating the accelerator at 4.5 K for systems testing and as a fall-back position if problems in maintaining 2 K occur. If both 4.5 K and 2 K are available operating temperatures, probably any temperature in between would also be available for operations. 4.5 K operation might be precluded from a system which relies on heat transport through stagnant, pressurized superfluid. The ability to force-flow the helium must be included, a deviation from the LHC scheme as we understand it. But the system could be similar to that for LHC, with the addition of lumped recooling and forced flow for 4.5 K operation not adding much complexity to the cryostat or cryogenics. A cryostat piping scheme is shown in Figure 2.

Fixed target operatings might be feasible at 4.5 K. The 2 K refrigeration capacity may be about 5 times greater when taken at 4.5 K, and this could be applied to the removal of AC heating due to ramping of the current in fixed target operations.

The beam screen, if needed for vacuum, is passively cooled by conduction to the beam pipe since the 50 W to 75 W over the machine is small enough to take at 2 K.

2. 30x30 TeV collider

A. Using 10 Tesla, 2 K, NbTi magnets
This is a bigger LHC. LHC is the prototype.

B. 12.5 Tesla, 4.5 K Nb_3Sn magnets, 3 W/m per beam synchrotron radiation

The synchrotron radiation is the dominant heat load. The benefit of an 80 K shield is relatively small, so one may choose to eliminate it with a relatively small penalty. Then one may have only 4 pipes plus the cold mass in the cryostat. A cryostat cross-section is shown in Figure 3.

Beam screen cooling is taken at 25 K in order to reduce the refrigeration power required. For 3 mm tubes on the beam screen one can only force flow through one or two magnets in series; one needs many parallel flows. One flow path per magnet means thousands of parallel channels. There are so many that these must operate passively, without valves. There is a large risk of a tube plugging and the over-heating of the beam screen. If one can make room for tubes of about 6 mm ID or larger, many magnets can be in series so that there are only a few parallel flow channels, a less risky arrangement.

The cryogenic system is divided into 8 plants of a size equivalent to 30 KW at 4.2 K each. A schematic of the division of the ring into strings of magnets is shown in Figure 4. This corresponds to 6.5 MW electrical input to each plant. This power is used as follows: 40% beam screen, 23% 4.5 K refrigeration, 22% cryostat thermal shield, 15% 4.5 K liquefaction.

C. 12.5 Tesla, 10 K - 15 K, high Tc. We discussed a machine with 1/2 W/m per beam synchrotron radiation, rapid cycling.

The relatively high magnet temperature and large helium stream delta-T allow lower flow rates or longer runs and a simpler cryostat than a tighter temperture constraint would. We considered a very simple case where part of the magnet flow is simply returned through the cryostat as shield flow. The result is just two pipes plus the cold mass (Figure 5).

The high magnet temperature allows the beam screen cooling to be done passively by conduction to the beam pipe like in the 2x2 TeV, 2 K machine.

Conclusions.

1. 3 W/m of synchrotron radiation dominates the magnet cooling and cryogenic system design. (Compare the SSC design which called for about 0.3 W per dipole!)

2. A significant constraint in previous large cryogenic system designs (Tevatron, HERA, SSC, LHC) is maintaining the magnet temperature in a narrow window (e.g., 250 mK). If the tolerance on magnet temperature is relaxed (e.g., 4.5 K to 5.5 K, or 10 K to 15 K), the cryostats and cryogenic system can become significantly simpler.

3. Each independently powered high-current (about 10 KA) circuit costs about $50,000 per year in current lead cooling operating costs, plus about $150,000 in refrigeration capital costs. It is desirable to minimize the number of independent high-current electrical circuits.

Recommended R&D.

1. Development of large-scale 2 K refrigeration cycles containing cold compressors, with studies of the operation of such systems under transient and off-design conditions (filling, 4.5 K, quench recovery, etc.), should be undertaken. Tests of existing cold compressors could be done in combination with analyses and simulations in order to understand the dynamic behavior of systems with cold compressors.

2. R&D is needed to improve the efficiency of large helium compressors. Approximately half the inefficiency in a large cryogenic plants are in the screw compressors. This should be a cooperative program with industry to improve the helium compressor efficiencies. For very large systems (>20 KW at 4.5 K), dynamic compressors for helium such as those used in large air plants could improve overall efficiency.

3. Large turbo-expanders on active magnetic bearing should be developed, as well as continued development of the large cold compressors on active magnetic bearings.

4. Current lead cooling is a significant operating cost for a cryogenic system, perhaps 20% to 30% of the total perating cost for a large accelerator cryogenic system. R&D including construction and thorough testing of more efficient current leads, whether high Tc or improved conventional ones, cold provide a significant payback.

DiTevatron Cryogenic Layout

(Figure 1)

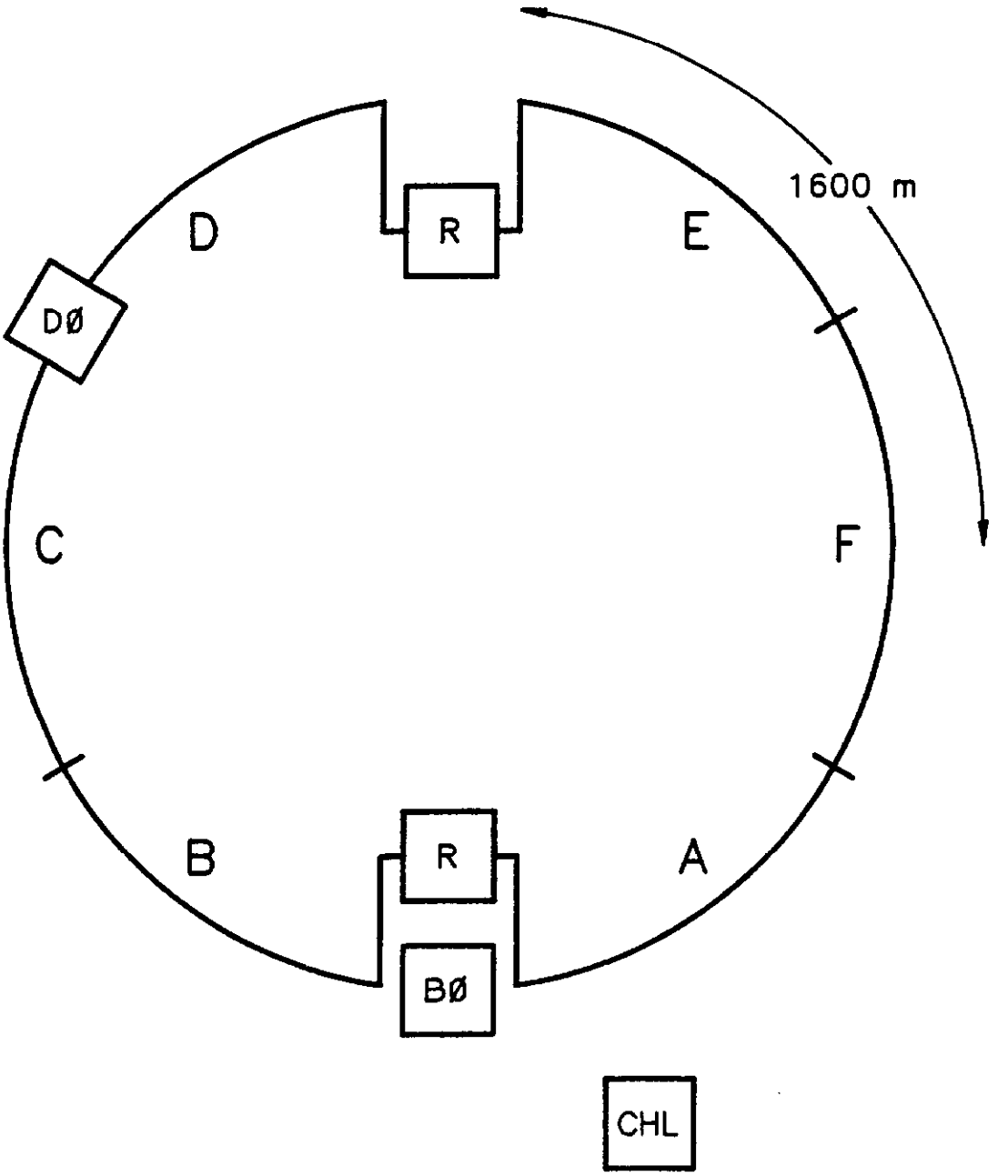

NOTE:
WARMUP UNIT MAY BE A FULL- OR HALF-SECTOR.

DiTevatron Full Cell

(Figure 2)

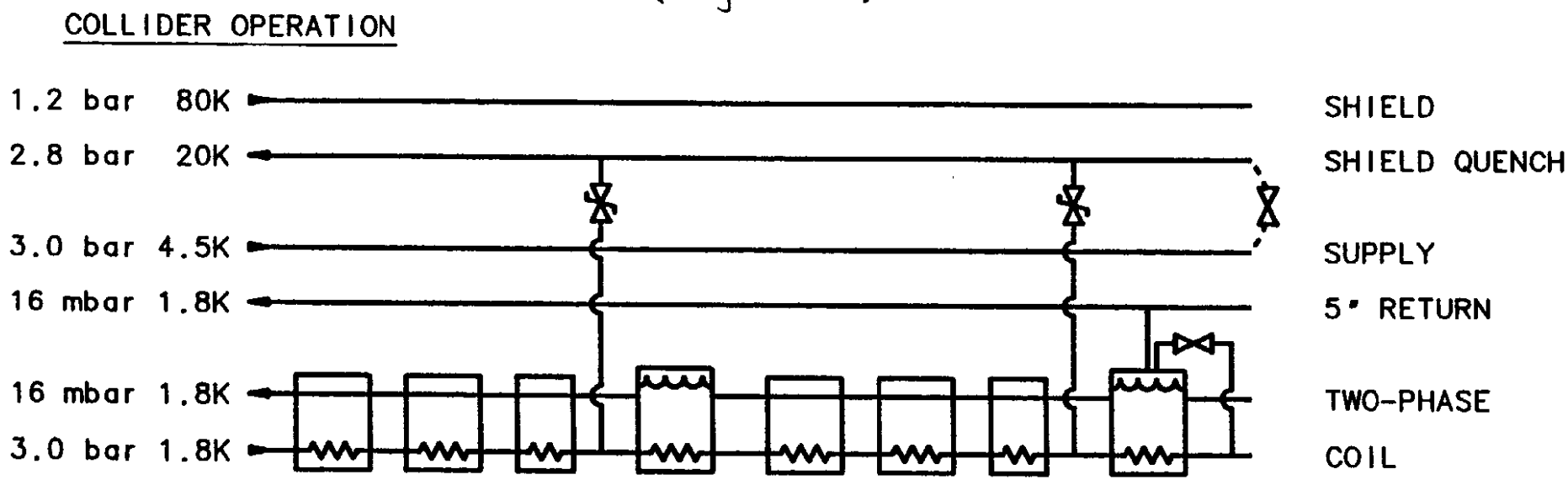

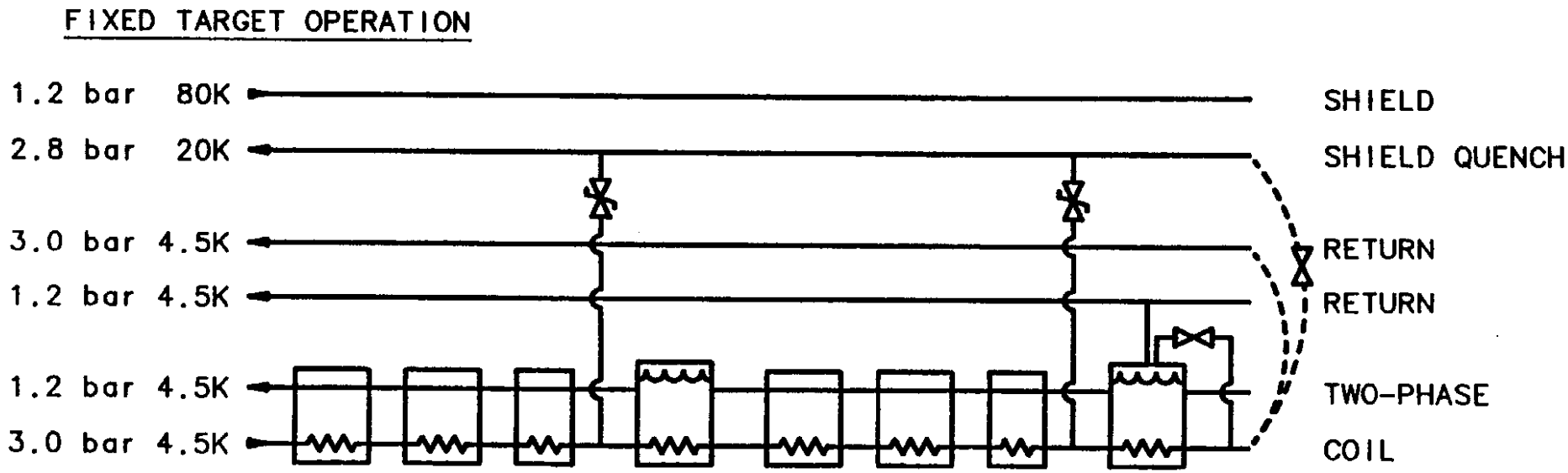

Figure 3

4- Pipe Cryostat Cross-section

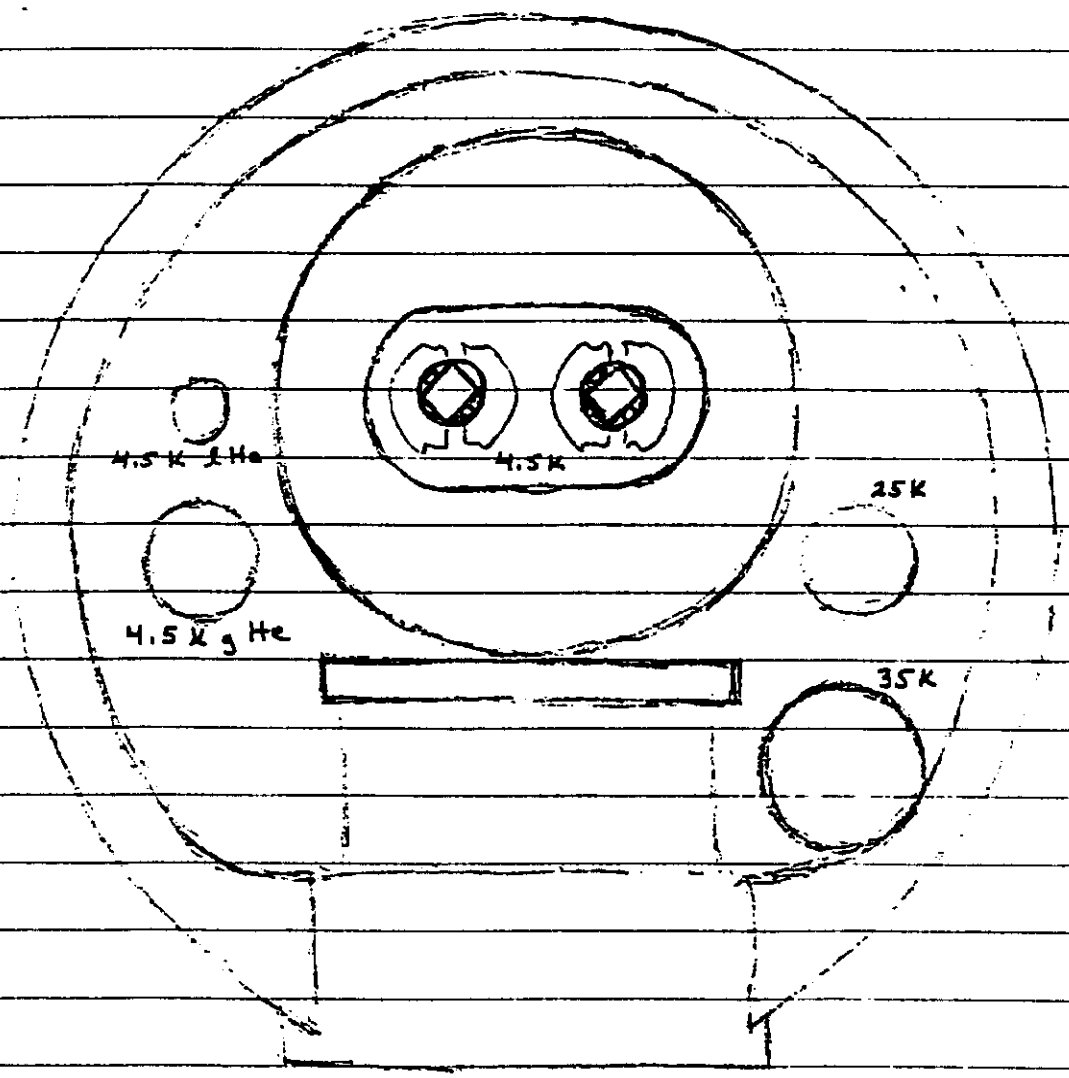

Cryogenic Plants around a 30 X 30 TeV Collider
with 12.5 Tesla Magnets at 4.5 K or 10 K - 15 K

(Figure 4)

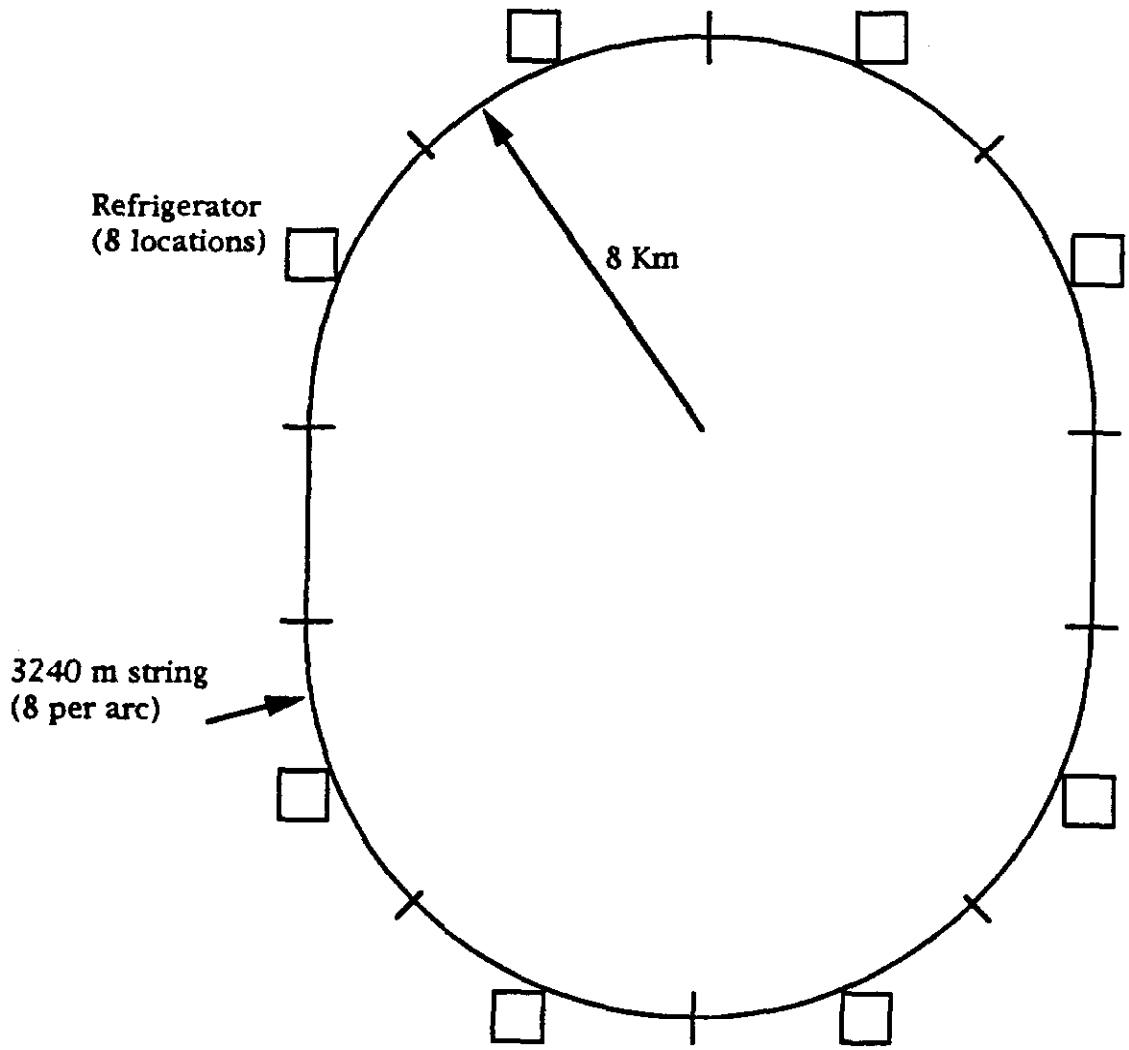

Figure 5

2- Pipe Cryostat Cross-section

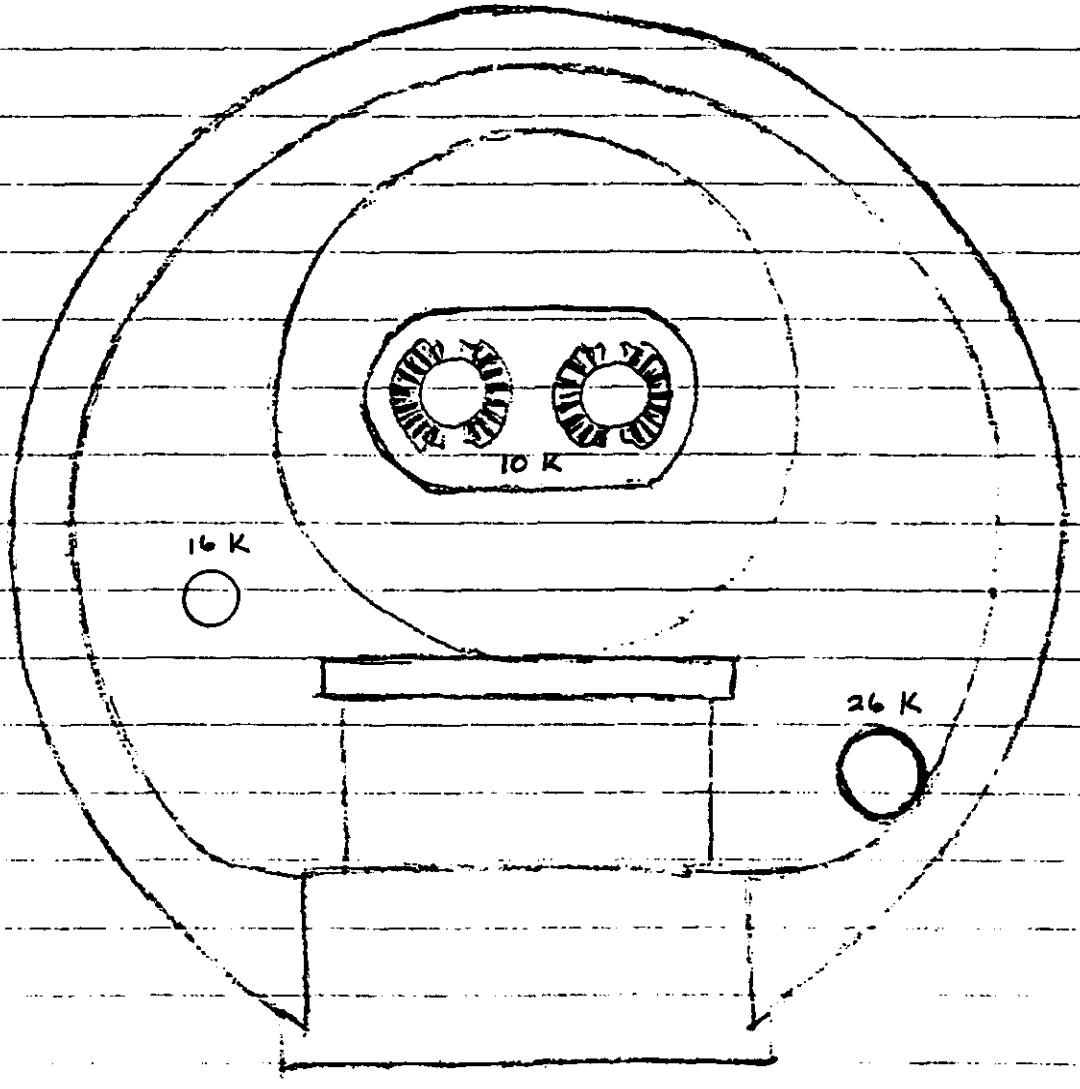

Fermi National Accelerator Laboratory

Vacuum Report for the 6-10 July 1994 DPF Workshop on Future Hadron Facilities

W. Turner

Lawrence Berkeley Laboratory
Berkeley, California

G. Chapman

SSC Laboratory
2550 Beckleymeade Avenue, Dallas, Texas 75237

Operated by Universities Research Association Inc. under Contract No. DE-AC02-76CHO3000 with the United States Department of Energy

Vacuum Report for the 6-10 July 1994 DPF Workshop on Future Hadron Facilities

William Turner and Gerry Chapman

I. Objectives

The overall objectives for the vacuum subgroup were to investigate three questions:

Is a liner necessary for a 2×2 TeV collider?
Is a liner feasible for a 30×30 TeV collider?
Will the SSC and LHC solutions for IR and warm bore vacuum apply to the 30×30 TeV collider?

II. 2×2 TeV collider

The primary synchrotron radiation parameters for the 2×2 TeV p-pbar collider are listed in Table 1. These have been derived from the originally distributed parameter list for the 2×2 TeV collider. The corresponding Tevatron parameters are also given for comparison. In the Tevatron the photon critical energy, flux and radiated power are low enough to have negligible consequences for beam tube vacuum and cryogenic refrigeration. Passing from the Tevatron to the 2×2 TeV collider the critical energy, photon flux and radiated power increase by factors of ten, two hundred and two thousand. With a bending radius ρ = 0.76 km the total radiated power is ~ 70 Watts for the entire ring and is still not a major factor for cryogenic refrigeration. However the critical energy and photon flux have increased to levels that may have beam tube vacuum consequences. Unfortunately there are no experimental measurements of photodesorption below a critical energy 12.4 eV. The experimental trend is that the photodesorption coefficients on electrodeposited Cu are increasing linearly with critical energy from 12.4 eV to 280 eV.[1] If the data are extrapolated to 3.8 eV, the initial photodesorption coefficient for H_2 from electrodeposited Cu is predicted to be 8×10^{-5} H_2 molecules/photon. For a photon flux 8×10^{16} photons/m/sec, the time to form a monolayer of physisorbed H_2 (~ 3×10^{15} H_2/cm^2) on the beam tube wall is of the order of five days. For a beam tube temperature 4.5 K the vapor pressure of H_2 rapidly increases approximately four orders of magnitude as one monolayer is approached, reaching a saturated value 8.6×10^{12} H_2/cm^3. This would be totally unacceptable for beam scattering lifetime and deposition of beam scattered power in the cold mass of the cryostats. At this point the cold mass would need to be warmed to ~ 20 K, the desorbed H_2 pumped out of the beam tube and the cold mass cooled to 4.5 K to resume operation. In practice the photodesorption of physisorbed H_2 and heavier gases would force beam tube warm up somewhat earlier than the H_2 monolayer formation time. Even if the bore tube temperature were reduced to ~ 3 K, so the saturation vapor pressure were not a problem, the increasing photodesorption of physisorbed H_2 and heavier gases would very likely force a beam tube warm up before one monolayer is reached.[2] It is worth pointing out that because of magnet quenching the

power deposition problem has a local aspect as well as the global one determined by refrigeration capacity. Because of this the least conditioned part of the beam tube determines the interruption sequence of the entire accelerator. Approaching a monolayer of H_2 anywhere in the machine would lead to a runaway increase in vacuum pressure and/or a magnet quench and require warming up and pumping out the beam tube at that location. At a magnitude 8×10^{-5} H_2 molecules/photon it is conceivable that the beam tube could take a very long time to clean up. If the warm up interval stayed at a few days for tens of monolayers of desorption this would be a serious detriment to accelerator operation and one would want to consider inserting a beam tube liner to pump the photodesorbed gases out of the view of the synchrotron radiation. Since the synchrotron power is low enough to be absorbed directly at 4.5 K, the liner could be at the same temperature as the magnet bore tube and relatively simple. The high pressure GHe cooling loops on higher temperature versions of a liner or beam screen could be eliminated. At 4.5 K cryosorber is needed outside the liner to increase the pumping capacity for H_2 over that of a bare metal surface. If the temperature of the cryostat were lowered to 3 K the H_2 saturation density falls to $3\times10^8/cm^3$ and the need for cryosorber is eliminated.

It is entirely possible that the vacuum consequences of synchrotron radiation in the 2×2 TeV collider are nil. The work function of Cu is 4.4 eV and photodesorption coefficients may decrease precipitously as the critical energy approaches the work function, particularly if photodesorption proceeds via production of a secondary electron leaving the surface. Only 6.3% of the photons have energy greater than the critical energy. On the other hand significant photodesorption may be caused by photoelectrons that do not leave the surface so there may not be any gross change of behavior as the critical energy decreases below the work function. It will take experimental data to resolve this issue.

A second issue examined for the 2×2 TeV collider was whether the beam tube surface facing the p and pbar beams needs to have high conductivity to insure long enough growth time for stabilization of the resistive wall instability at injection. The growth time for the resistive wall instability is inversely proportional to the beam current so there is a factor of eighty decrease compared to the Tevatron due to this factor. The growth time also increases as the third power of the beam tube diameter and linearly with the injection energy. For an injection energy 150 GeV, characteristic of the FNAL Main Ring, and beam tube ID = 40 mm the growth time was calculated to be 14.4 turns for a 1 mm thick stainless steel beam tube and 182 turns for a beam tube plated with 5 μm of Cu with RRR = 100. If a liner were needed and the beam tube ID decreased to 30 mm these growth times decrease to 6.1 and 77 turns. The stainless steel cases are marginal while the Cu plated cases are in the range of what was regarded as an acceptable growth time for the SSC. Raising the injection energy to 1 TeV would bring the stainless steel case into an acceptable range for 40 mm ID.

During the meeting a second parameter list was circulated for 132 nsec bunch spacing in the 2×2 TeV collider instead of the original 19 nsec. The beam current and radiated photon intensity decreased to ~ 0.6 of the original values; the resistive wall growth time increased by ~ 1/0.6 = 1.7. These changes do not significantly alter the discussion given above.

III. 30×30 TeV collider

A. Liner specifications

There is no doubt that a perforated, warm (4 to 50 K) liner or beam screen is needed for removing the synchrotron radiation heat load and pumping the photodesorbed gas for the 30×30 TeV collider. Attention was therefore turned to examining the technical feasibility of a liner for certain chosen design parameters. Synchrotron radiation characteristics are listed in Table 2 for the 30×30 TeV collider and for the LHC for comparison. The design luminosity for both of these machines is ~ $10^{34}/cm^2$-sec. Looking at Table 2, two concerns for 30×30 TeV compared to LHC are the factor of ~ 25 increase in photon critical energy and consequent increase in the magnitude of photodesorption coefficients and the factor of ~ 15 increase in radiated power. In order to assess the situation with the limited time available, a liner design was specified and the consequences worked out. The magnet bore tube was assumed to have ID = 40 mm and temperature 4.5 K. The liner was specified to be an LHC type, square cross section, inside dimensions 27×27 mm with 4 mm inside radius rounded corners. This geometry allows horizontal and vertical mechanical apertures of 35 mm and space for the external cooling tubes on the outside flat faces. The liner material was assumed to be 1 mm thick stainless steel plated on the inside with 100 μm of Cu, RRR = 100. The 1 mm stainless steel is strong enough to withstand quench forces up to ~ 300 T^2/sec without the liner contacting the bore tube. Studies at SSC and LHC indicate that the yield point of Cu in the corners is exceeded during a magnet quench. There is some worry this may cause de-lamination. However no visible changes were noted in a dipole magnet bore tube at SSC that had undergone more than 80 quenches so this does not seem to be an important issue. Liner cooling is by high pressure flow of GHe through two parallel stainless steel tubes ID = 3 mm, OD = 4.5 mm brazed to the outside flat faces of the liner. Liner temperature was assumed to be in the range 4 to 50 K; liner vacuum performance does not depend critically on the temperature. The liner is perforated with 2×6 mm rounded end slots, 75 per meter, geometric hole area fraction = 1%. The maximum allowable local gas scattered beam power without causing a runaway increase in vacuum pressure and/or a magnet quench was taken to be 1 W/m; the maximum average gas scattered beam power that could be accommodated by the cold mass refrigeration was assumed to be 0.1 W/m per beam tube, or 5 kW per beam tube for the entire cold bore circumference. With these parameters specified the issues examined were vacuum limited luminosity lifetime, beam power scattered by beam gas interactions, transverse and longitudinal liner impedances, resistive wall instability growth time, heating by beam image currents and liner cooling by flow of GHe.

B. Vacuum performance

In order to assess the vacuum performance of a liner it is necessary to know the photodesorption coefficients. There is no experimental data between 490 eV and 3.75 keV however the magnitudes of desorption coefficients at 280 eV, 490 eV and 3.95 keV are roughly the same suggesting relatively flat energy dependence over this range. Consequently we assume the photodesorption coefficients that have been measured on room temperature electrodeposited Cu at 490 eV.[3] This data may be represented by the following H_2 equivalent photodesorption coefficient that includes desorption of CH_4, CO

and CO_2 as well as H_2: $\eta = \eta_0 / (\Gamma / \Gamma_0)^a$ for $\Gamma \geq 10^{19}$ photons/m with $\eta_0 = 1$, $\Gamma_0 = 10^{19}$ photons/m and $a = 2/3$. We assume an effective temperature of photodesorbed molecules of 60 eV, consistent with recently reported data for photodesorbed H_2 from a 4.2 K beam tube.[4] Because of the larger scattering cross sections and reduced conductances of CO and CO_2 relative to H_2, CO and CO_2 amount to 93% of this H_2 equivalent desorption coefficient. If the 30×30 TeV collider were operated at full beam current with an unconditioned section of liner having this desorption coefficient, the H_2 equivalent density would increase to $> 4\times10^{11}/cm^3$. The gas scattered beam power would be > 26 W/m which would very quickly lead to a quench of the superconducting dipole magnets. It is therefore necessary to condition the liner at reduced beam current until the gas scattered beam power falls below acceptable limits at full operating current. These limits were taken to be 0.1 W/m for cleanup of the entire accelerator and 1.0 W/m for cleanup of components that have been replaced in an otherwise conditioned accelerator. At 0.1 W/m gas scattered beam power over the entire cold bore circumference of the collider the total operating time before reaching 192 mA per beam was found to be the order of tens of operating days for the liner specified in the previous paragraph. Once full current was reached the luminosity lifetime had increased to ~ 30 hrs. and continued to improve with operation time, reaching ~ 120 hrs. at 100 days. The time to cleanup the liner to the point where full current operation can proceed depends approximately on the inverse 3/2 power of the assumed limit for gas scattered beam power. Consequently the time to clean up a component at 1.0 W/m was found to be in the range of a day. If the temperature of the superconducting magnet bore tube is less than or equal to 3 K then the bare metal surface has sufficient H_2 pumping speed and capacity to pump all of the photodesorbed H_2. Above 3 K cryosorber would have to be added to the surface of the bore tube with a capacity of the order of ten or more monolayers of physisorbed H_2. Anodized metal surfaces, porous metal and charcoal are among the possibilities. Recently anodized aluminum has been shown to have a very high capacity for absorbing H_2 at 4.2 K.[5] This is an attractive option for a liner system cryosorber and could have other useful applications, such as pumping small helium leaks in the insulation vacuum of the magnet cryostats. Development of a liner for the beam tube vacuum in a superconducting accelerator is a reasonably complex task and of course has not yet been done since the SSC and LHC are the first accelerators to encounter such a need. The best place to focus efforts on research and development on cold bore tube vacuum and liner development is the LHC at CERN.

C. Liner impedance

With 75 2×6 mm rounded end slots per meter, an equivalent liner ID = 30 mm and an assumed liner length equal to 80% of the total collider circumference, the transverse and longitudinal impedances below the beam tube cutoff frequency were estimated to be Z_T = 0.8 MOhms/m and Z_L/n = 0.01 Ohms. The single bunch instability thresholds for the SSC were Z_T ~ 170 MOhms/m and Z_L/n ~ 4 Ohms so there seems to be a large safety margin. Near and above the cutoff frequency there is some danger of narrow band resonances leading to multi-bunch instabilities. Recent work shows that randomizing the spacing and length of holes in the liner to break up

periodicity is an effective means of reducing these high frequency impedances to manageable levels.[6]

D. Resistive wall instability growth time

The resistive wall instability growth time was calculated to be 112 turns assuming an effective liner ID = 30 mm, fractional tune equal to 0.1, a 100 μm thick Cu layer with RRR = 100 and injection energy 1 TeV. Other relevant parameters were taken from the parameter list for the 30×30 TeV collider. The magnetoresistivity correction (Kohler's rule) for Cu was included in the calculation. A growth time of the order of 100 turns was generally regarded as adequately long for feedback stabilization at the SSC. Since the resistive wall growth time scales with the third power of the beam tube ID, decreasing the ID from 30 to 20 mm would reduce the growth time to 33 turns. At this point consideration should be given to design requirements of the transverse feedback damping system before proceeding. Of course the thickness of Cu could be increased to lengthen the growth time. However the quench forces are then increased proportionally and the thickness of stainless steel would have to be increased, which further decreases the available aperture.

E. Wall heating by the beam image current

Resistive wall heating by the beam image current occurs at high enough frequencies ($f \sim c/2\pi\sigma_z \sim 1$ GHz) that increased resistivity in Cu due to the anomalous skin effect is important. Beam image current heating was estimated using a surface resistivity $R_s = 2\times10^{-3}$ Ohms measured at 1 GHz and 4.2 K on electrodeposited Cu.[7] The result obtained for an RMS bunch length 4.5 cm was 1.0 kW per beam, a negligible refrigeration impact compared to the synchrotron radiation heat load of ~ 150 kW per beam.

F. Liner cooling

A critical concern for the implementation of a liner is the removal of 3 W/m of synchrotron radiation per beam in the limited space allowed between the liner and magnet bore tube. Two 3 mm ID tubes brazed to the outside of the liner and at the middle of two of the four flat faces were specified for removal of heat by the flow of high pressure GHe. Up to four tubes of this size are possible. The cryogenics subgroup considered a particular solution with two headers in the cryostat specified for input and output of GHe at 20 bar, 15 K and 18 bar, 25 K respectively. The self consistent length of 3 mm tubing and flow rate of GHe that satisfy these boundary conditions were calculated to be 42 m and 2.5 gm/sec (1.25 gm/sec per cooling tube) respectively. An individual GHe circuit could then go down one beam tube for ~ 20 meter (one 20 m dipole, 2 ten meter dipoles etc.) and return along the second beam tube in a two in one cryostat. The total length of dipoles in the 30×30 TeV collider is ~ 50 km so the total flow of GHe between the two headers would be ~ 6.3 kg. Quadrupole and spool piece liners could be cooled by the same scheme or from the ends. The actual choices of inlet and outlet temperatures and pressures would depend on an overall optimization of the magnet, cryogenic and vacuum systems however the example given shows at least that a reasonable solution exists. Similar results were obtained at LLNL by J. Zbasnik, who had worked on this type of problem for the SSC liner, and R. Wong but they could not attend the workshop.

G. IR vacuum

The IR region of a proton collider presents challenging vacuum design problems due to limited access and the need to minimize detector background due to beam gas interactions and interactions of IR collision products with the beam pipe, supports and vacuum pump materials. To achieve the required IR beam tube vacuum it is necessary to locate vacuum pumps inside the detectors; the innermost one within a few meters of the IP. Very high reliability and compatibility with the magnetic field of the detector are required. Supporting the beam tube inside tens of meters long movable sections of the detector, remote disassembly and handling of radioactive components are also required. These problems are essentially identical with those that were being dealt with at the SSC[8] and are now being dealt with at the LHC. The 30×30 TeV collider parameters were examined to see if there are important differences that fall outside the scope of work at SSC and LHC. Bunched beam induced multipactoring, ion pressure bump instability and beam gas scattering were discussed at the workshop; the overall conclusion was that there did not seem to be insurmountable vacuum IR problems in the 30×30 TeV collider beyond the SSC and LHC experience. Due to the three times higher beam current in 30×30 TeV collider compared to SSC it will probably be desirable to reduce the IR pressure requirement from 10^{-8} Torr to ~ 3×10^{-9} Torr. Compared to the SSC GEM detector, for example, this could be accommodated by increasing the diameter of the beam pipe inside the central tracker from 80 mm to 120 mm. The overall conclusion was that the work being done at the LHC will be the best source of future information on research and development in IR vacuum relevant to the 30×30 TeV collider.

IV. Summary, recommendations for future work

For the 2×2 TeV collider:

1. Photodesorption data at ~ 3.8 eV critical energy are needed to decide whether a liner is needed for the cold bore tube vacuum. Extrapolation of existing data above 12.4 eV down to 3.8 eV critical energy predicts an initial H_2 monolayer formation time of the order of one week at design intensity. The cleanup rate is unknown.

2. There is a possible need for a high conductivity coating on the beam tube wall to obtain long enough growth time for the resistive wall instability. The issue it tied to the injection energy. If the injection energy is 150 GeV then the resistive wall growth rate for stainless steel was calculated to be 14 turns, which is short compared to present experience. A 5 μm coating of Cu was calculated to increase the growth time to 182 turns, which is within the range of present experience. If the injection energy is increased to 900 GeV then the growth rate for stainless steel increased to 86 turns, which seems acceptable without a high conductivity coating.

3. If a liner is needed it will be for vacuum only and it can be at the same temperature as the magnet cryostats. This greatly simplifies the

liner design since GHe cooling tubes are not needed. If the cryostat temperature is lowered to ~ 3 K then the bare metal bore tube outside the liner serves as an adequate cryopump. This eliminates the need for a porous cryosorber for H_2 and the liner design is further simplified.

4. If a liner is needed, an extruded aluminum composite magnet bore tube/liner and aluminum bore tube plus aluminum sheet metal liner options should be considered as possible cost optimized solutions in addition to stainless steel (copper clad if necessary).

For the 30×30 TeV collider:

1. Eventually to make accurate predictions of cold bore tube vacuum it will be necessary to measure photodesorption coefficients at 1.2 keV critical energy up to an integrated photon flux ~ 10^{23} to 10^{24} photons/m on the particular material that is chosen for the liner.

2. Estimates of liner performance were made using existing room temperature photodesorption data at 490 eV, 1% geometric open hole area for pumping, square cross section with 36 mm vertical and horizontal mechanical aperture and fabricated from stainless steel with 100 μm RRR = 100 copper cladding. This type of liner is similar to that being considered for the LHC. The general conclusion was that such a liner is feasible. The operating time for conditioning the entire liner before reaching full current was calculated to be tens of days and for conditioning a short section the order of a day. The upper bounds on gas scattered beam power deposition in the cold mass was assumed to be 0.1 W/m for conditioning the entire ring and 1.0 W/m for conditioning a short section. The growth rate for the resistive wall instability, impedance margins below beam tube cutoff and beam image current heating were all examined and found to be satisfactory. Quench forces up to BdB/dt ~ 300 T^2/sec can be sustained without flexing the liner into the bore tube.

3. Short slots are preferred for liner pumping holes to reduce the impedance for a given pumping speed. Rounded end 2×6 mm slots, 75 per meter were assumed in the calculations. The slot lengths and axial spacings should be randomized to reduce the impedance of narrow band resonances near and above the beam tube cutoff frequency.

4. Reasonable solutions exist for removing the 3 W/m of synchrotron radiation heat load per beam tube impinging on the liner. A particular example assumed two parallel 3 mm ID cooling tubes attached to the outside of the liner with GHe inlet manifold at 20 bar, 15 K and outlet manifold at 18 bar, 25 K. For these boundary conditions the length of tubing between connections to the inlet and outlet manifolds was calculated to be ~ 40 m and the throughput of GHe 2.5 gm/sec per beam tube. With two beam tubes and approximately 50 km of cold bore tube the total GHe throughput would be 6.25 kgm/sec. Liner performance is not too sensitive to operating temperature in the range 5 to 50 K.

5. A cost optimized design for a liner should complete a trade study of aluminum versus copper clad stainless steel options.

6. The IR beam tube vacuum for the 30×30 TeV collider does not appear to present any problems not already encountered at the SSC and LHC.

7. The beam tube vacuum problems and solutions for the 30×30 TeV collider are largely similar to the LHC. The LHC will be a good focus and source of information on beam tube research and development for the 30×30 TeV collider.

8. At the workshop the 30×30 TeV synthesizing group was considering high T_c magnet (~ 15 K) and rapid cycling, low stored beam energy options. The high T_c option would simplify the liner if the synchrotron radiation is absorbed at T_c since the GHe cooling tubes could be eliminated. The H_2 adsorption capacity and pumping speed of cyrosorbers at T_c would need to be investigated. However a temperature above somewhere in the range Tc = 15 to 20 K would greatly complicate the beam tube vacuum because cryosorption could no longer be counted on for pumping photodesorbed hydrogen. The rapid cycling low stored beam energy option reduces the synchrotron radiation intensity from 3 W/m to ~ 0.5 W/m. This simplifies the liner since the pumping and heat removal requirements are reduced.

References

[1] J. Gomez-Goni, O. Grobner and A. Mathewson, "Comparison of Photodesorption Yields Using Synchrotron Radiation of Low Critical Energies for Stainless Steel, Copper and Electrodeposited Copper Surfaces", to be published in J. Vac. Sci. Technol. A 12(5), Jul/Aug 1994.

[2] V. Anashin, O. Malyshev, V. Osipov, I. Maslennikov and W. Turner, "Investigation of Synchrotron Radiation Induced Photodesorption in Cryosorbing Quasi-closed Geometry", SSCL - Preprint - 517 (1994). to be published in J. Vac. Sci. Technol. A 12(5), Sep/Oct 1994.

[3] I. Maslennikov, W. Turner, V. Anashin, O. Malyshev, V. Osipov, V. Nazmov, V. Pindyurin, A. Salimov, C. Foerster and C. Lanni, "Photodesorption Experiments on SSC Collider Beam Tube Configurations", Proc. of the 1993 Particle Accelerator Conference, Washington D. C., pg. 3876.

[4] N. Alinovsky, V. Anashin, P. Beschansy, G. Derevyankin, V. Dudnikov, A. Evstigneev, O. Malyshev, V. Osipov, I. Maslennikov and W. Turner, "A Hydrogen Ion Beam Method of Molecular Density Measurement Inside a 4.2 K Beam Tube", SSCL - Preprint - 563 (1994), to appear in Proc. of the 1994 European Particle Accelerator Conference, London (June 1994).

[5] M. G. Rao, P. Kneisel and J. Susta, "Cryosorption Pumping of H_2 and He with Metals and Metal Oxides at 4.3 K", CEBAF-TN-94-036 (1994).

[6] S. Kurennoy, "Limitations on Pumping Holes in the Thermal Screen of Superconducting Colliders from Beam Stability Requirements", to appear in Proc. of the 1994 European Particle Accelerator Conference, London (June 1994).

[7] E. Gray, "SSC Beam Tube Resistance Measurements", LANL Tech. Note No.: AT-1:93-344(1993).

[8] G. Chapman and J. Zhou, "The Proposed Warm Bore Beam Pipe Assemblies and Associated Vacuum Systems for the World's Two Largest Particle Detectors", to be published in J. Vac. Sci. Technol. A 12(5), Jul/Aug 1994.

Tables

Table 1: Comparison of Tevatron and 2×2 TeV Collider Synchrotron Radiation Parameters

Parameter	Tevatron	2×2 TeV
E(TeV)	0.9	2.0
I_{p+pbar}(mA)	5	434
ρ(km)	.76	.76
E_{crit}(eV)	0.34	3.8
$d\Gamma/dt$(phot/m/sec)	4.1×10^{14}	8×10^{16}
$P/(2\pi\rho)$(mW/m)	.007	15.0

Table 2: Comparison of LHC and 30×30 TeV Collider Synchrotron Radiation Parameters

Parameter	LHC	30×30 TeV
E(TeV)	7	30
I(mA)*	530	192
ρ(km)	2.7	8.0
E_{crit}(eV)	45.6	1200
$d\Gamma/dt$(phot/m/sec)*	9.6×10^{16}	5×10^{16}
$P/(2\pi\rho)$(W/m)*	.22	3.0

* per beam

Fermi National Accelerator Laboratory

Antiproton Source Production

J. Marriner

Fermi National Accelerator Laboratory
P.O. Box 500, Batavia, Illinois 60510

Operated by Universities Research Association Inc. under Contract No. DE-AC02-76CHO3000 with the United States Department of Energy

Antiproton Source Production

for a 2-TeV Proton-Antiproton Collider and

at a Peak Luminosity of 2×10^{33} cm^{-2}-sec^{-1}

D. Amidei, V. Bharadwaj, F. Bieniosek, M. Church,
W. Foster, J. Griffin, R. Johnson, S. Werkema

ABSTRACT

We have considered the antiproton production rate requirements of a 2-TeV Proton-Antiproton Collider operating at a peak luminosity of 2×10^{33} cm^{-2}-sec^{-1}. We find that the collider will require a antiproton stacking rate of approximately 90×10^{10} antiprotons per hour assuming that the unused antiprotons are recovered from the collider. This stacking rate can be achieved by building 2 or more new storage rings using extensions of existing technology. Major technological considerations include energy deposition in the antiproton target, antiproton acceptance, and stochastic cooling.

GENERAL CONSIDERATIONS

We have considered antiproton production within the constraints that we expect will exist at Fermilab after the construction of the Main Injector. The Main Injector will be capable of accelerating 6 batches of 84 bunches. Each batch contains 5×10^{12} protons. The current plan for antiproton production with the main injector is to use a single batch to produce an antiproton accumulation rate of 15×10^{10} antiprotons per hour.

The antiproton production rate must be increased by a factor of 6 to achieve the luminosity of 2×10^{33} cm^{-2}-sec^{-1}. This increase may be obtained simply by increasing the number of batches targeted or by increasing the transverse acceptance. We have considered a number of different schemes for increasing the antiproton production rate. Once the antiprotons are produced, they must be cooled to sufficiently high densities to satisfy the collider requirements. The major considerations in obtaining the increased stacking rate involve targeting and stochastic cooling.

REQUIRED ANTIPROTON PRODUCTION

We have considered the number of antiprotons that would be required to support a collider with an integrated luminosity of 400 pb^{-1} per week. We estimate that a stacking rate of 90×10^{10} hr^{-1} is required. According to this estimate, about 2/3 of the antiprotons are lost in proton-antiproton interactions in the collider. Appendix I shows some of the parameters of this estimate.

ANTIPROTON PRODUCTION AND TARGET CONSIDERATIONS

The antiproton production rate can be increased by either increasing the number of protons collected or by increasing the phase space area of the collected antiprotons. The existing antiproton source produces 16×10^{-6} antiprotons per targeted proton. The production ratio can be increased by about 25% by increasing the lithium lens gradient from 800 T/m to 1000 T/m, increased by roughly a factor of 2 by increasing the transverse emittance collected from 20π mm-mrad to 40π mm-mrad, and increased proportionately to the momentum bite (nominally 4% for the existing antiproton source). The increased gradient in the lithium lens requires an improvement in lens technology; the other factors are obtained by building a collection ring with a larger acceptance.

The proton beam currently deposits 700 J/g in the antiproton target. This energy density is nearly the maximum energy density allowed that can be sustained by any known solid target. Target damage may be avoided by using a system of kicker magnets to sweep the proton beam across the face of the target to maintain a maximum energy deposition of 700 J/g. It is envisioned that a sweeping system will already be in place in the Main Injector era. Increasing the number of protons targeted will require higher fields in magnets that are already technically challenging.

STOCHASTIC COOLING

The antiproton flux that can be accumulated is proportional to the bandwidth of the cooling systems. One major limitation is the maximum bandwidth that can be achieved, particularly in the stack tail cooling system. The current antiproton source uses a 1-2 GHz stack tail cooling system and was designed for a stacking rate of 10×10^{10} antiprotons per hour. To date it has achieved a stacking

rate of 5×10^{10} antiprotons per hour. The stacking rate is currently limited by antiproton production—not by cooling—so the system capability is probably somewhat higher. We will assume that a practical 1-2 GHz cooling system can achieve a stacking rate of 7.5×10^{10} antiprotons per hour.

Stochastic cooling systems have been built using 4-8 GHz bandwidths We believe that an extension of the existing techniques to the 8-16 GHz region should be possible. Higher bandwidths probably require new techniques. Thus, we imagine that it would be possible to stack 8 times the assumed present capability of 7.5×10^{10} per hour by simply scaling the existing stack tail cooling design in the accumulator. We further assert that it would be possible to achieve the additional 50% in stacking rate that is required by performing some of the cooling in the additional rings that are required to perform the pre-cooling, post-cooling, and beam manipulation.

Another consideration is the power requirements of the pre-cooling system. The power requirements for high gain precooling systems may become prohibitive when fast cooling of high emittance beams is required. In order to keep the power demands in a reasonable range, we have had to make the somewhat optimistic assumption that an effective 50 Ω pickup can be built in the 8-16 GHz frequency range to work with a 30-40π mm-mrad emittance beam.

HIGH ENERGY ACCUMULATOR

The High Energy Accumulator is a storage ring that is rather similar to the existing accumulator except that the only cooling systems are core cooling systems. The ring requires high vacuum, good magnetic field quality, and the absence of beam heating mechanisms (except for intrabeam scattering). The High Energy Accumulator is to be built at some energy which is higher than the Main Injector transition energy to facilitate transfer and of antiprotons to and from the Tevatron. We have assumed that this machine would be installed in the Main Injector tunnel. However, there may be significant advantages to a smaller circumference storage ring including smaller intrabeam scattering rates, cost of the vacuum system, and signal transmission for the stochastic cooling systems.

SCENARIOS CONSIDERED

We considered four example scenarios to achieve the required antiproton production rates. All scenarios begin with 120 GeV protons in the Main Injector. All scenarios present the same beam parameters to the current accumulator where momentum stacking is accomplished. Finally, all scenarios include a high energy accumulator where a beam of 1×10^{13} particles can be stored.

Scenario I: The Main Injector is loaded with 6 booster batches. The Main Injector performs a "batch rotation" on the 6 batches to produce a super-batch that is about 400-800 nsec long. This batch is then targeted immediately.

Comments on Scenario I: We found that this scenario was unattractive. At best, the batch rotation would take 0.5 sec to perform—extending the production cycle and substantially increasing the Main Injector power dissipation. Furthermore, the energy density in the target is a serious problem in this scenario. The required sweeping system was deemed to be impractical. However, a scheme that coalesced 3 batches and increased the acceptance in momentum and in transverse phase space could be attractive. The targeting problem could, in this case, be solved by defocusing the beam on the target and accepting a lower yield (but compensating with a higher acceptance).

Scenario II: The Main Injector is loaded with 6 booster batches. Each batch is rotated to achieve the narrow time spread in the normal way. Once rotated the bunches are captured in a 956 MHz rf system. Each booster batch is targeted at approximately 10 msec intervals. The batch is rotated in the existing Debuncher (in the normal way) to yield a narrow momentum spread. The beam is then transferred to a new Pre-cooling Ring, where it is stochastically cooled an transferred to the existing Accumulator Ring.

Comments on Scenario II: The targeting issues are also fairly serious in this scenario. The most straight-forward solution would require 6 parallel target stations. One might guess that the target station alone in this scenario could cost in the range of 20M$ to 50M$.

Scenario III: The Main Injector is loaded with 6 batches of protons. After a normal bunch rotation all batches are extracted, targeted, and

collected in a large Debuncher/Compressor ring placed in the Main Injector tunnel. The beam is then transferred to the existing Debuncher where it is cooled stochastically and transferred to the existing Accumulator Ring.

Comments on Scenario III: The high γ_T in the Debuncher/Compressor requires very high rf voltages to perform the bunch rotation at 8.9 GeV collection energy. The possibility of collecting the beam at 16 GeV, performing the bunch rotation at high energy, and decelerating in the Main Injector is a possible solution. However, the large circumference of the ring precludes stochastic cooling at practical power levels.

Scenario IV: A single booster batch is accelerated in the Main Injector and targeted. The beam is debunched using a linear accelerator and injected into a Precooling Ring. The increase in flux is obtained by collecting a larger transverse emittance and a larger momentum spread. A parameter list for this scenario is given in Appendix II. The parameters are more of a wish list than a design. Many parameters are the result of calculations, but many are the result of guessing what might be possible.

Comments on Scenario IV: This scenario is very friendly for the targeting. The scenario also has the potential for increased flux—beyond the 90×10^{10} per hour requirement—by targeting more booster batches. However, the rf requirements are substantial.

R&D ISSUES TO BE ADDRESSED

Stochastic cooling: Stochastic cooling at 8-16 GHz needs to be demonstrated. Of particular concern is the need to cool physically large beams with short wave-lengths. These systems not only require high frequencies, but high powers. Previously used techniques are probably inadequate for higher power levels. Some consideration should be given to techniques that could potentially cancel the effects of the "bad mixing" between pickup and kicker. Finally, one should consider more exotic techniques for higher frequency cooling. In particular, one should consider stochastic cooling at optical frequencies[1]—for the collider if not for the antiproton source.

---

[1] Zholents and Zolotorev, Phys. Rev. Lett. 71:4146-4149 (1993) and SLAC-PUB-6476, "Transit-time Method of Optical Stochastic Cooling"

rf: The 800 MHz rf system proposed for the linear debuncher scheme is a large and expensive system. R & D would be necessary to investigate economical methods of obtaining high gradients and possibly for tuning and de-Qing the cavities that would be placed in the Main Injector.

Targeting: A sweeping system is desirable or essential for the scenarios described here. In all scenarios we have assumed that one can develop a lithium lens that is capable of producing a gradient of 1000 T/m. One more exotic possibility is the development of a lithium lens using liquid instead of solid lithium. Finally, a plasma lens could possibly be developed, but the pulse length of 500 nsec obtained[2] at CERN would have to be increased.

Magnets: The possibility of using either super-ferric or permanent magnets for the high energy accumulator ring has been suggested. We did not investigate these technologies although both possibilities have some attractive features. The large apertures (40π mm-mrad and 10% $\Delta P/p$) required of the collection ring in at least some of our scenarios may present challenges for both conventional and exotic magnets.

CONCLUSION

It is clear that an Antiproton Source capable of stacking 90×10^{10} antiprotons per hour is technically feasible. However, all the scenarios that we considered require substantial investments new components.

---

[2]H. Riege, et al., CERN Note PS/AR Note 91-10.

Appendix I

Stacking Rate Required for 2x10**33 Luminosity			
Initial Luminosity	1.98E+33	cm-2-sec-1	
Initial Pbar Intensity in Tevatron	1.24E+13		
Initial Proton Intensity in Tevatron	4.50E+13		
Cross-section	7.50E-26		
Number of Interaction Regions	2		
Pbar Lifetime (excluding beam-beam)	50	hr	
Proton Lifetime (excluding beam-beam)	50	hr	
Length of Store	13	hr	
Time Between Stores	15	hr	
Average Luminosity	1.02E+33		
Final Pbar intensity	4.44E+12		
Final Proton Intensity	3.59E+13		
Pbar Recovery Efficiency	85%		
Pbars Recovered	3.78E+12		
HE Accumulator Initial Intensity	3.78E+12		
HE Accumulator to Tev Xfer Efficiency	85%		
HE Accumulator Final Intensity	1.46E+13		
HE Accumulator Lifetime	300	hr	
HE Accumulator Average Loss Rate	3.06E+10	hr-1	
Stacking time per store	13	hr	
Efficiency of transfer to HE Accumulator	95%		
Stacking Rate Required	9.10E+11		
Store Lifetime Scale Factor	1		

Appendix II

Antiproton Source Parameter List

Scenario IV - Linear Debuncher - Version 2

Target Parameters			
Protons on target per batch	5.00E+12		
Number of batches	1		
Number of target stations	1		
Beam size (sigma)	0.1	mm	
Sweeping Radius	0.33	mm	
Sweep Time (sine wave period)	1.6	usec	
Sweeping Field	2	kG	
Target Material	Ni		
Maximum Energy Deposition	700	J/g	
Lithium Lens Gradient	1000	T/m	
Momentum Acceptance (Dp/p)	14	%	
Transverse Acceptance	40	pi-mm-mrad	
Production Efficiency (pbar/p)	140	E-6	
Repitition Rate	2	sec	
Main Injector Parameters			
Energy	120	GeV	
Emittance (all bunches)	59	eV-sec	
Gammat	20		
Harmonic	8913		
Revolution Frequency	94	kHz	
Voltage	18	MV	
Bunch length	8	degrees	
Emittance dilution	1.2		
Emittance/bunch	0.0066	eV-sec	
Eta	0.0024		
RF freq	837.8	MHz	
Momentum spread	0.299	GeV	
Bucket area	0.382	eV-sec	
Bucket Height	0.503	GeV	
LINAC			
Beam Parameters			

Pbar Params v2

Energy	8.938		
Gamma	9.53		
Intensity	7.00E+08		
Initial Momentum Spread (Dp/p)	14	%	
Final Momentum Spread (Dp/p)	0.6	%	
r.f. Parameters			
drfift length meters	141		
linac MV/m	25		
linac length	40		
beam line energy (MEV)	8000		
Pre-Cooling Ring Parameters			
(Formerly the Debuncher Ring)			
Beam Parameters			
Energy	8.94	GeV	
Gamma	9.53		
Transfer Efficiency	90.00	%	
Intensity	6.30E+08		
Initial Momentum Spread	0.6	%	
Final Momentum Spread	0.05	%	
Initial Transverse Emittance	40	pi-mm-mrad	
Final Transverse Emittance	1	pi-mm-mrad	
Lattice Parameters			
Magnetic Field	1.7	Tesla	
Transition Energy	7.99		
Tune	9.75		
Circumference	505.24	m	
Revolution frequency	590	kHz	
Eta	0.0046		
Acceptance	40	pi-mm-mrad	
r.f. Parameters			
Harmonic Number	Broad band		
Voltage	5	kV	
Cooling Systems - Longitudinal			
System Bandwidth	8	GHz	
Number of Pickups	1024		
Pickup Impedance	50	Ohm	
Noise Temperature	100	deg K	
Pickup Sensitivity	0.8		
Length of pickup array	12	m	
Number of Kickers	1024		

Kicker impedance	50	Ohm	
Kicker Sensitivity	0.8		
Length of kicker array	12	m	
Kicker power	10000	W	
Cooling Systems - Transverse			
System Bandwidth	8	GHz	
Mixing Factor	1.6		
Number of Pickups	1024		
Pickup Impedance	25	Ohm/cm	
Noise Temperature	100	deg K	
Pickup Sensitivity	0.8		
Length of pickup array	12	m	
Number of Kickers	1024		
Kicker impedance	25	Ohm/cm	
Kicker Sensitivity	0.8		
Length of kicker array	12	m	
Kicker power	10000	W	
Vacuum	1.00E-08	Torr	
Stacking Ring			
(Formerly the Accumulator)			
Beam Parameters			
Energy	8.94	GeV	
Gamma	9.53		
Transfer Efficiency	90		
Stacking Efficiency	90		
Stacking Rate	9.19E+11	hr-1	
Maximum Stack Size	9.00E+11		
Initial Emittance	1	pi-mm-mrad	
Final Emittance	1	pi-mm-mrad	
Initial Density	200	eV-1	
Final Density	1.00E+05	eV-1	
Lattice Parameters			
Magnetic Field	1.7	Tesla	
Transition Energy	6.6		
Tune (H)	6.6		
Tune (V)	8.6		
Circumference	474	m	
Revolution frequency	628	kHz	
Eta	0.012		
Acceptance	10	pi-mm-mrad	

Cooling Systems - Stacking			
System Bandwidth	8	GHz	
Mixing Factor	3		
Cooling Time (50%)	2	hr	
Number of Pickups	512		
Pickup Impedance	50	Ohm	
Pickup Sensitivity	0.8		
Length of pickup array	10	m	
Number of Kickers	512		
Kicker impedance	50	Ohm	
Kicker Sensitivity	0.8		
Length of kicker array	10	m	
Kicker power	1000	W	
Cooling Systems - Core Momentum			
System Bandwidth	8	GHz	
Mixing Factor	3		
Cooling Time (50%)	2	hr	
Number of Pickups	512		
Pickup Impedance	50	Ohm	
Pickup Sensitivity			
Length of pickup array	1	m	
Number of Kickers	512		
Kicker impedance	50	Ohm	
Kicker Sensitivity			
Length of kicker array	1	m	
Kicker power	100	W	
Cooling Systems - Core Transverse			
System Bandwidth	8	GHz	
Mixing Factor	3		
Cooling Time (50%)	2	hr	
Number of Pickups	64		
Pickup Impedance	50	Ohm/cm	
Pickup Sensitivity			
Length of pickup array	1	m	
Number of Kickers	64		
Kicker impedance	50	Ohm/cm	
Kicker Sensitivity			
Length of kicker array	1	m	
Kicker power	100	W	
r.f. Parameters			
Harmonic number	84		
Voltage	100	kV	

Pbar Params v2

Vacuum			
Average Pressure	3.00E-10	Torr	
Accumulator			
(Recycler/Depository,etc)			
Beam Parameters			
Energy	40	GeV	
Gamma	42.63		
Beam Intensity	1.46E+13		
Beam Current	218.96	mA	
Transverse Emittance (95%)	4	pi-mm-mrad	
Longitudinal Emittance (95%)	100	eV-sec	
Momentum spread	0.020	%	
Lattice Parameters			
Magnetic Field	0.4	Tesla	
Transition Energy	20.2		
Tune	20.3		
Circumference	3145	m	
Revolution frequency	94	kHz	
Eta	0.0019		
Acceptance	40	pi-mm-mrad	
Cooling Systems - Longitudinal			
System Bandwidth	8	GHz	
Cooling Time (50%)	2	hr	
Number of Pickups	64		
Pickup Impedance	50	Ohm/cm	
Pickup Sensitivity			
Length of pickup array	1	m	
Number of Kickers	64		
Kicker impedance	50	Ohm/cm	
Kicker Sensitivity			
Length of kicker array	1	m	
Kicker power	100	W	
Cooling Systems - Transverse			
System Bandwidth	8	GHz	
Mixing Factor	3		
Cooling Time (50%)	2	hr	
Number of Pickups	64		
Pickup Impedance	50	Ohm/cm	
Pickup Sensitivity			
Length of pickup array	1	m	
Number of Kickers	64		

Kicker impedance	50	Ohm/cm	
Kicker Sensitivity			
Length of kicker array	1	m	
Kicker power	100	W	
r.f. Parameters			
r.f. harmonic	Broad band		
r.f. Voltage	5000	V	
Vacuum			
Pressure	3.00E-10	Torr	
Dipole Vacuum Chamber i.d.	4x6	cm	
Dipole Vacuum Chamber o.d.	6x8	cm	
Number of Ion Pumps	300		
Ion Pump Capacity	30	l/sec	
Number of Sublimation Pumps	500		
Sublimation Capacity	200	liter/sec	
Collider			
Protons/bunch	6.00E+10		
Antiprotons/bunch	1.65E+10		
Number of bunches	750		
Bunch length	80	cm	
Proton emittance	5	pi-mm-mrad	
Antiproton emittance	5	pi-mm-mrad	
Initial Luminosity	1.98E+33	cm-2-sec-1	
Number of Protons	4.50E+13		
Number of Antiprotons	1.24E+13		
Transfer Efficiency	85%		
Total Cross Section	7.5E-26		
Number of IRs	2		
Average Luminosity	1.00E+33	cm-2-sec-1	
Store Hours	110	wk-1	
Integrated Luminosity	396	pb-1/wk	
Stacking Rate Required	9.10E+11	hr-1	

Fermi National Accelerator Laboratory

Injector Working Group Report

R. York

Michigan State University
East Lansing, Michigan

Operated by Universities Research Association Inc. under Contract No. DE-AC02-76CHO3000 with the United States Department of Energy

Injector Working Group Report

Guharay, Samar
Huang, Yun-Xiang
MacLachlan, James
Nagaitsev, Sergei
Popovic, Milorad
York, Richard C.

Introduction

The charge to the working group was to evaluate the injector chain for two facilities:

1. 2x2 TeV p-$\bar{p}$ collider with an emittance (rms) of 3 π mm mrad, an intensity of 2.38×10^{11} particles/bunch, and a bunch spacing of 132 ns (seven 53 MHz buckets).
2. 30x30 TeV p-p collider with an emittance (rms) of 1 π mm mrad, an intensity of 2.4×10^{10} particles/bunch, and a bunch spacing of 132 ns (seven 53 MHz buckets).

Other issues such as $\bar{p}$ production, lattice considerations, and magnet design were the purview of other working groups. Therefore, the transverse emittance through the injector chain in light of FNAL experience and SSCL design evaluations was the primary thread used for the evaluations. Given the specifications of the two facilities (2x2 and 30x30 TeV), the most problematic relative to emittance is the 2x2 TeV p-$\bar{p}$ collider. However, even for the 2x2 TeV case, solutions appear to be relatively straight forward in regard to the brightness requirements.

Tables 1 and 2 outline the possible injector chains giving the proposed emittance budget at each stage. The precise energy range of each segment is soft, but as a practical matter FNAL parameters were used. The emittance budget allocation is also somewhat arbitrary and could benefit from further evaluation. A scheme discussed below whereby three of the 53 MHz buckets are coalesced in the Medium Energy Booster (MEB) has been assumed. That is, the space charge tune shifts were calculated assuming $2.38 \times 10^{11}/3$ and $2.4 \times 10^{10}/3$ protons/bunch for the 2x2 and 30x30 TeV cases respectively. It has been assumed that the present and envisaged (main ring specifications) FNAL proton production are adequate to meet the $\bar{p}$ production requirements.

Injection Chain - Ion source to Drift Tube Linac (DTL)

To achieve the 2x2 TeV specifications, the FNAL Cockroft-Walton system with its 0.2-0.3 π mm mrad at 53 mA is more than adequate. To achieve the 1 π mm mrad for the 30x30 TeV case, an ion source/LEBT/RFQ with an emittance of ~0.2 π mm mrad at a current of ~45 mA is necessary. Therefore, an R&D program which would develop a prototypical system to be used for proof-of-principle and parameter optimization should be begun now in order to realize these goals in the next 5-10 years. This becomes increasingly important for cases where final emittances less than 1 π mm mrad are desirable. In addition, consideration should be given to determining the degree to which the present FNAL system could be improved.

Table 1. 2x2 TeV Injector

Accelerator Element	E_{final} (GeV)	Emittance $\varepsilon^N rms$ (π mm mrad)	Comment
Ion source - DTL	0.00075	1	(FNAL ~0.3 π mm mrad)
DTL	0.1	1.5	(FNAL ~1.1 π mm mrad)
SCL	0.85-1.0	2	(FNAL ~1.3 π mm mrad)
LEB	8	2.4	$\Delta\nu_{spacechg}$= 0.37-0.3
MEB	150	2.7	$\Delta\nu_{spacechg}$= 0.07 Coalescing in

Table 2. 30x30 TeV Injector

Accelerator Element	E_{final} (GeV)	Emittance $\varepsilon^N rms$ (π mm mrad)	Comment
Ion Source - DTL	0.0025	0.2	Prototype
DTL	0.1	0.3	Evaulate 1st tank ε dilution
SCL	0.4	0.5	
LEB	8	0.7	$\Delta\nu_{spacechg}$= 0.32
MEB	150	0.8	$\Delta\nu_{spacechg}$= 0.02 Coalescing in
HEB	2,000	1	

Injection Chain - DTL/Side Coupled Linac (SCL)

To achieve the 2x2 TeV specifications, the linac energy must be increased from 400 MeV to 850 - 1,000 MeV to maintain the space charge tune shift in the Low Energy Booster to 0.37 - 0.3 respectively. Under these conditions, the choice of a continuation of the previous FNAL linac upgrade is probably preferable to undertaking an R&D program to develop appropriate high gradient structures. However, during the workshop alternative 30x30 TeV specifications were proposed for which a several (3-8) GeV linac would have been required. Hence, it would be prudent to consider a high gradient structure program, or at a minimum, track progress of other accelerator groups in this area. To achieve the 30x30 TeV specifications, the emittance growth through Drift Tube Linac (DTL) region must be diagnosed and rectified. The FNAL 400 MeV linac may be adequate presuming that a space charge tune shift of 0.32 provides acceptable performance.

Injection Chain - Low Energy Booster (LEB)

For the 2x2 TeV case, an injection energy of 850 - 1,000 MeV would be required to maintain the space charge tune shift at 0.37 - 0.3 respectively for an emittance of 2 π mm mrad. The FNAL LEB presently provides ~4 x 10^{10} protons/bunch with an emittance of 2 π mm mrad. This performance is the result of a significant and continued diagnosis and correction program. It is important that activities in this vein

continue. For the 30x30 TeV case, it may be possible to achieve the specifications given in Table 2 even with the present linac energy of 400 MeV since this would result in a presumed acceptable space charge tune shift of 0.32. Inasmuch as this result maybe marginal, it is important that the LEB performance improvement program be continued. Also, the viability of 1 GeV H^- injection into the present FNAL booster should be evaluated.

Injection Chain - Medium Energy Booster (MEB)

The transverse emittance is not anticipated to be a significant issue in the MEB. With the present specifications, the space charge tune shifts are small. (See Tables). This conclusion is also supported by the systematic investigation of emittance dilution for the SSCL MEB under similar conditions. Although probably not required with the present specifications, electron cooling in the MEB could be considered. Roughly speaking, a 6 MeV, 2 A electron beam over a 40 m section of the ring could be used to reduce the emittance by half in approximately 2 minutes. A development of this concept is provided in these proceedings.[1]

Injection Chain - High Energy Booster (HEB)

While the High Energy Booster is not anticipated to have significant problems in achieving the required emittances, care will be required to achieve the 30x30 TeV emittance.

Coalescing

Both the 2x2 and the 30x30 TeV specifications stipulate a bunch spacing of 40 m. To achieve a 40 m bunch spacing for example, it is proposed that segments of the LEB batch be extracted such that a pattern of 3 full buckets - 4 empty buckets (53 MHz) would be created in the MEB. This pattern would then be accelerated to flat top (150 GeV) and coalesced to create the required bunch spacing. This sequence has been assumed in the space charge analysis where the 53 MHz bunch intensities where assumed to be $2.38 \times 10^{11}/3$ and $2.4 \times 10^{10}/3$ for the 2x2 and 30x30 TeV cases respectively. Clearly, the viability of this scheme and the hardware implications particularly the fast kickers for the LEB and the rf in the MEB require further study.

1. "Multi-MeV Electron Cooling - A Tool for increasing the Performance of High Energy Hadron Colliders?", Sergei Nagaitsev, These Proceedings.

Fermi National Accelerator Laboratory

Report of the Interaction Region Working Group

S. Peggs

Brookhaven National Laboratory
Upton, Long Island, New York 11973

Operated by Universities Research Association Inc. under Contract No. DE-AC02-76CHO3000 with the United States Department of Energy

Report of the Interaction Region Working Group

S. Peggs
Brookhaven National Laboratory, Upton, NY 11973

Abstract

This paper is a summary of work done at the "Workshop on Future Hadron Facilities in the US" that was held July 6-10, 1994, at Indiana University, in Bloomington.

1 INTRODUCTION

The optics of a high energy hadron collider are conceptually divided into the arcs and the interactions regions (IRs). Arcs bend the beam, and comprise most of the collider circumference. They are usually made from a large number of repetitive FODO cells, with as small an average bending radius as practically possible. Interaction regions are relatively straight, and transport the beam between arc ends and interaction points (IPs). The IR optics focus the beam down to a small spot at the IP, with an rms size

$$\sigma^* = \sqrt{\epsilon\beta^*/(\beta\gamma)} \qquad (1)$$

where ϵ is the rms normalised emittance, β^* is the beta function at the IP, and $\beta\gamma$ is a relativistic factor. Two storage rings were considered at the workshop, a 2 x 2 TeV collider with $\beta\gamma \approx \gamma \approx 2 \times 10^3$, referred to here as "T2", and a 30 x 30 TeV collider with $\gamma \approx 3\times10^4$, dubbed "T30". This summary adopts the same nominal parameters for T2 and T30; an initial emittance of $\epsilon = 10^{-6}$ m, and a collision beta as low as $\beta^* = 0.2$ m. Nominal collision beam sizes σ^* for T2 and T30 are therefore 10.0 μm and 2.6 μm, respectively.

General statements can be made for T2 and T30 if the IR optics are simplified by assuming:

1. There are no prior geometric constraints.
2. The optics are designed as interconnecting modules, each with a specific function.
3. Small beam separation of $\Delta \leq 0.1$m.
4. Dynamical analysis is limited to general comments on local tolerances and correction.

It is worth classifying hadron colliders on the basis of these assumptions, before turning to more detailed discussions in succeeding sections.

Prior geometric constraints and modularity. T2 is conceived as replacing the Tevatron, in the existing tunnel. Similarly, the LHC must fit in the LEP tunnel. The footprint of a new machine must fall (generally) within a fraction of a meter of the old, and so careful attention must be paid to the layout of bending dipoles. This has had important consequences in limiting the amount of IR modularity that is possible in the LHC. Similarly, it appears to be difficult to increase the length of the IR straight in T2 (see below). By contrast, RHIC, SSC, and T30 are essentially free of prior geometric constraints.

Small beam separation. RHIC and the SSC separate two beams of identical particles into independent magnets with centers about a meter apart. This generates a spurious "separation dispersion" η of approximately the same size as the beam separation. The magnets are horizontally separated in RHIC, and correction of the separation dispersion is included in the role of the dispersion suppressor module that sets $\eta^* = 0$ but leaves η'^* non-zero. Beam separation is vertical in the SSC, and the "M = -I" vertical dispersion correction section adds a significant complication to the IR design. If the beams are only separated by $\Delta \leq 0.1$ m, then the separation dispersion is comparable to other random sources, and the problem becomes moot. This condition is met in proton-antiproton colliders such as the Tevatron or T2 where two beams circulate in a one-in-one magnet, and in the LHC which uses a two-in-one magnet. It is also assumed that T30 would also use a two-in-one magnet.

Limited dynamical analysis. The dynamic aperture of a collider is often limited by IR performance, but its accurate evaluation for T2 and T30 falls well beyond the scope of the workshop. It is not possible to unequivocally say that $\beta^* = 0.2$ m is achievable, for example, although it looks reasonable at first glance. This summary limits iself to overviews of linear effects and nonlinear harmonics in the dominant IR triplet quadrupoles.

2 IR MODULES

The prime virtue of modularity is that the separation of functions leads to a conceptually easier and more flexible lattice. For example, modules can be connected together more or less like a toy train set. Figure 1 shows the modular implementation of a RHIC IR, tuned for collisions with $\beta^* = 1.0$ m. Dipoles and F and D quadrupoles are shown as rectangles centered on, above, or below the main axis.

2.1 A simple telescope

Figure 1 illustrates the simplest possible telescope module. After traveling for $L^* = 25$m (and passing through beam splitting dipoles), a hadron leaving the RHIC IP encounters a close packed triplet of quadrupoles, where the ring-wide maximum β of

$$\hat{\beta} \equiv L_e^2/\beta^* \qquad (2)$$

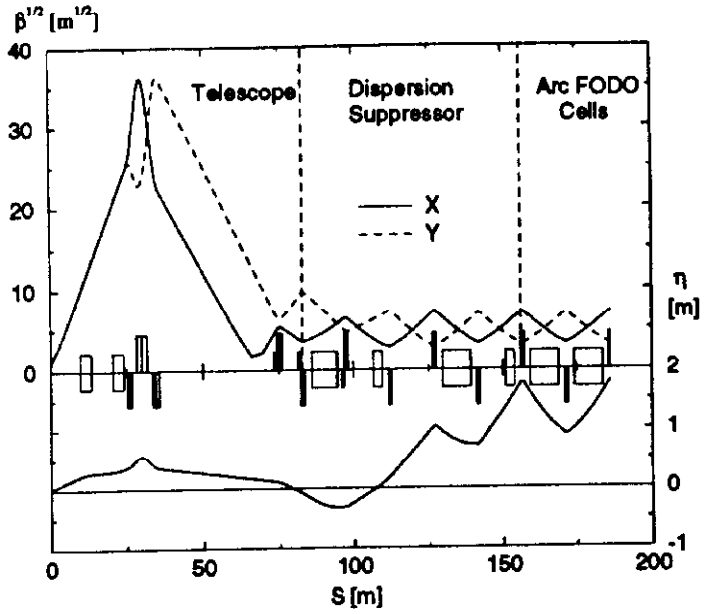

Figure 1: Modular IR design: the RHIC interaction region.

is encountered. The "effective length" L_e remains essentially constant independent of β^*, since the triplet quadrupole strength $K[\mathrm{m}^{-2}]$ is almost (or exactly) held constant.

Figure 2 shows how L_e varies with the common triplet quadrupole strength K, following work by Peck[1]. This assumes that the quads are separated by 1 m gaps, and that the same $\widehat{\beta}$ is encountered in both planes. It shows that L_e is only weakly dependent on L^* and on the quadrupole strength available. The gradient G T/m in T30 quadrupoles is related to the strength by

$$G = K/B\rho \approx 10^5 K \tag{3}$$

A not impossible gradient of $G = 400$ T/m therefore yields $L_e = 62$ m in a T30 IR with $L^* = 20$ m, so that $\widehat{\beta} = 19.2$ km when $\beta^* = 0.2$ m, and the maximum beam size $\widehat{\sigma}$ is

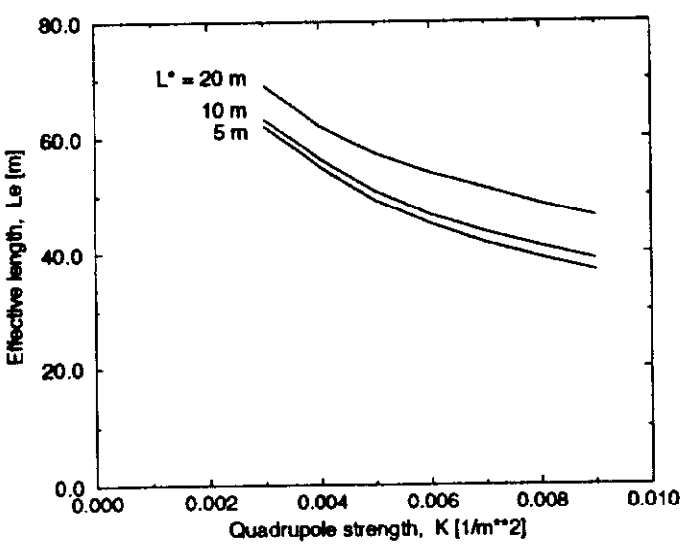

Figure 2: Effective length L_e in long triplets.

still only 0.8 mm. Triplet physical aperture is therefore not expected to be a problem in T30 (or T2). This remains true when a non-zero crossing angle is included to separate the beams by, say, $7\sigma(s)$, thereby ameliorating parasitic long range beam-beam interactions. Small L_e values (and large K values) are desirable for dynamic aperture, not physical aperture, reasons.

A fourth quad Q4 is at the end of the long drift after the triplet, followed, half of a half FODO cell length later, by a fifth quad Q5. It is natural in general to separate the beams into separate beampipes between Q3 and Q4, although this is not done in RHIC. Since Q4 is primarily responsible for matching into the FODO cell twiss functions at Q5, its strength varies strongly with β^*. (The requirement for perfect FODO cell β matching is relaxed in the RHIC implementation shown.) The absence of a secondary β peak is a great advantage of this simple telescope, which tunes robustly over a large range of β^* values[2].

2.2 *Dispersion control and utility straights*

The collision dispersion η^* is zero for all the colliders under discussion in order to suppress odd order beam-beam resonances and to minimize the collision beam size, while the SSC design is alone in also setting the slope η'^* to zero. Full dispersion suppression is a design choice for T2 and T30. A telescope can be connected to a variety of 180 degree phase advance FODO dispersion suppressors (ie, suppressors with constant quadrupole spacing). For example, a natural suppressor with a high dipole packing fraction can be made using cells with a quadrupole spacing 3/4 of the arc cells, each cell bending by 2/3 of the angle of the arc cell. Or, a missing dipole suppressor with twice the arc bending radius can be made by keeping the quad spacing the same, while halving the bend angle per half cell. Note, however, that the phase advance from the IP to Q5 is $\approx 3\pi/2$ in one plane, and $\approx \pi/2$ in the other. So, if the two telescopes on either side of an IP are powered antisymmetrically, they will naturally provide $\eta^* \approx 0.0$ even when matched directly into arc FODO cells with full bending strength! Perfect partial suppression can be achieved by allowing small variation in the strength of the first few quadrupoles outside the triplet - a desirable feature for other reasons.

Utility drift spaces have to be provided, for kickers, Lambertson magnets, electrostatic separators, spin rotators and snakes, general instrumentation, et cetera. One way is to follow the telescope with a bend free set of cells in a utility module, before entering (for example) a high packing fraction dispersion suppressor module. The RHIC implementation in Figure 1 uses a dipole layout scheme that partially suppress η'^*, and at the same time provides utility drift spaces. Since this region serves more than one function, it is not strictly proper to call it a module. In fact, most of the quadrupoles in Figure 1 are tuned simultaneously when a new optics is designed.

2.3 Betatron oscillation polarisation

The eigenmodes of betatron oscillation conventionally lie in the horizontal and vertical planes, with an obvious analogy to plane polarisation in light optics. It has been proposed that the beam-beam effect could be ameliorated if the planes are rotated locally, at the IP, by 45 degrees [4]. A "quarter wave plate" module on one side of the IP can do this, matched by a compensating module on the other side. Such a module was presented in conceptual form at the workshop[5]. Crudely speaking, it consists of a section containing only skew quadrupoles and drifts, where the phase advance in one 45 degree plane is $\pi/2$ larger than in the other. It has also been proposed that global circular polarisation ameliorates nonlinear dynamics and correction schemes in general[3]. One way to achieve this is to place identical quarter wave modules on either side of the IP.

These two proposals have a lot in common, even though they are independently motivated. However, although the schemes appear to be attractive, they both need a significant amount of research and development before they become practical, well justified, proposals.

3 TEVATRON GEOMETRIC CONSTRAINTS

The prior geometric constraints of the Tevatron tunnel are crudely evaluated by modeling each sextant as an IR straight $L_S = 35$ meters long, followed by an arc of constant bending radius, followed by another IR straight. If L_S in T2 is increased by ΔL, as dipoles are pushed back out of the telescope, the radial distances from the center of the ring to an IP and to an arc center increase by ΔR_{IP} and ΔR_{ARC}, where

$$\Delta R_{IP} = -0.18\,\Delta L \qquad \Delta R_{ARC} = 0.09\,\Delta L \tag{4}$$

It appears difficult to move the T2 dipoles much further away from the IP. Although the ground rules can be changed, for example by allowing missing dipoles in the middle of the arcs, it will probably remain impossible to have a bend free T2 telescope. Directly or indirectly, efforts to lengthen the IR straight in T2 tend to raise the dipole field required for a fixed energy. The modified geometric demands of beam separation, injection and extraction in T2 also conflict with prior geometric constraints, and with IR design in general.

4 TRIPLET QUADRUPOLE ERRORS

The large lengths, strengths and beta functions of the IR triplet quadrupoles make them particularly vulnerable to various error effects, some of which are discussed below. However, even perfect triplet quadrupoles indirectly limit collider performance, through the "chromatic aberration" $\beta(\delta)$ effects that they create. Multiple sextupole families may be necessary. It is almost definitely these chromatic effects that set the ultimate limit on the lowest β^* available in T30, and maybe also in T2. A more quantitative statement is beyond the scope of this report.

4.1 Misalignment errors

When a triplet quad of focal length f is displaced transversely by Δx, an angular kick of $\Delta x/f$ is created. Taking the quad beta function to be $\widehat{\beta}$ and using equation 2, the closed orbit is displaced at the IP by

$$\Delta x^* \approx L_e\,(\Delta x/f)\,F_1 \tag{5}$$

where F_1 is a factor, close to 1, that is a function of the fractional tune. Using $L_e = 62$ m and $f = 20$ m, displacements of only 1.0 μm or 0.26 μm move the closed orbit by σ^* in T2 or T30, respectively. This is much less than conventional alignment and surveying accuracies, at the 100 μm level.

If the displacement is constant (DC) in time, closed orbit correction is relatively straightforward. However, the triplet quads will probably vibrate at mechanical frequencies of a few Hz, with amplitudes large enough to cause the "colliding" beams to miss altogether. This makes local closed orbit feedback necessary, at frequencies that are (fortunately) much less than the revolution frequency. The feedback algorithm becomes somewhat more complicated if the triplet BPMs move with the triplet, but the problem remains linear, with a non-singular solution - at least on paper.

4.2 Normal quadrupole errors

The quadrupole integrated strength is subject to errors that distort the lattice optics. For example, if the magnetic length is wrong by ΔL, a beta wave is launched with an amplitude

$$\frac{\Delta\beta}{\beta} \approx \frac{\widehat{\beta}}{f}\frac{\Delta L}{L}F_2 \tag{6}$$

where $F_2 \approx 1$ is another form factor. A 10% beta wave is introduced in T30 when the length of a single quad is wrong by only about 10^{-4}, a plausible number in practice. Independently controllable quadrupoles - ideally about 10 on either side of each IP - can be used as both diagnostics and correctors for DC errors. The beta wave is observed by measuring tune shifts as individual quads are perturbed. Then the linear problem is inverted, much as in closed orbit correction, to derive slightly modified quad strengths.

Dangerous levels of tune modulation can easily result from power supply ripple, even when state of the art regulation practices are employed. Preliminary experience at HERA suggests that it is useful to feed back the Fourier analysed signal from a sensitive beam loss monitor into the regulation circuitry[6].

4.3 Skew quadrupole and roll angle errors

Skew quadrupole errors in triplet quadrupoles are indistinguishable, in practice, from roll angle misalignments. A roll angle of θ results in a minimum tune split of

$$\Delta Q_{min} = \theta\sqrt{\beta_H\beta_V}/(f\,\pi) \tag{7}$$

so that a 1 mrad error has serious consequences, even in RHIC. If the horizontal dispersion function at the quad is non-zero, a 1 mrad roll also produces a measurable vertical dispersion wave, providing a usable diagnostic. A single skew quadrupole corrector in a triplet simultaneously corrects linear coupling and vertical dispersion errors coming from all three triplet quads[7]. The need to have diagnostics that enable this correction argues in favor of NOT having full dispersion suppression.

4.4 *Nonlinear errors*

Some conventional wisdoms about nonlinear magnetic errors in triplet quadrupoles are worth recording, without the numerical justification that depends on a detailed analysis, since the topic is vitally important to collider performance.

"Tuning shims" are highly desirable. Eight small air gaps may be spread out azimuthally, with quadrupole symmetry, on the inside arc of the iron yoke of each triplet quadrupole. As many as eight harmonics may then be corrected, on a magnet to magnet basis, after low current (warm) field quality measurements. At RHIC, shims of a variable mixture of brass and iron are inserted along the length of the quadrupole body, and mechanically fixed in place, to correct the $b_3, b_4, b_5, b_6, a_3, a_4, a_5$ and a_6 harmonics[8].

End multipoles may dominate. Significant nonlinear fields - thin multipoles - are driven by the conductor configuration at the end of the quadrupoles where the current leads emerge to connect to the outside world. Field errors at the other end, where the conductors turn around to reenter the yoke, are less important, although non-negligible. These systematic end effects are the dominant triplet field nonlinearities, if random body errors are removed using tuning shims.

Lumped correctors are useful. The rapid variation of horizontal and vertical beta functions makes it impossible to correct tune versus amplitude effects by simply adjusting the integrated harmonic content of each triplet. A final nonlinear correction may be achieved by powering lumped correctors in the triplet package. In RHIC their strengths will be dead reckoned, since they mainly correct systematic end effects, and since no easy beam based diagnostics are available[8].

5 NON-SUPERCONDUCTING IR QUADRUPOLES

Non-superconducting quads have a fundamental potential role of protecting the superconducting triplet quads in T30 against particle spray from the IP, by acting as collimators. Electromagnetic or permanent (Samarium Cobalt, SmCo) quadrupoles are resilient to energy deposition - they don't quench. They can also have a much smaller pole tip radius than the practical lower limit of $R_{pole} = 2.5$ cm that seems to apply to superconducting (SC) quads. However, non-SC quads have the disadvantage of a lower pole tip field - $B_{pole} \approx 1.3$ Tesla, instead of, say, $B_{pole} \approx B_{dipole} \approx$ 12 Tesla for T30. Nonetheless, non-SC quads are useful optical elements, as well as collimators.

The working group first considered a non-SC quad location close ($\approx$ 1 m) from the IP, embedded in a detector. Both iron and SmCo quads have particular mechanical difficulties at this location, due to the need to power and cool the former, and the need to detune the latter at injection. Also, they are not optically effective close to the IP, and so their proposed location was moved to just in front of the triplet. The SC quads are well protected by iron "Q0" quads about 3 metres long. Since this is short compared to $L^* = 20$ m, say, the strongest physical aperture limitation occurs at storage, when $\beta^* = 0.2$ m implies $\beta_0 \approx 2.0$ km, and consequently $\sigma_0 \approx 1.0$ mm and 0.26 mm in T2 and T30, respectively. Taking $R_{pole} = 10.0$ cm $= 10\sigma$ in T2, and $R_{pole} = 5.0$ mm $= 19.4\sigma$ in T30, leads to Q0 gradients of about 130 T/m and 260 T/m, respectively. These apertures are unconventionally small for hadron colliders, and give rise to the fear that a kicker pre-fire, for example, could cause beam to strike a "collimator" from the wrong side, and severely damage a detector. Such apertures are not a mechanical issue, however, as quadrupoles with similar apertures have been built for use in electron colliders.

A more detailed analysis of all the performance, aperture, and cost issues could even lead to the recommendation that the T30 triplet should consist solely of conventional iron magnets.

6 ACKNOWLEDGEMENTS

Many people attended the IR working group sessions, to a greater or lesser extent. Sincere thanks go to J. Johnstone, W. Scandale, Y. Derbenev, S. Tepikian, R. Talman, A. Chao, A. Garren, S. Holmes, M. Syphers, and to any other participant whose name I have overlooked.

7 REFERENCES

[1] S. Peck, "Minimizing chromaticity in interaction regions with long weak quadrupoles", Proc. 1984 SSC Summer Study, pp. 384-387, Snowmass 1984

[2] S. Peggs, "Accelerator physics issues in large proton storage rings", Proc. 13th Intnl. Conf. on High Energy Accs., Novosibirsk, 1986

[3] R. Talman, "Möbius twisted accelerator", CESR internal note CBN-94-1, 1994

[4] Y. Derbenev, "Invariant colliding beams", University of Michigan note UM-HE-93-27, 1993

[5] Y. Derbenev, "Circular optics for the IR", unpublished, July 1994

[6] M. Seidel, "Messungen mit kollimatoren und schauerzählern", pp. 133-144, DESY-HERA 94-03, 1994

[7] T. Satogata et al, "IR quadrupole roll and solenoid misalignment in RHIC", Proc. 1994 EPAC, London, to be published

[8] J. Wei et al, "Magnetic correction of RHIC triplets", Proc. 1993 PAC, pp. 258-260, Washington, 1993

Fermi National Accelerator Laboratory

Lattice/Beam Dynamics Working Group

M. Syphers

Brookhaven National Laboratory
Upton, Long Island, New York 11973

Operated by Universities Research Association Inc. under Contract No. DE-AC02-76CHO3000 with the United States Department of Energy

Lattice/Beam Dynamics Working Group
Summary Report

Mike Syphers
BNL

Introduction

The Lattice/Beam Dynamics Working Group was charged with reviewing and identifying technical issues and their potential solutions for (a) a 2x2 TeV high luminosity p-pbar collider, and (b) a 30x30 TeV high luminosity pp collider. Rather than attempting to solve very specific problems for these devices in the relatively short time scale of a workshop, the group attempted to look at more general questions to try to indicate in which directions future work in these areas should procede. The emphasis of the group tended toward lattice issues and general accelerator design issues for the above two cases, with more specific questions being addressed as directed by the needs seen by the Workshop Synthesizers.

Since this was a Workshop, formal presentations were kept to a minimum. A few, slightly more "formal" Working Group presentations were made during the workshop on topics such as a "Mobius Accelerator" (R. Talman), "Robinson Wigglers" (S. Y. Lee), "Phase Trombones" (A. Garren) and the "CERN LHC Combined Function Lattice" (R. Talman). Most of these were results of discussions which occured during the course of the workshop.

2 TeV x 2 TeV

Lattices

For the 2 TeV pbar-p collider, the lattice discussion consisted of a review of work performed at Fermilab in 1988-89 on Tevatron upgrade lattices.[1] In this work, several alternatives were investigated, including:

a) lengthening of the long straight sections in the Tevatron from 53 m to 73 m. This option required two different dipole magnets, with fields of 8 T and 9 T (for 1.8 TeV beams). The strong dipoles were used in the vicinity of the straight sections.

b) lowering the ring dispersion function by using new quadrupole magnets/trims near the straight sections to match the dispersion to the standard cells of the arcs. The dispersion peaks were reduced from 6 m to under 4 m.

c) increasing the cell length in the arcs from 30 m to 40 m. The existing Tevatron arcs contain "missing dipole magnets" at the "17" and "48" locations; this new design has the same amount of free space, but with the missing magnets arranged to better control the dispersion mismatch. Dispersion suppressors are used at the ends of the arcs to make zero dispersion straight sections. While the geometry of this accelerator is slightly different than that of the existing Tevatron, the radial excursions within the tunnel were estimated to be typically 6-9 in., with a maximum of 13 in.

Table 1 shows general parameters of the above three cases. The general conclusion was that while a new Fermilab accelerator would be constrained by the Tevatron tunnel, it is possible to make improvements to the lattice design to provide longer straight sections,

better matched lattice functions, and perhaps both. With the introduction of 90° cells, the dispersion function is lowered substantially, and this phase advance along with the smaller beam size for coalesced bunches may improve the performance of the separated beams accelerator.

Table 1

	TEV	OPT1	OPT2	OPT3	
Energy	1.0	1.8	1.8	1.8	TeV
Radius	1000	1000	1000	1000	m
Str. Sect. Length	53	73	53	53	m
Cell phase adv.	68	74	90	90	deg
Cell β_{max}	98	98	99	135	m
Global β_{max}	110	110	180	144	m
Cell D_{max}	4.0	3.5	2.6	4.7	m
Global D_{max}	5.9	5	3.6	5.6	m
D in str. sec.	2.5	3.2	2.4	0.0	m
Magnet field	4.4	8,9	8.0	7.8	T
Cell Quad Strength	0.038	0.041	0.050	0.036	1/m
Cell Half-length	29.7	29.7	29.7	39.7	m

Beam Intensity Issues

Two beam intensity issues of the 2 TeV pbar-p collider were discussed. The first involved the impedance thresholds for the parameter sets provided by the Workshop Synthesizers. The longitudinal impedance threshold for the microwave instability was computed to be on the order of $Z_{\|}/n = 2$ Ohms, and was not believed to pose any new technical challenges. The transverse impedance of the accelerator needs to be less than about $Z_{\perp}/n = 800$ kOhms/m, which also is not pushing any presently obtainable limits.

The second intensity issue looked at for the pbar-p collider was the long-range beam-beam interaction. This collider will have 1-2 orders of magnitude more long-range interactions than the present Tevatron collider. As an estimate of the magnitude of the effects, consider a head-on beam-beam tune shift of $\Delta\nu_{HO}$ for each of two interaction points. Around the accelerator, there will be $2*n_B$ long-range interactions, where n_B is the number of bunches in each beam. Assuming the two beams are separated by several beam sigmas (4-5, say) by the helical orbit separators, then a proton bunch will produce a long-range force on the antiproton bunch which is decreasing roughly as $1/r = 1/(d \pm x)$. (Here, d is the separation between the centers of the two bunches, and x is the displacement of an antiproton from the center of it's bunch.) The expansion of $1/(1 \pm x/d)$ generates all multipoles, giving rise to steering errors, tune shift errors, chromaticity, and tune spread. For simplicity, if we assume a simple 1-D model, then these errors can be written in terms of $\Delta\nu_{HO}$ as:

a) $$(\Delta x_{co}/\sigma)_{max} \approx 4\pi\, \Delta\nu_{HO} / (d/\sigma) = 0.025$$

b) $\Delta\nu = 2\,\Delta\nu_{HO} / (d/\sigma)^2 \qquad = 0.0008$

c) $\Delta\xi = 4\,\Delta\nu_{HO}\,(D/\sigma) / (d/\sigma)^3 \qquad = 3.2$

(D is the dispersion function = 4 m, say,
and take $\sigma = 0.4$ mm at $\beta = 100$ m)

d) $\Delta\nu_{max} \approx 9\,\Delta\nu_{HO} / (d/\sigma)^4 \qquad = 0.00014$
(for particles at $a = 2.4\,\sigma$)

where these expressions are for a single long-range encounter. The numerical results are for $\Delta\nu_{HO} = 0.01$, and $d/\sigma = 5$. One can see that the effects of hundreds of such encounters (1500, for one parameters list considered) are significant The most recent parameters list for the 2 TeV accelerator reduces the number of long-range interactions to 216, which makes some of the numbers more tolerable, though the issues remain, especially for chromaticity compensation. The analysis should be carried through further, looking at the details of the 2-D long-range interactions along the helical orbit. In addition, the effects of uneven bunch spacing (which is surely to be the case for scenarios with several hundred bunches) need to be investigated -- in particular, the Pacman effect due to average corrections of the long-range beam-beam interactions.

30 TeV x 30 TeV

For the 30 TeV x 30 TeV Collider, most of the discussion was centered around optimization of the lattice. Drawing upon the lessons from the SSC, the group felt that simplification of the lattice -- from a hardware standpoint -- was absolutely necessary. This entailed developing a workable lattice in which the number of different types of components are minimized, long cable runs for correctors are avoided and the number of power leads are minimized. This philosophy led to a design with "sparse/lumped" correctors, and assumptions about having power and vacuum hardware physically attached to the same cryostat containing the main quadrupole magnets, thus avoiding the need for separate "spool pieces" in every half-cell.

The group also held discussions on magnet aperture and field quality, and instabilities thresholds. Impedance issues were not seen to be an immediate issue which could be addressed by this group in this workshop. The prominent impedance issue will be the beam tube liner, and so will depend very strongly on the magnet and cryogenic/vacuum design.

One of the more exciting aspects of the new accelerator was the possibility of reducing the transverse emittance damping time due to synchrotron radiation by a factor of 2 or 3. The Working Group also spent time on the design of a standard cell to perform this function.

Lattice Issues

It was realized by the Working Group that the lattice of a new, large, high energy collider could be simplified in such a way that may have a significant impact on the cost of the accelerator. The emphasis on much of the discussion was how to avoid the need for

"spool pieces," which are devices used in present superconducting accelerators to interface the accelerator to power and vacuum systems, beam instrumentation systems, and which typically contain accelerator correction magnets. In the SSC, each 90 m half cell of the Collider ring contained a 5 m spool piece, at least half of which was used for correction magnets -- dipoles, quadrupoles, and sextupoles in particular, with occasional other correctors such as skew quadrupoles. There were a variety of spool pieces, some of which contained recooling apparatus, some having power and vacuum interfaces, different ones with different corrector packages, etc.

The Working Group envisioned a scenario as follows. The "arcs" of the accelerator are made up of 90° FODO cells. Each FODO cell is composed of a quadrupole and 5 dipole magnets. As a working example, the Working Group compared these concepts to the general lay-out of the SSC arcs. In the SSC, roughly every 24 cells there was an interface point to the power and cryogenics systems. In the new scheme, the lattice would contain a section of 4 cells which would have free space generated by leaving out a sequence of dipole magnets (10, in our example) as a "dispersion-matched insertion." These "free spaces" would contain "empty cryostats," which could then be converted to function as spool pieces as required. That is, there would be devices which are of the same length and outer diameter as standard dipole cryostats, but which may contain correctors, power feeds, cryo feeds, etc. as needed. An example of such an insertion is shown in Fig. 1.

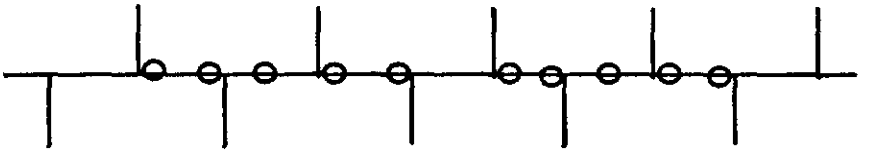

Fig. 1

To avoid having spool pieces in each half cell, standard systems hardware, which occurs every cell, would be designed into the quadrupole assembly resulting in a single piece of hardware. It was assumed that the quadrupole stands would be remotely moveable with stepping motors to perform orbit adjustments throughout each arc. In regions such as the IRs and utility straight sections (not discussed by this Working Group), steering correction magnets could be implemented (as well as in the free-space insertions discussed above, as necessary) to perform injection bumps, etc.. However, in the arcs, where such distortions generally are not necessary, the quadrupole alignment could be set and left alone. To make a 5 mm orbit bump in the ring, one would need only about ±1 mm movement of a standard quadrupole. Such remotely controllable magnet stands could also allow one to relax the alignment requirements of the accelerator upon installation. It was pointed out, however, that if this accelerator incorporates a 2-in-1 magnet design, simultaneous alignment of both beams using moveable magnets may be more difficult operationally.

The adjustment of the global tunes of the accelerator will be performed by Phase Trombones -- one at each end of each arc. These consist of 5 "standard" cells with 5 independently controlled quadrupole circuits, allowing one to tune the phase advance across the Trombone in each plane, while keeping the section matched to the rest of the ring. If it is found that such sections cannot meet the required tuning range (roughly 1-2

units), then other measures would need to be considered, the most straightforward being the placement of trim quadrupoles in the "free-space" insertions.

Chromaticity adjustments will be made using sextupoles in the free-space insertions. In our example, each insertion contains four straight sections by F quads, four next to D quads, each the length of a standard dipole. It was felt that this would be plenty of space to encorporate the sextupoles necessary for chromaticity correction. Naturally, the effects on dynamic aperture of such a lumped scheme will have to be studied carefully.

In addition, the free-space insertions contain "missing magnets" in the middle of half cells, which can contain skew quadrupoles to perform decoupling.

A schematic layout of one arc of the accelerator is shown in Fig. 2

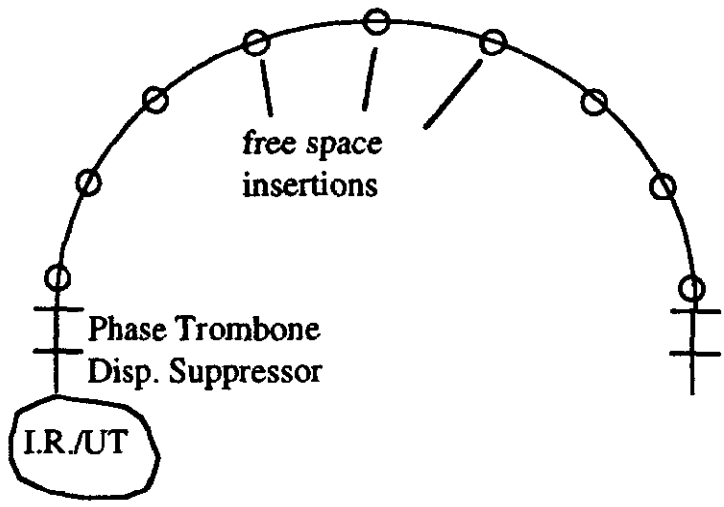

Fig. 2

Damping Time Enhancement

The damping rates, or damping partition numbers, of the collider are constrained to add up according to Robinson's Theorem[2]:

$$J_x + J_y + J_s = 4,$$

where $J_x = 1-D$, $J_y = 1$, and $J_s = 2+D$. Here, D is given by

$$D = \langle (D/\rho^2)(1/\rho + (2B'/B)\rangle / \langle 1/\rho^2\rangle$$

where the averages are taken over the entire ring. For a pure FODO lattice, where B'=0 when B is not zero, and vice versa, then $J_x = J_y = 1$, and $J_s = 2$. To take advantage of the synchrotron radiation damping inherent in a 30 TeV proton collider, schemes were investigated to enhance the damping rate. A design of a combined function lattice for the LHC[3] was reviewed by the group, and a combined function lattice was briefly discussed

for the 30 TeV ring. This was initially discussed in the spirit of simplifying the componets of the standard cell. But, it was quickly realized that the pure combined function lattice would lead to anti-damping in the horizontal plane. Next, two lattices consisting of defocusing bending magnets were envisioned. The first lattice used cells containing a single focusing quadrupole and defocusing bending magnets elsewhere. Analytical expressions for this simple system were developed. Though the hardware layout is simple (one quadrupole type, and one bending magnet type), to obtain increased damping one needs a gradient of about 3 T/m in a 10 T magnet. ($D \approx 2\langle DB'/B\rangle = -1$, which for B=10T, and $\langle D\rangle = 1.5$ m leads to B'=-3 T/m.) This leads to rather long cells (if we demand 90° phase advance in both planes) and unacceptable amplitude functions. The second lattice used defocusing bending magnets, but retained both F and D quadrupoles in the standard FODO-type structure. In this case, the two quadrupoles are of different strengths (lengths), and so one gives up the simplicity one was after.

Another, simpler scheme involves misaligning the quadrupoles by roughly 5 mm. If the otherwise standard quadrupole magnets are all moved radially outward by this amount, then the quadrupoles will steer the beam and hence generate radiation. For this case,

$$
\begin{aligned}
D &= -(8\,\delta / (L\,\theta_b))\,(L_b/L_q) \\
&= -(8\,\delta / ((90\text{ m})(7.5\text{ mrad}))\,)\,(80\text{ m})/(5\text{ m}) \\
&= -1 \\
\text{--->}\ \delta &= 5.5\text{ mm, for SSC-type cell parameters.}
\end{aligned}
$$

The 5.5 mm shift would thus double the transverse damping rate. On the other hand, it may be more economical or simpler to design a quadrupole magnet with a small central bend field of order 1.2 T to perform the same task. And, if the quadrupole positions are remotely tunable, as we have previously assumed, then one could contemplate "tuning" the damping rate.

Magnet Apertures

One afternoon's discussion focused on magnet aperture issues. It was the concensus of the Working Group that a 50 mm magnet design was acceptable for a 2 TeV x 2 TeV pbar-p collider. For the 30 TeV x 30 TeV collider, the group held the assumptions that this accelerator would use a 2 TeV injector, and would have a fill time of under 30 minutes. For this case it was felt, primarily from SSC experience, that ±5 mm were required for a "good field region," and ±10 mm of physical aperture was required to perform injection and beam abort procedures. It was felt that the field quality generated by present 50 mm magnets was satisfactory. Because the nonlinear field quality suffers in a minor way by going through the magnet off-axis, one could consider having the 20 mm beam pipe off-center through the (presumed) 50 mm magnet bore, if this simplified any engineering efforts of the vacuum/liner designs. It was later noted that if full advantage of synchrotron radiation damping enhancements can be realized in this collider -- by appropriate choice of lattice, or quadrupole offsets, for example -- then the field quality at injection could perhaps be relaxed. In this scenario, a smaller magnet bore, or lower injection field might be tolerable.

Bibliography

[1] A. A. Garren and M. J. Syphers, "1.8 TeV Tevatron Upgrade Lattices," proc. 1989 Part. Accel. Conf., IEEE 1989.

[2] K. W. Robinson, "Radiation Effects in Circular Electron Accelerators," Phys. Rev. **111**, No. 2 (1958).

[3] F. Meot and T. Tortschanoff, "Combined Function Focusing, Combined Function Superconducting Dipole for the LHC," CERN **SL/94-20(AP)**, CERN, 1994.

Fermi National Accelerator Laboratory

LEBT for High-Luminosity Colliders

S.K. Guharay and M. Reiser

Institute for Plasma Research, University of Maryland
College Park, Maryland 20742

Operated by Universities Research Association Inc. under Contract No. DE-AC02-76CHO3000 with the United States Department of Energy

LEBT for High-Luminosity Colliders

S. K. Guharay and M. Reiser
Institute for Plasma Research
University of Maryland
College Park, MD. 20742

I. Introduction

The design considerations of a high-luminosity collider usually impose a tight emittance budget through the accelerator chain.[1] The decomposition of the budget through various elements of the accelerator chain reveals that a major problem remains at the low-energy section involving ion source, low-energy beam transport (LEBT) and radio-frequency quadrupole accelerator (RFQ); here an RFQ accelerator is considered as the first acceleration column after extraction of an ion beam. A good deal of work has been done in the past on these individual components, and significant progress in their state-of-the-art has been achieved. However, an efficient handshake among the three units has not been demonstrated experimentally, and this issue warrants a critical investigation. The matching problem in an ion source-LEBT-RFQ section can be translated to two basic questions: (1) What is available from an ion source? This generates the input conditions for the LEBT. (2) What is required at the RFQ input? This defines the output parameters of the LEBT. In the premises of the current accelerators H^- ion beams are commonly chosen as the initial beam from an ion source.[1-4] The beam from an ion source is normally very diverging (envelope divergence ~ 50 mrad at the extractor), and the RFQ acceptance requires a highly converging beam (beam radius of about 1.5 mm and the beam convergence at the maximum envelope radius ~ -70 mrad). Furthermore, a differential pumping is required between the ion source and the RFQ so that the RFQ can be isolated from the ion source. This demands that certain buffer space be included between the ion source and the RFQ. These constraints need to be considered in the design of a LEBT. The problems of intense, high-brightness beam transport were discussed in other articles.[5]

A LEBT system can be developed using (a) a magnetic lens with gas neutralization, (b) electrostatic lenses, and (c) RFQ lens. While the scheme (c) has remained primarily at the conceptual level, there has been considerable amount of work on the other two schemes. A lot of working experience exists with the scheme (a) in the context of experiments at Brookhaven[6] and Los Alamos[7]. The scheme (b) has been used very successfully in heavy-ion fusion research at LBL[8]; long transport channels using electrostatic quadrupole lenses (ESQ) were developed for transport and focusing. Preliminary experiments using einzel lenses[9] and helical ESQ lenses[10] were conducted at the SSC Laboratory. Mori presented some interesting experimental results with helical ESQ lenses in the context of transporting heavy ions[11]. At Maryland, we have examined the design problems of LEBT taking into account the practical considerations specifically relevant to a high-brightness accelerator. It has been found that a LEBT system consisting of ESQ lenses and an einzel lens offers a very attractive solution. This composite electrostatic LEBT scheme has a strong potential to satisfy many desired features for developing a low-emittance injector in the context of advanced accelerators.

Some of the notable features are:

(1) An adequate buffer space between an ion source and an RFQ can be provided for differential pumping.

(2) An optimized combination of first-order (ESQ lenses) and second-order (einzel lens) focusing elements can satisfy extreme matching requirements without allowing any significant emittance dilution[12].

(3) The tuning can be done by adjusting low-voltage power supplies of ESQ lenses.

(4) Some variation of input conditions can be accommodated.

(5) Reliable simulation of the beam dynamics can be done, and this will provide a good guideline to recognize the sensitivity of various experimental control knobs.

(6) Beam steering can be done by coupling a dipole field to an ESQ lens.

A combination of ESQ lenses with a "ring" lens was used very effectively in LBL[13]; however, the experiment was conducted in the context of rather low-perveance beam.

In this article, we wish to present the key points of our understanding on developing an efficient LEBT for low-emittance injectors. Some specific examples have been considered here to shade some light on the particular problem.

II. LEBT for a Low-Emittance Injector

The design studies of a LEBT system have been conducted here using the parameters of H^- beams corresponding to different types of high-brightness ion sources, namely, (a) Penning-Dudnikov type source at Los Alamos[14], (b) volume ionization sources at Brookhaven[15] and SSCL[12], and (c) magnetron-type ion source at SSCL[15].

Figure 1 shows schematics of the LEBT components developed at Maryland. A combination of six ESQ lenses and a short einzel lens section has been cascaded to cover a length of about 30 cm; the whole system has been designed compact enough to minimize the drift space between the lenses. The lens parameters were determined following a hierarchy of numerical schemes developed by and large at Maryland. The phase-space distribution of particles and the evolution of emittance through the ESQ lenses were determined by using a modified version of the Los Alamos particle simulation code, PARMILA; the modifications were done at Maryland to include nonlinear effects due to fringe-fields of lenses.[16] The parameters of the einzel lens section were determined by beam dynamics studies using the SNOW code. Details of the simulation method have been discussed in our earlier papers on this topic as referenced above.

Continuing the discussions along the line of designing ESQ lenses we refer to our previous studies on the transport of a 30 mA, 35 kV H^- beam from the SSCL volume source[12]. Figure 2(a) shows the estimated rms normalized emittance $\tilde{\epsilon}_n$ as the beam

propagates through the six ESQ lenses in the LEBT. The maximum beam excursions in the two orthogonal directions (X and Y) are shown in Fig. 2(b). Here each set of two data points corresponds to the values of the parameters in the two orthogonal directions. The data at z = 0 correspond to the input values; afterwards, each dataset represents the values at the end of the subsequent lenses. Note that the emittance grows as the beam excursion through the lenses increases. This suggests that the external focusing force on the beam should be applied adiabatically to avoid any sudden increase of amplitude and thereby to control the emittance growth. In the above example, the emittance growth in the ESQ LEBT was estimated to be a factor of about 1.5; the einzel lens section didn't contribute to the emittance growth. This result satisfied the emittance budget allowed in the SSCL ion source-LEBT-RFQ section.

In a recent study on transporting a 30 mA, 35 kV H^- beam from a magnetron source we examined the criticality of various elements; the ESQ LEBT parameters are same as in the previous example. Figure 3 shows envelope solutions of the beam for two different lengths of the drift space between the LEBT and the extractor of the ion source: (a) LEBT at a distance of 5 cm from the extractor, and (b) LEBT at a distance of 2.5 cm from the extractor. The beam envelope could be maintained within about 80% of the lens aperture in the case (b), while the envelopes show larger excursion in the case (a) resulting a higher emittance growth. This example reveals that a close coupling between the LEBT and its interfacing components is desired to maintain a tight emittance budget. In this example, the einzel lens section has not been considered; however, if a long drift space is required between the LEBT and the RFQ (~ several cms) as in the case of the SSC injector, an einzel lens needs to be included for a satisfactory solution.

III. Conclusions

The above analysis gives us some guidelines to design an efficient ion source-LEBT-RFQ section. In view of the parameters of the proposed 30 x 30 TeV collider it has been noted that a strong R&D program on the low-emittance injector is warranted. In this area, the crux of the problem is found to be related to the following points:

(1) Optimization of ion source parameters to deliver a nearly parallel beam to the LEBT;
(2) Close coupling between an ion source and a LEBT and between a LEBT and an RFQ;
(3) Detailed experimental investigation on LEBTs using intense, high-brightness beams.

In this article, we have showed a scheme to develop an efficient LEBT using a combination of ESQ lenses with an einzel lens when a quite difficult matching requirement was imposed. In general, electrostatic LEBT schemes are expected to work well at the low-energy end, especially for a short-pulsed (< 50 μs) beam with a beam current of ~ 30 mA at a beam voltage of ~ 35 kV. Higher beam currents can also be efficiently transported using electrostatic lenses, particularly ESQ lenses, if the beam voltage is increased and the perveance remains close to typically the 30 mA, 35kV

case. We have been conducting experiments on a test stand at Maryland to develop an efficient ion source-LEBT system which can couple beams with an RFQ very efficiently.

Acknowledgments:

This work was supported by the Office of Naval Research and the SSC Laboratory.

References:

1. "Site-Specific Conceptual Design", SSCL report# SSCL-SR-1056, July 1990.
2. C. W. Schmidt and C. D. Curtis, BNL 50727, p.123; C. D. Curtis, C. W. Owen and C. W. Schmidt, Proc. LINAC Conf., SLAC, June 2-6, 1986, p.138.
3. J. G. Alessi, D. McCafferty, K. Prelec, Proc. LINAC conf., Aug. 24-28, 1992, p.335.
4. H. Haseroth, et al., Proc. LINAC conf., Aug. 24-28, 1992, p. 58.
5. M. Reiser, Nucl. Instrum. & Meth. in Phys. Res. B**56**, 1050 (1991); IEEE Trans. on Nuclear Science, vol. NS-32, No.5, 2201 (1985); Proc. LINAC Conf., Oct. 3-7, 1988, p. 451; M. Reiser, et al., Microwave and Particle Beam Sources and Propagation, SPIE vol. 873, 1988, p. 172.
6. J. G. Alessi, et al., Proc. LINAC Conf., Oct. 3-7, 1988, p. 196.
7. R. R. Stevens, AIP Conf. Proc. No. 287, 1994, p. 646.
8. T. J. Fessenden, AIP Conf. Proc. No. 253, 1992, p. 160.
9. K. Saadatmand, et al., Rev. Sci. Instrum. **65**, 1173 (1994).
10. D. Raparia, et al., Rev. Sci. Instrum. **65**, 1457 (1994).
11. Y. Mori, et al., Proc. LINAC conf., Aug. 24-28, 1992, p. 642.
12. S. K. Guharay, et al., Rev. Sci. Instrum. **65**, 1774 (1994).
13. O. A. Anderson, et al., Proc. 2nd European Particle Accelerator Conf., Nice, June 12-16, 1990, LBL-28962.
14. S. K. Guharay, C. K. Allen and M. Reiser, Nucl. Instrum. & Meth. in Phys. Res. A, **339**, 429 (1994); S. K. Guharay, et al., Intense Microwave and Particle Beams III, SPIE vol. 1629, 1992, p. 421.
15. S. K. Guharay, et al., AIP Conf. Proc. No. 287, 1994, p. 672.
16. C. R. Chang, E. Horowitz and M. Reiser, Microwave and Particle Beams, SPIE vol.1226, 1990, p.483.

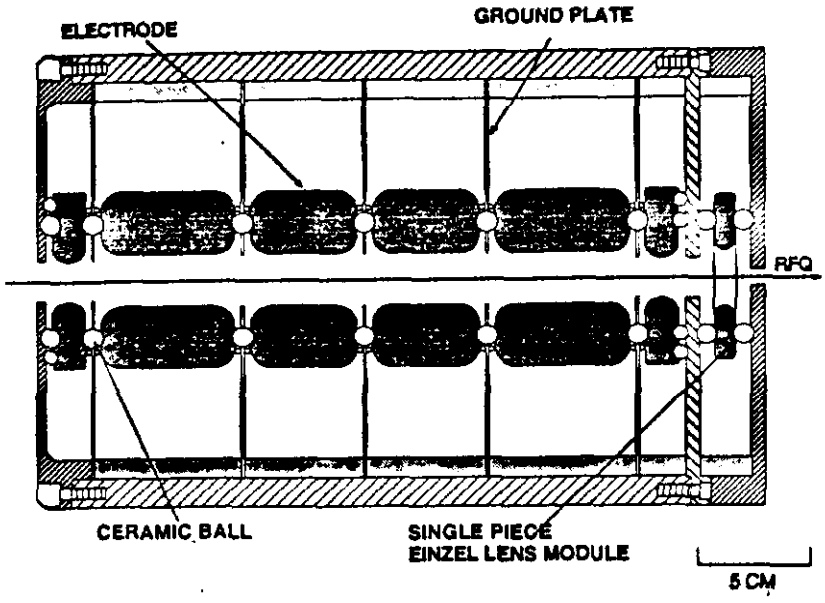

Fig. 1

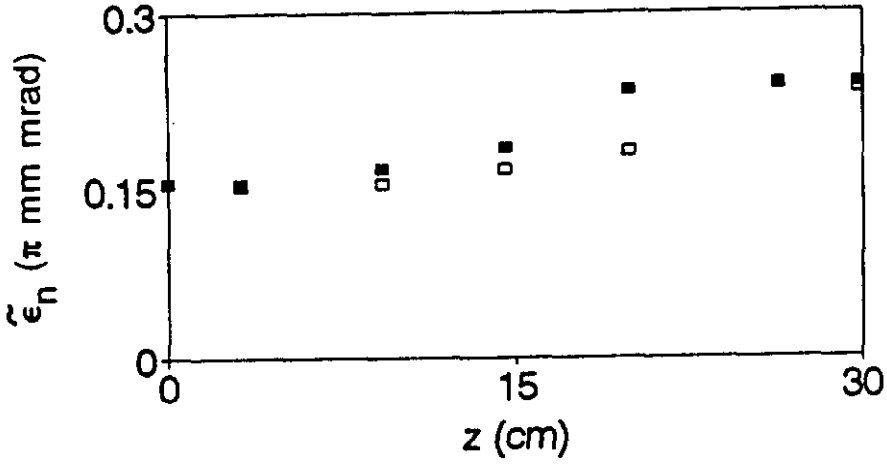

Fig. 2(a)

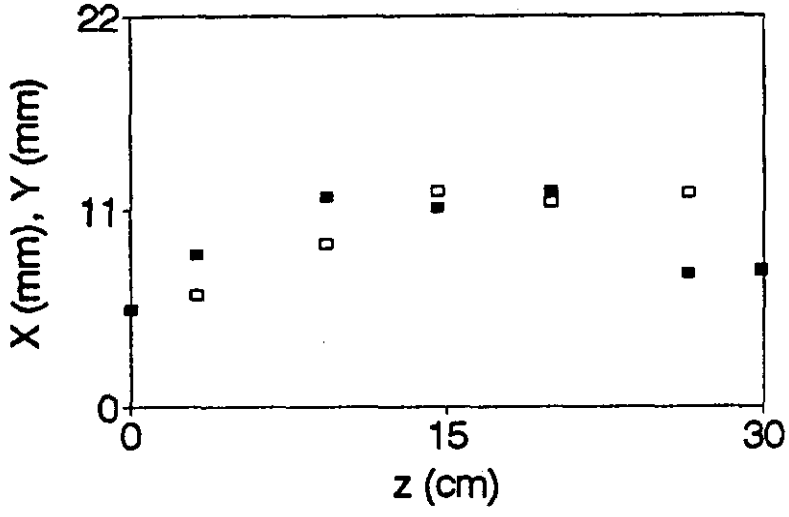

Fig. 2(b)

x-component y-component

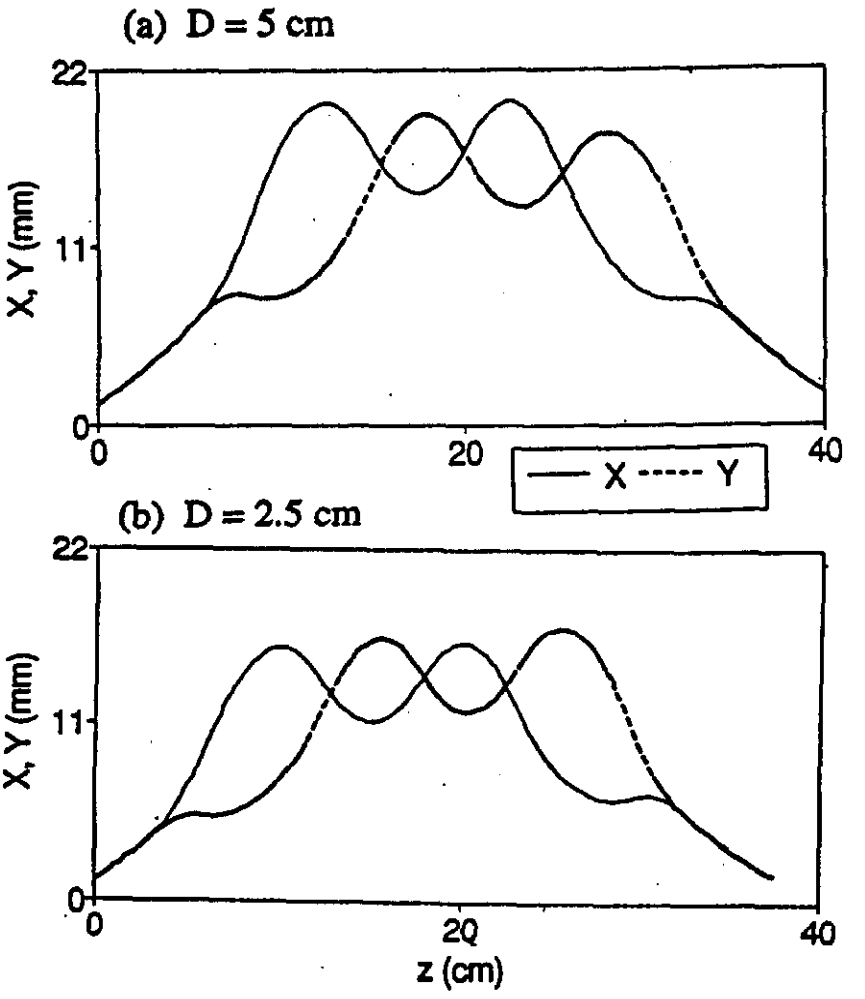

Fig. 3

Fermi National Accelerator Laboratory

Some Notes on Long-Range Beam-Beam Effects for the 2 TeV Collider

M. J. Syphers

Fermi National Accelerator Laboratory
P.O. Box 500, Batavia, Illinois 60510

Operated by Universities Research Association Inc. under Contract No. DE-AC02-76CHO3000 with the United States Department of Energy

Some Notes on Long-Range Beam-Beam Effects for the 2 TeV Collider

M. J. Syphers

The 2 TeV $\bar{p}$-p collider discussed at this workshop would necessarily have hundreds of long-range interactions between the counter-rotating bunches and some of the low-order effects of these interactions are estimated below. As we will see below, the helical orbit around the accelerator will help alleviate some of these effects, though the tune spread due to the long-range interactions will be present.

First, we consider the forces on an antiproton due to the passage of a single proton bunch. The force from the proton bunch varies as the distance from the center of the bunch as

$$F(r) \sim \frac{1 - e^{-r^2/2\sigma^2}}{r}$$

which, if we assume that the two bunches are sufficiently separated, varies approximately as $1/r$. The magnitude of the force is given by

$$F(r) = \frac{-\lambda e^2}{\pi \epsilon_0 r}$$

where e is the unit charge of the proton, and λ is the number of charges per unit length along the proton bunch.

Next, consider an antiproton whose equilibrium orbit is a distance d away from the proton bunch. For simplicity, we consider only the effect in one degree of freedom (horizontal, say). If x is the displacement from this equilibrium orbit then the force on the antiproton as a function of x is just

$$F(x) = \frac{-\lambda e^2}{\pi \epsilon_0 d(1 + x/d)}$$

which, under our assumptions, can be expanded to

$$F(x) = \frac{-\lambda e^2}{\pi \epsilon_0 d}\left(1 - \frac{x}{d} + \left(\frac{x}{d}\right)^2 - \left(\frac{x}{d}\right)^3 + \ldots\right).$$

For the above expression, we have assumed that the antiproton bunch is to the "radial outside" of the proton bunch. If it were on the "radial inside" of the proton bunch, the force would be

$$F(x) = \frac{\lambda e^2}{\pi \epsilon_0 d(1 - x/d)}$$

which, expanded, yields

$$F(x) = \frac{\lambda e^2}{\pi \epsilon_0 d}\left(1 + \frac{x}{d} + \left(\frac{x}{d}\right)^2 + \left(\frac{x}{d}\right)^3 + \ldots\right).$$

We see immediately that the long range force will generate steering errors on the antiproton trajectory, as well as a tune shift along the principal trajectory, a contribution to the chromaticity along the principal trajectory, plus there will be a tune shift with amplitude, which will generate a tune spread among the antiproton bunch. Below we make estimates of the magnitudes of these four effects.

1 Orbit Distortion

The change in the slope of the antiproton trajectory due the long-range force from the proton bunch will be

$$\Delta x' = \int \frac{F(s)ds}{pv} = \int \frac{-\lambda e^2}{\pi \epsilon_0 dpv} ds = \frac{-Ne^2}{2\pi \epsilon_0 d\gamma mc^2}$$

where N is the total number of protons in the bunch, and γ is the normal relativistic factor. This expression can be re-written in terms of the proton's classical radius, r_0, as

$$\Delta x' = \frac{-2Nr_0}{\gamma d}.$$

This single steering error will then produce a closed orbit distortion of the principal trajectory of magnitude:

$$\Delta \hat{x} = \frac{|\Delta x'|\sqrt{\beta_0 \hat{\beta}}}{2|\sin \pi\nu|} \approx \frac{Nr_0}{d}\frac{\sqrt{\beta_0\hat{\beta}}}{\gamma}.$$

Rewriting the displacement in units of beam sigma's,

$$\frac{\Delta \hat{x}}{\hat{\sigma}} \approx \frac{Nr_0}{(d/\sigma)}\frac{\pi}{\epsilon_N} = \frac{4\pi \Delta\nu_{HO}}{(d/\sigma)}$$

where $\Delta\nu_{HO}$ is the standard beam-beam head-on tune shift parameter:

$$\Delta\nu_{HO} \equiv \frac{Nr_0}{4\epsilon_N}$$

and ϵ_N is the rms normalized emittance,

$$\epsilon_N \equiv \frac{\pi\sigma^2(s)}{\beta(s)}\gamma.$$

2 Tune Shift

The tune shift due to the gradient term in the force equation can be estimated using the standard tune shift formula:

$$\Delta\nu = \frac{1}{4\pi}\beta q \rightarrow \frac{1}{4\pi}\int \frac{\beta F'(s)ds}{pv} = \frac{1}{4\pi pv}\int \frac{\lambda e^2}{\pi\epsilon_0 d^2}\beta ds$$

which reduces to

$$\Delta\nu = \frac{2\Delta\nu_{HO}}{(d/\sigma)^2}.$$

This is the change in tune of an antiproton along the ideal trajectory which is caused by the long-range passage of a proton bunch.

3 Chromaticity

The contribution to the ring chromaticity due to a sextupole field can be written as

$$\Delta\xi = \frac{1}{4\pi}\beta SD = \frac{1}{4\pi}\beta D\frac{B''\ell}{(b\rho)} \rightarrow \frac{1}{4\pi}\int \frac{\beta DF''(s)}{\gamma mc^2}ds$$

which, for our case, can be simplified to

$$\Delta\xi = \frac{-4\Delta\nu_{HO}(D/\sigma)}{(d/\sigma)^3}.$$

4 Tune Spread

The tune shift with amplitude due to a zero-th harmonic octupole field distribution can be written as

$$\Delta\nu(a) = \frac{1}{2\pi}\frac{3}{8}Ka^2$$

where

$$K \equiv \frac{\beta_0}{(B\rho)}\oint\left(\frac{\beta}{\beta_0}\right)^2\frac{B'''}{6}ds.$$

Here, β_0 is the amplitude function at the point corresponding to the amplitude a. For our case,

$$K = \frac{\beta_0}{pv}\oint\left(\frac{\beta}{\beta_0}\right)^2\frac{\lambda e^2}{\pi\epsilon_0 d^4} = \frac{\pi^2\gamma}{\beta_0}\frac{2r_0N}{\epsilon_N^2}\frac{1}{(d/\sigma)^4}.$$

Thus, the tune shift with amplitude becomes

$$\Delta\nu(a) = \frac{3}{8}\frac{\pi a^2\gamma}{\beta_0}\frac{Nr_0}{\epsilon_N^2}\frac{1}{(d/\sigma)^4}$$

which reduces to

$$\Delta\nu(a) = \frac{3}{2}\frac{\epsilon_a}{\epsilon_N}\frac{\Delta\nu_{HO}}{(d/\sigma)^4}.$$

Here, ϵ_a is the emittance of a particle with amplitude a.

We can write down the average tune shift of the distribution of particles by noting that $< a^2 >= 2 < x^2 >= 2\sigma^2$ and hence $< \epsilon_a >= 2\epsilon_N$. Thus,

$$\langle\Delta\nu\rangle = \frac{3\Delta\nu_{HO}}{(d/\sigma)^4}.$$

A tune "spread" for the distribution can be estimated by taking one's favorite maximum emittance particle. For example, the particles at $a = 2.45\sigma$ (the phase space radius which contains 95% of the particles) will have a tune shift of

$$\Delta\nu(a = \sqrt{6}\sigma) = \frac{9\Delta\nu_{HO}}{(d/\sigma)^4}.$$

This would correspond to the spread in tunes the particles would have beyond the tune "shift" along the central trajectory which was calculated earlier.

5 Remarks on Adding the Contributions

For the purpose of the Workshop, we are interested in looking at the order of magnitude of these effects to see if they warrant considerable further study. We estimate the above effects using a head-on beam-beam tune shift parameter of $\Delta\nu_{HO} = 0.01$ for a single head-on collision. We also assume that the counter-rotating bunches are separated along a helical orbit with the bunches separated by about 5σ. Then, just plugging in numbers to the above, we have

$$\begin{aligned}
(\Delta x_{co}/\sigma)_{max} &\approx \frac{4\pi(0.01)}{5} = 0.025 \\
\Delta\nu &= \frac{2(0.01)}{5^2} = 0.0008 \\
\Delta\xi &= \frac{-4(0.01)(4\mathrm{m}/0.4\mathrm{mm})}{5^3} = -3.2 \\
\Delta\nu_{max} &\approx \frac{9(0.01)}{5^4} = 0.00014
\end{aligned}$$

In the third line, we have assumed a typical dispersion of 4 m at a location where the beam-size is 0.4 mm just as a numerical example. We see the very strong chromatic effect of the long-range interaction.

We now have to realize that the beams are moving along helical orbits and so will encounter each other sometimes with the $\bar{p}$ bunch to the radial outside, sometimes to the inside, and of course the vertical and horizontal deflections will be shared at some

(most?) points. For the cases discussed at the workshop in which there are hundreds of long-range encounters we readily point out a few consequences. First of all, if there are n_B bunches of protons and antiprotons circulating the ring, and if n_B is large, then there will be approximately $2n_B$ long-range encounters. At the Workshop's end, the typical number being used was $n_B = 108$. Multiplying the above expressions by a number like 200 will yield

$$\begin{aligned}(\Delta x_{co})_{max} &\approx 2\text{mm} \\ \Delta\nu &= 0.16 \\ \Delta\xi &= -600 \\ \Delta\nu_{max} &\approx 0.03\end{aligned}$$

In fact, the first three entries are gross overestimates. The antiprotons will pass the proton bunches half to the inside and half to the outside, in which case the dipole deflections will roughly cancel. In addition, the deflections are divided up between the horizontal and vertical planes. The exact orbit distortions will depend upon the phase advance between and the amplitude functions at the crossing points $(\pi\nu/n_B)$ along the helical orbit.

In addition, the actual tune shifts will be smaller than those calculated above for much the same reason. When the beams pass each other horizontally, the horizontal tune shift is of one sign, while the vertical tune shift is of the opposite sign. The tune shifts are reversed for vertical passages. If roughly half of the passages are vertical and half horizontal, then the effects will tend to cancel.

Similarly, a horizontal crossing will generate a sextupole component which adds to the chromaticity of the accelerator. A vertical crossing, however, generates a skew sextupole component which does not contribute to the global chromaticity. Also, the signs of the chromaticity due to the horizontal crossings are opposite for radial outside and radial inside crossings. Hence, the contributions to the chromaticity of the ring will tend to cancel each other. Again, the exact residual tune shifts and chromaticities will depend upon the details of the helical orbit.

Finally, however, the tune spread of the antiproton beam will be approximately that computed above. The sign of the octupole term is independent of whether the bunch is to the radial inside or outside. Furthermore, the sign of the octupole due to vertical crossings is the same as the sign for horizontal crossings. Thus, the tune spread in each plane for 200 crossings will be on the order of $\Delta\nu_{max} = 0.03$ due to the long-range interactions.

A proper detailed analysis of these effects for particular helical orbits and bunch spacing scenarios should be performed. It is interesting to note that the tune shift due to the two head-on collisions is 0.02 – this is the shift for the zero-amplitude particles; the large amplitude particles see essentially no tune shift. On the other hand, the long range interactions yield a tune shift of 0.03 for the large amplitude particles; the zero-amplitude particles see essentially no tune shift due to the long range interactions in the helical orbit.

Fermi National Accelerator Laboratory

Synchrotron Radiation Masks for High Energy Proton Accelerators

R. Talman

Laboratory of Nuclear Studies, Cornell University
Ithaca, New York 14853

Operated by Universities Research Association Inc. under Contract No. DE-AC02-76CHO3000 with the United States Department of Energy

July, 1994

SYNCHROTRON RADIATION MASKS FOR HIGH ENERGY PROTON ACCELERATORS

Richard Talman

Laboratory of Nuclear Studies
Cornell University
Ithaca, NY 14853

ABSTRACT

An important design challenge for a superconducting high energy proton accelerator (such as the LHC or a conjectural 30×30 TeV machine) is preventing the synchrotron radiation energy from being dissipated at liquid helium temperature. Here a system of warm masks is proposed for capturing the radiation. Radiation is absorbed in thin "scrapers" placed at the end of every bending magnet, just outside the central orbit, rather than in a continuous cylindrical liner. The scrapers could be made retractable in order to preserve a large aperture during commissioning and operational procedures. A less elegant but possibly more economical scheme has one or more scrapers inside each magnet.

Submitted to *to Future Hadron Facilities Workshop, Bloomongton, Indiana, July, 1994*

In the original SSC design it was assumed that all synchrotron radiation energy would be dissipated at liquid helium temperature and this set the luminosity limit. Later a "liner" configuration, illustrated on the left of Fig. 1, was introduced to raise this limit.[1] All radiation was to be trapped in the warm, centered, liner. Since a similar design has been proposed for the LHC it can be called the "standard" configuration. Typical values for the main dimensions are coil-inner-radius $r_c = 25\,\mathrm{mm}$, liner-inner-radius $r_l = 15\,\mathrm{mm}$, and beam-stay-clear-radius $r_b = 10\,\mathrm{mm}$. The magnetic field is essentially uniform out to coil radius r_c, which is much greater than r_b, even allowing for closed orbit errors, injection errors, momentum dispersion and operational procedures that cause central orbit deviation, all of which contribute to r_b. There is no great incentive to reduce r_c however, since the magnet cost would not be much reduced by reducing the bore, say to 20 mm radius. (At least, based on SSC experience, cost as a function of r_c has a broad minimum at about 20 mm radius and the extra cost at 25 mm is modest.) In any case the extra space was required to make room for the liner.

The suggested alternate design is shown on the right of Fig. 1. The beam has been intentionally offset toward the center of the ring, and masks are placed on the outside to catch the radiation. Thus the "excess" good field region allotted to warm absorber is an offset vertical strip rather than the annulus of the standard design.

A top view of the proposed masking scheme is shown in Fig. 2. The distance between adjacent masks is L. Quadrupole magnets, being situated just past masks, can be centered on the design orbit. Radiation emitted in the region between two masks is absorbed in the next few masks. Installation, retractability and heat removal from the masks would be simplest if the masks are between magnets. For the present discussion that will be assumed, but a design with masks in the interior of dipoles is probably feasible and may lead to a cheaper overall design.

The geometry is further clarified in Fig. 3. It is assumed that all radiation is emitted exactly forward. (With the typical cone angle of the radiation being $1/\gamma$ the spot size at the mask is of order 1 mm—almost negligible.) Furthermore the source location of all radiation is taken to be on the central orbit. This will be approximately true after the beam is at full energy (and hence at its most slender), and after closed orbit deviations have been operationally reduced. This situation will hold during the long data taking intervals

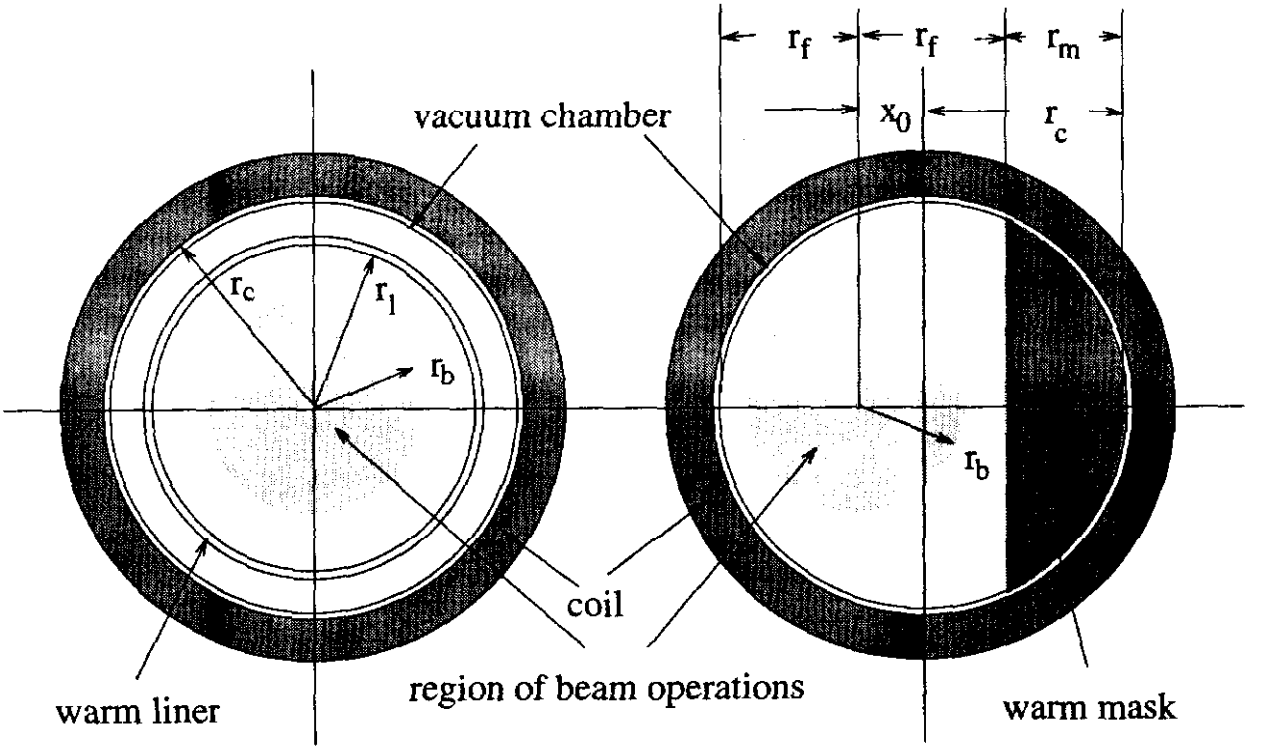

Figure 1: The figure on the left shows the "standard" configuration with radiation absorbed in a continuous, centered, warm, cylindrical liner. The figure on the right shows the proposed configuration with radiation being absorbed in judiciously located warm masks, and with the beam eccentrically displaced toward the inside of the ring.

and the energy radiated during the shorter time intervals when these assumptions are not true will be small by comparison. This operational time structure also favors making the masks retractable so that the beam offset x_0 can be small or zero and the masks inserted only as required.

The special rays illustrated have the property of grazing one mask and just barely clearing the wall as they strike the next mask. This condition determines how slim the masks can be (how little they encroach on the beam) while still catching all the radiation. The closer together the masks are, the slimmer they can be. The greatest possible mask separation is illustrated on the right—all radiation emitted between mask 1 and mask 2 is absorbed in mask 3. In terms of radius of curvature R, this results in mask width $r_m = 1.5L^2/R$, and "free radius" $r_f = 0.5L^2/R$ as shown. This may be too extravagant since it leaves only 40% of the good field volume for beam operations. For the case on the

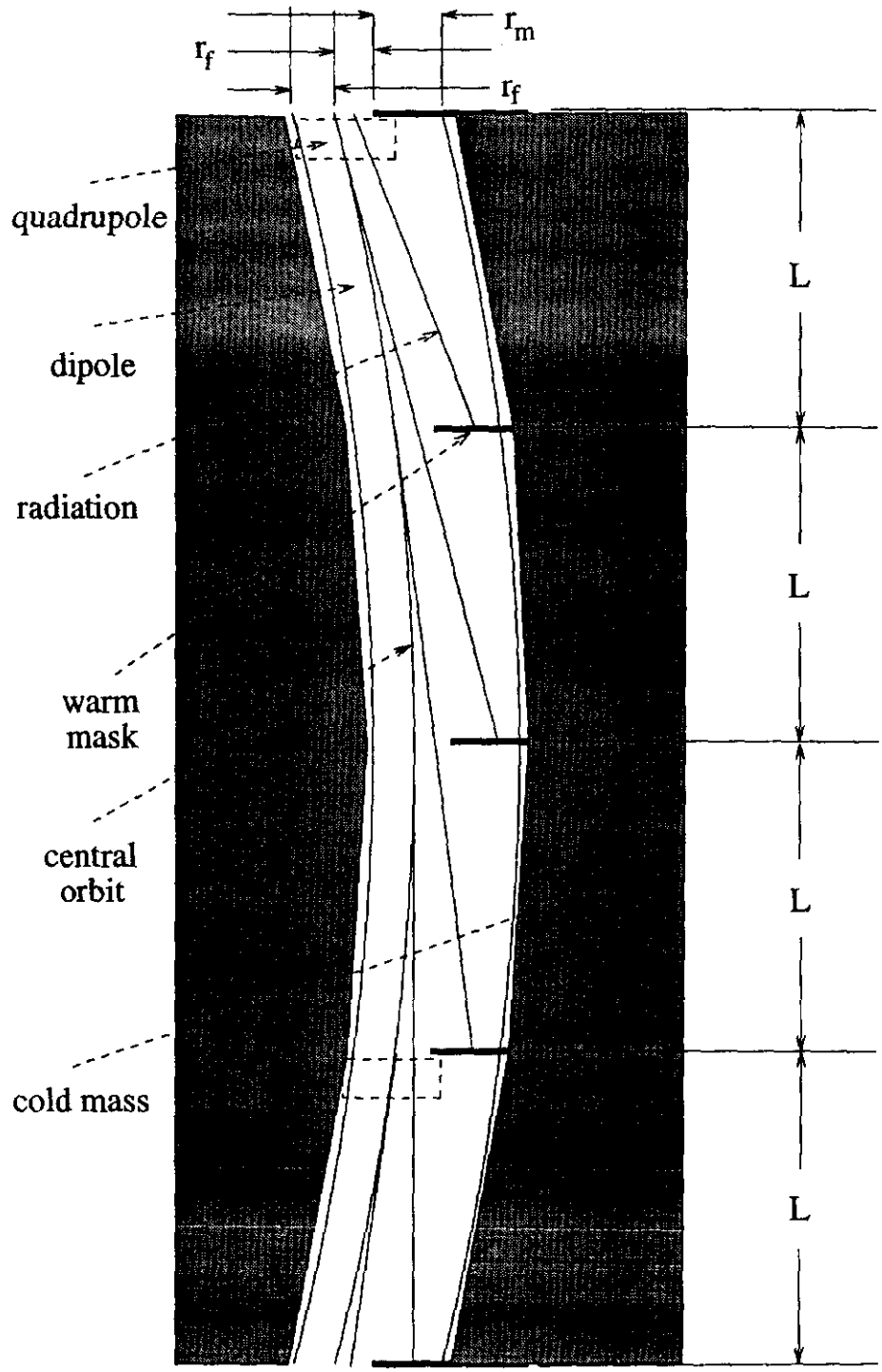

Figure 2: Top view of regular arc masking. In the simplest possibility masks are situated at every dipole end.

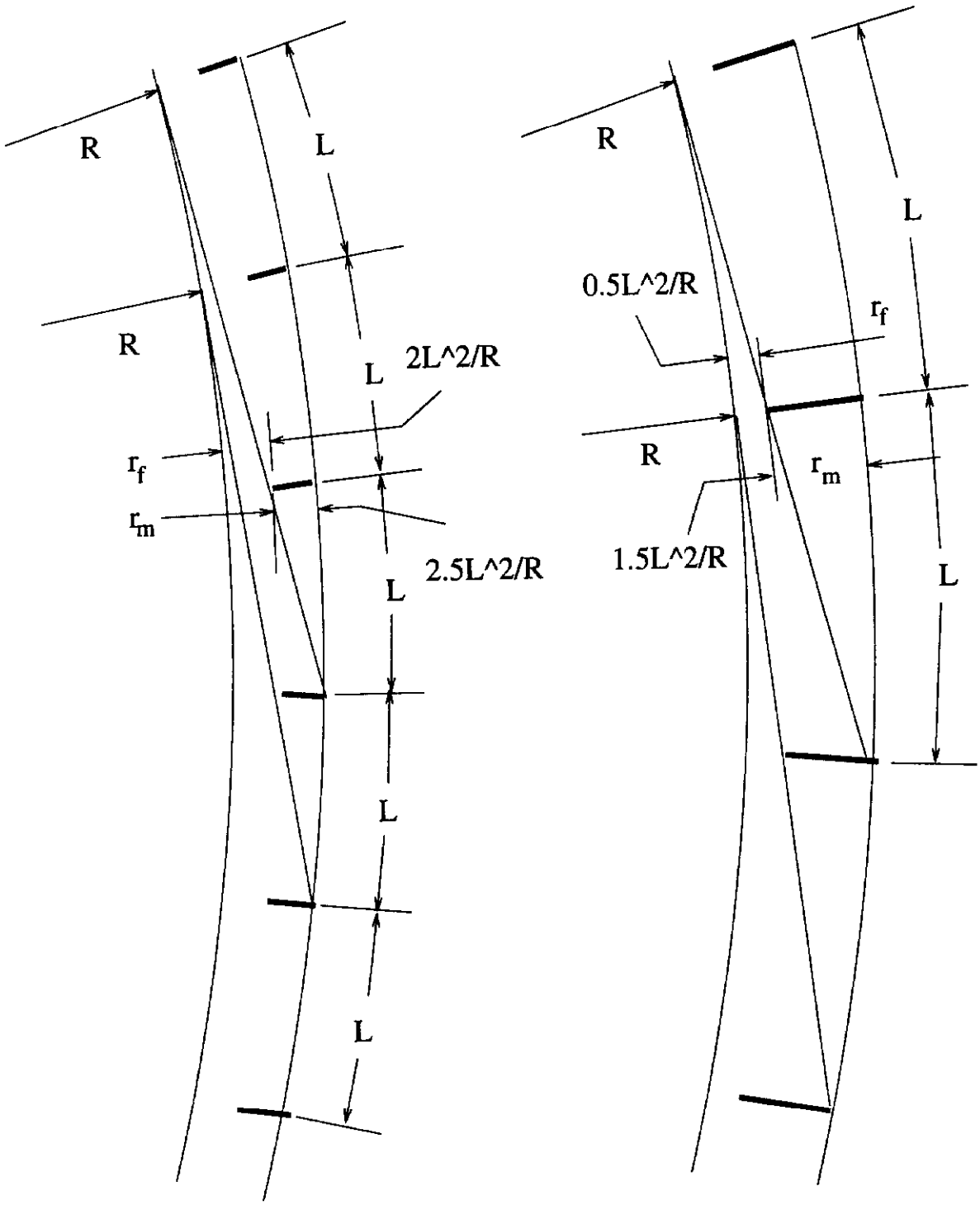

Figure 3: Two choices of mask geometry, both having the property that a ray grazing one mask just barely reaches the next mask as it is about to hit the cold magnet bore.

Table 1: Mask geometry for maximum mask separation and next-to-max separation, for coil radius, $r_c = 25\,\mathrm{mm}$.

accelerator	separation case	r_f/r_c	R km	L m	r_m mm	$2r_f$ mm	L-design m	x_0 mm
LHC	maximum	1/2.5	2.7	7.3	30.0	20.0	9	15.0
	next-to-max	4/6.5		4.6	19.2	30.8		9.4
SSC, 30x30	maximum	1/2.5	10	14.1	30.0	20.0	15	15.0
	next-to-max	4/6.5		8.8	19.2	30.8		9.4

left radiation emitted between mask 1 and mask 2 is absorbed in mask 4. This "next-to-max" solution leaves almost 2/3 of the volume free and will tentatively be put forward as the design of choice. The dimensions are determined by the following equations,

$$2r_f + r_m = 2r_c = 50\,\mathrm{mm}, \quad L\,(\mathrm{maximum}) = \sqrt{\frac{2r_cR}{2.5}}, \quad L\,(\mathrm{next\text{-}to\text{-}max}) = \sqrt{\frac{2r_cR}{6.5}}, \quad (1)$$

and numerical results for LHC [2] SSC, and 30×30 are given in Table 1.

Also listed in Table 1 are the current-design magnet lengths. It can be seen that the values of L required for radiation masking, are shorter than the current-design dipole magnet lengths, though not by much. For example, for the LHC with next-to-max mask separation, the magnet lengths would be halved compared to current design. This would certainly increase the cost. However the great design simplification and improved vacuum situation might make this good value. An alternative would be to suspend one or more masks in the interior of each dipole of current-design length. It would be possible to remove the heat either transversely or through longitudinal tubes (placed to not intercept any radiation)—neither approach is attractive, but both are simpler than a full liner.

It will certainly be argued, and cannot be denied, that the field quality in the eccentric geometry will be less good than in the standard azimuthally symmetric geometry. Several points can be made to show that this degradation may be acceptable. Superficially it might be thought that offset x_0 could not exceed, or even approach, the radius r_b, expected to exceed the "dynamic aperture" in the standard configuration. This is certainly wrong since,

to a first approximation, the dynamic aperture "moves with the central orbit". This has been observed at the Fermilab main ring and at the CERN SPS[3] as well as in numerical simulations [4] and is consistent with the following theoretical argument. Making the unnecessarily pessimistic assumption that the coil is not redesigned for off-center operation, the multipole expansion is

$$B_y + iB_x = B_0 \sum_{n=0}^{n_{max}} (b_n + ia_n)(x - x_0 + iy)^n , \tag{2}$$

differing from the expansion about the physical magnet center only by the term x_0. When units are chosen such that $r_c = 1$ the coefficients a_n and b_n are expected to be approximately constant, at least out to $n = 8$.[5] In these units, for the next-to-max mask separation case, the beam offset value is $x_0/r_c = 0.38$. This offset has a "feed-down" effect such as $b_n \rightarrow b_n - (n+1)x_0 b_{n+1}$. By this estimate the lowest nonlinear coefficient (which controls the "linear aperture") could be approximately doubled in the eccentric operation, and the effect on higher multipoles would be worse. Such a degradation would be close to or beyond the limit of acceptability. As a result special attention would have to be paid to reducing the unwanted multipoles, especially the multipoles b_3 and b_5, unallowed about the origin, but allowed about the displaced central orbit. Alternatively, L could be reduced further, but that would entail suspending masks in dipole interiors.

The physical requirements for a material from which to manufacture radiation masks do not appear to be unduly demanding. Table 2 shows some relevant parameters for a low Z insulator and a high Z conductor, either of which appear to lead to power reflection at the few percent level, and attenuation lengths short enough that mask thickness considerably less than one centimeter would be adequate [6–7]

Numerous uncertainties prevent arriving at a unique, definitive conclusion or mask design. It seems though that halving the magnet length, for example from 9 m to 4.6 m in the LHC case, would permit the use of masks far simpler than the liners presently contemplated. Making the masks retractable would greatly simplify commissioning.

Table 2: Properties of materials at critical energy u_c. Approximately half the radiated energy is below wavelength λ corresponding to u_c. The "extinction coefficient" k is the imaginary part of the index of refraction. Except for a numerical factor of order 2π, λ/k is the attenuation length in the material.

					graphite		gold	
	E	B	u_c	λ	reflectance	k	reflectance	k
	TeV	Tesla	eV	μm	%		%	
LHC	7	8.65	46	0.027	2.6	$\simeq 0.1$	4.3	0.4
SSC	20	6.67	287	0.0043	< 2.6	$\simeq (\frac{46}{287})^2 0.1$	< 4.3	$\simeq (\frac{46}{287})^2 0.4$
30x30	30	10	968	0.0013	< 2.6	$\simeq (\frac{46}{968})^2 0.1$	< 4.3	$\simeq (\frac{46}{968})^2 0.4$

1. References

1. SSC—A Retrospective Summary, 1989-1993. SSCL-SR-1235, April, 1994.
2. Design Study of the Large Hadron Collider (LHC), CERN/AC/DI/FA/90-06, October, 1990, updated at this workshop.
3. Observations described by Stiening and Wilson at the 1977 Erice School, and in subsequent private communications.
4. Operational simulation of collider injection procedures at the SSC by Ben Cole, using TEAPOT, 1993.
5. SSC Conceptual Design Report, Figure 2.4-2, SSC-SR-2020, 1986.
6. G. Hass and L. Hadley, Amer. Inst. of Phys. Handbook, 6-118, McGraw Hill, 1972.
7. Handbook of Optical Constants of Solids, II, E. Palik, editor, Academic Press, 1991, A. Borghesi and G. Guizzetti, p. 454, and D. Roessler and D. Huffman, p. 942.

Fermi National Accelerator Laboratory

Emittance Preservation in a Proton Synchrotron

Y. Huang

Superconducting Super Collider Laboratory
2550 Beckleymeade Avenue, Dallas, Texas 75237

Operated by Universities Research Association Inc. under Contract No. DE-AC02-76CHO3000 with the United States Department of Energy

EMITTANCE PRESERVATION IN A PROTON SYNCHROTRON

Y. Huang
SSCL, 2550 Beckleymeade Ave., Dallas, TX 75237

INTRODUCTION

To achieve high luminosity in a chain of high energy colliders, one can either increase the beam intensity or lower the transverse emittance. The SSC scenario is to use moderate current and small emittance(1 πmm.mrad) to achieve its goal of luminosity $10^{33}/\text{cm}^{-2}/\text{sec}$. This imposes a stringent emittance budget on its injectors(Linac, LEB, MEB and HEB). For MEB, it is 0.6πmm.mrad at injection with a growth allowance of 17%.

It is very challenging to preserve such a small emittance in a proton synchrotron since there are many different sources which might cause the emittance to grow, such as:

A) multipoles in magnetic field(from both systematic and random errors) and power supply ripple;

B) space-charge tune spread at injection and transition;

C) decoherence due to residual chromaticity and nonlinearity of fields when the beam is injected with transverse errors;

D) coherent instabilities, etc.

We have performed a systematic investigation of these effects on MEB emittance growth by both scaling law and computer modeling. Wherever it is possible, a quantitative analysis has been given. For each of the problems, some precations are suggested. Their improvements on the beam quality are also described.

MULTIPOLE EFFECT AND OPTIMIZATION OF LATTICE STRUCTURE

Various elements present in a real lattice structure cause the beam to cross different resonance lines which lead to a reduction of beam dynamic aperture or the growth of the beam emittance. In the study of the MEB, the simulation is filled with all of the errors according to the SSC specifications. First, the closed orbit is corrected to better than 0.6 mm rms using the correction dipoles. The analysis then addresses:

1) linear coupling resonances: $\nu_x - \nu_y = 0$ and $\nu_x + \nu_y = 51$;

2) third order and other second order resonances;

3) the fourth order difference resonance $2\nu_x - 2\nu_y = 0$.

The beam tracking by TEAPOT in the MEB lattice specified with 3B document and the following Fast Fourier Transform (FFT) clearly indicated the above sources.

Skew quadrupoles, misaligned quadrupoles and solenoids cause coupling between horizontal and vertical betatron motion. To overcome this problem, eight skew quads have been

placed in the MEB lattice. Based on the 4x4 linear matrix description of coupled betatron motion, the minimum split of the eigentune can be expressed through

$$|Q_a - Q_d|_{min} = \frac{\sqrt{det|C+B|}}{\pi(\sin\mu_a - \sin\mu_d)} \tag{1}$$

For MEB this value is about 6×10^{-4} after the correction.

Our study revealed that, when chromaticity correcting sextupoles were included at every quadrupole location, the main driving source for the third order resonances comes from those sextupoles (164 in MEB). Guignard's formula is used to estimate the strength of the driving term based on summation of all the sextupoles contribution. However, removing a few sextupoles at strategic locations has significantly reduced the strength of driving term for major third order resonances. As a result of this optimized arrangement, the beam dynamic aperture is increased from 50 $\pi mm.mrad$ to 80 $\pi mm.mrad$.

It is well known that an isolated difference resonance does not lead to an instability since the particle motion is bounded. However, an initially very small emittance in one direction may grow to a large value due to the coupling with the motion in another direction. Therefore, much attention should be paid to the correction of difference resonance, especially for the machine emphasizing small emittances. For the MEB, a tracking result analysis by FFT indicated that after the third order resonance correction, the fourth order coupling resonance, $2\nu_x - 2\nu_y = 0$, becomes the main obstacle to a further increase in the dynamic aperture. Although octupole correctors can be included to reduce the driving term for this resonance, the study shows that a simple and effective scheme is to use tune splitting mode: changing the operating point from (25.4, 25.4) to (26.4, 25.4). With this scheme, the strength of the difference resonance is greatly reduced. The simulation with the new operating point shows a significant increase in beam dynamic aperture, from $80\pi mm.mrad$ to $150\pi mm.mrad$.

Experience at the CERN SpS and other machines has shown that power supply ripple affects the long term dynamic aperture through modulation of the tune. Especially, a betatron frequency near resonance with ripple frequencies can lead to emittance growth through driven betatron oscillations. For the SSC collider, the betatron frequency is about 700 - 800Hz which is around the ripple frequency 720 Hz. A tracking study up to ten thousand turns shows an increase in vertical emittance of 222%. For MEB, the betatron frequency is 30000 Hz, far away from the ripple frequency. So the ripple is not a problem.

SPACE CHARGE TUNE SPREAD AND CHOICE OF OPERATING POINT

The repulsive electric force produced by the beam itself often can not be ignored, resulting in the betatron tune of the particles being depressed. The maximum tune shift from the bare tune is given by Laslett formula for the Gaussian distribution:

$$\Delta\nu = -\frac{r_p n_t B_f}{4\pi\beta^2\gamma^3\epsilon^{un}} \tag{2}$$

For the MEB with an injection momentum of 12 GeV/c, the maximum tune shift is -0.083. This shift may make a motion of the the beam cross low-order resonances. The initial operating point was originally set to (25.42, 25.38). Due to space charge effects the tunes of the particles spread out downward on the plane. The particles near the center of bunch are depressed the most, reaching tunes of (25.34, 25.30); very close to the horizontal third-order resonance, $3\nu_x = 76$. Some outer particles in the beam would fall in the vertical third-order region, $3\nu_y = 76$. The beam simulation code, SIMPSONS indicates that there is an increase in both horizontal and vertical emittances, and this increase in the vertical plane can reach approximately 10% when the MEB injection process is finished.

To solve the above problems, the operating point has been adjusted from (25.42, 25.38) to (25.43, 25.46). After the tune shift due to the space charge, the operating point is moved to (25.35, 25.38), still far away from the third integer resonances. A beam stimulation shows that no significant emittance grow is found.

When the beam crosses the transition energy, the bunches become much shorter. The bunching factor increases from 8.1 to about 65. However, the dispersion beam size, which is proportional to $D\frac{\delta p}{p}$, where D is dispersion function and $\frac{\delta p}{p}$ is rms relative momentum spread, becomes relatively big at the transition. Therefore, the tune shift is smaller than the injection value. Our simulation does not show any significant growth through the transition.

DECOHERENCE AND SUPPRESSION OF INJECTION ERROR

When a beam is injected on a path different from the closed orbit, it begins making betatron oscillations about the closed orbit. If the beam contains a spread of tunes, the motion will decohere as the individual betatron phases of the particles disperse. The phase space distribution of the beam spreads from a localized bunch to an annulus which occupies all betatron phases.

In the MEB, the injection errors come from the LEB extraction system (kicker and septum), the MEB injection kicker and other elements on the beam transmission line. The statistical errors at the injection point are 0.7 mm in horizontal plane and 1.1 mm in vertical plane. The emittance dilution factors, which are defined by

$$F \equiv \frac{\delta\epsilon}{\epsilon} = \frac{\pi}{2}\frac{\Delta x^2(\beta\gamma)_{Lorenz}}{\beta\epsilon} \tag{3}$$

will be 20% in horizontal plane and 85% in vertical plane. Here, Δx is the equivalent injection error given above, and ϵ is the normalized beam emittance.

A damper has been specified to suppress the coherent oscillation due to injection errors. The damping speed should be much faster than the dilution time which is expressed in number of turns by

$$\tau_D = \frac{1}{\Delta\nu} \tag{4}$$

where $\Delta\nu$ is the tune spread in the beam. In the MEB, there are two sources of the betatron tune spread: transverse nonlinearity where tune varies as a function of particle amplitude

and nonzero chromaticity where tune varies as a function of momentum spread through chromaticity, which is expressed by

$$\Delta\nu_c = \xi\frac{\Delta p}{p} \tag{5}$$

According to our simulation, the emittance dilution due to the first factor is very slow in MEB. The second action is periodic. The emittance decoheres each synchrotron oscillation, as expected. In a real machine, the chromaticity should not be corrected to zero exactly because of the concern of the coherent instability. Suppose residual chromaticity is -5.0, then the emittance will be diluted completely within 310 turns. So a damping period of 25 turns is good enough for limiting the emittance.

The MEB damper system consists of beam position monitor, electronic processing, time delay, filter and deflector. The input of the feedback system is the measurement of the transverse position of a longitudinal fraction of the beam. This position information is treated in a signal processing chain and ends up in the deflector. This beam deflector should transmit the information to the same fraction of the beam that was measured. To ensure that the information is transmitted to the correct beam portion it is further necessary that electronic phases or delays of the electric signal are well matched to the speed of the particle in the MEB. A set of basic properties have to be available to guarantee the function of the damper system.

COHERENT INSTABILITIES AND CURES

The interaction between the charged beam and the environment (wake field) might excite many different coherent oscillations in the beam. In some case it can lead to the transverse emittance growth and even a beam loss. By their original mechanism, the coherent instabilities in MEB may be classified into three categories: single bunch caused by the broad band impedance, couple bunch by the high-Q impedance of RF cavity and resistive wall by the non-purely conductive vacuum pipe. A code ZAP has been used to estimate the threshold value or growth time of these instabilities. Around transition, where the theoretical mode used in ZAP no longer works well, the six-dimensional tracking code SIMPSONS is used, as well as the two-dimensional code ESME.

Many efforts have been made in the design to reduce broad band impedance of the MEB. These include shielded bellows and screened pump ports, etc. As a result of these efforts, the broad band impedance is expected to be reduced to 1.65 MOhm/m. Our study indicates that there is big margin of the impedance budget in comparison with the threshold value of the single instability(36 MOhm/m at the injection).

However, the beam in the MEB does have a problem with the coupled bunch instability which is caused by the transverse high-mode impedance inside the RF cavities. The coherent oscillation modes can then be determined by these high mode impedances. Some of them might lead to beam instability. When it happens the amplitude of the coherent oscillation will increase with time exponentially and can be expressed by

$$y_n(t) = y_n e^{\frac{t}{\tau_\theta}} \tag{6}$$

where y_n is displacement and τ_g is defined as growth time. According to our calculation, the growth time is about 1 second. This obviously can not be tolerated, considering the beam will circulate in the ring for 5 second. High Order Mode dampers are proposed for the RF cavities. A significant improvement on growth time can be seen to be around 20 sec.

The resistive-wall instability is a common problem for large hadron accelerators and colliders. It grows very fast. It is caused by the large real part of the transverse coupling impedance of the nonpurely conductive ring. It may be triggered in many different modes. For the MEB, the lowest mode frequency is 41KHz. This is also the fastest growing mode with a growth time of 2.5ms. The highest mode is about 30MHz. To suppress this instability, a feed-back system has been planned. It will consists of beam position monitor, electronic processing, time delay, filter and kicker. To ensure suppression, the specifications of the system have been set as follows:

bandwidth: 30KHz-30MHz; deflection: 3.2μrad/turn, at P_{inj}=12GeV/c; damping period: 25 turns; acceptance: 2mm; peak power: 700W

Special attention has been paid to the transition region of the MEB where the dynamic process is nonadiabatic. As the phase slip factor,

$$\eta \equiv \frac{1}{\gamma_t^2} - \frac{1}{\gamma^2} \tag{7}$$

, approaches zero, less Landau damping is provided. Since the chromaticity is not zero in a real machine, a large shift in coherent mode frequencies, which is estimated through

$$\omega_\xi \equiv \frac{\xi}{\eta}\omega_0\nu_0 \tag{8}$$

, occurs, where ξ is chromaticity, ω_0 is the revolution frequency and ν_0 is the betatron tune. A strong coupling of m=0 mode to the resistive part of the broad band impedance can be expected, as indicated by Jacques Gareyte. One option to cure the head-tail instability during crossing the transition is to introduce some external nonlinearity, such as magnetic octupole. However, if the beam has small transverse dimension like in the MEB, the induced frequency spread by the octupole can be insufficient to cure the instability. In such case, the only cure to this head-tail instability is a chromaticity-jump. By reversing the sign of the chromaticity before and after transition correctly, one can guide the shift to the right direction so to avoid the coupling. This technique has been successfully implemented in both the main ring of Fermilab and the PS at CERN.

CONCLUSION

In a high energy proton synchrotron like the MEB, there are many different sources which might lead to a transverse emittance growth. However, with a good machine design and some necessary precautions it is possible to control this growth within tolerable level and achieve the design goal: a machine of high luminosity with a relatively low transverse emittance.

Fermi National Accelerator Laboratory

Beam-Beam Interaction Effects on Betatron Tunes

J.Y. Liu and L. Wang

Indiana University Cyclotron Facility
2401 Milo B. Sampson Lane, Bloomington, Indiana 47405

Operated by Universities Research Association Inc. under Contract No. DE-AC02-76CHO3000 with the United States Department of Energy

Beam-Beam Interaction Effects on Betatron Tunes

J.Y. Liu and L. Wang
IUCF, Indiana University, Bloomington, IN 47405

The beam-beam interaction significantly affects the betatron motion of particles in the collider. Betatron tune shifts are evaluated by considering effects from the head-on collision at the IR points and the long range interaction of $p\bar{p}$ beams in the 2×2 TeV collider. The stability limits are calculated analytically using the averaging method.

I. Head-on Collision

A particle receives a transverse kick at an interaction point [1],

$$\begin{aligned} \frac{\Delta x'}{x} &= \frac{\Delta y'}{y} = -\frac{2N_p r_p}{\gamma(x^2+y^2)}\left(1 - e^{-\frac{x^2+y^2}{2\sigma^2}}\right) \\ &= -\frac{N_p r_p}{\gamma\sigma^2}\left[1 - \frac{1}{4\sigma^2}(x^2+y^2) + \frac{1}{24\sigma^4}(x^2+y^2)^2 \cdots\right] , \end{aligned} \tag{1}$$

where N_p is the particle number per bunch, σ is the rms beam size of a round Gaussian beam, and $r_p = \frac{e^2}{4\pi\epsilon_0 m_p c^2} = 1.5347 \times 10^{-18}$ m.

For a small amplitude betatron oscillation, the tune shift due to the beam-beam interaction, namely head-on collision, is given by

$$\Delta\nu_x = \Delta\nu_{HO}\left[1 - \frac{1}{4}(3\alpha_x + 2\alpha_y) + \frac{1}{12}(5\alpha_x^2 + 6\alpha_x\alpha_y + 3\alpha_y^2)\cdots\right] , \tag{2}$$

where $\Delta\nu_{HO}$ is the linear tune shift per crossing, given by

$$\Delta\nu_{HO} = \frac{N_p r_p}{4\pi\epsilon_N} , \tag{3}$$

and $\epsilon_N = \gamma\sigma^2/\beta^*$ is the normalized beam emittance, and $\alpha_{x,y} = (A_{x,y}/2\sigma)^2$, here the betatron amplitude $A_{x,y}$ is defined by $x = A_x \cos\phi_x$, and $y = A_y \cos\phi_y$. One can also obtain $\Delta\nu_y$ which is the same as $\Delta\nu_x$ with x and y interchanged.

The tune spread is contributed by higher order terms, which gives $\delta\nu \leq |\Delta\nu_{HO}|$. At $A_x = A_y = \sqrt{2}\sigma$, a particle has a net tune shift $\Delta\nu_x = 0.6\Delta\nu_{HO}$.

[Numerical values] A 2×2 TeV $p\bar{p}$ collider [2]:
$N_p = 2.38 \times 10^{11}$/bunch, $N_{\bar{p}} = 9 \times 10^{10}$/bunch, and $\epsilon_N = 3$ (π mm-mr).

$$\begin{aligned} p: &\quad \Delta\nu_{HO} = 0.0073 \quad \text{(two crossings)} , \\ \bar{p}: &\quad \Delta\nu_{HO} = 0.0194 \quad \text{(two crossings)} . \end{aligned}$$

II. Long-Range Interaction

Transverse kicks caused by the long range force are given by [1]

$$\begin{aligned}\Delta x' &= -\frac{2N_p r_p}{\gamma}\frac{x+d}{(x+d)^2+y^2} \\ &= -\frac{2N_p r_p}{\gamma d}\left[1-\frac{x}{d}+\frac{x^2-y^2}{d^2}+\frac{3xy^2-x^3}{d^3}+\cdots\right] . \qquad (4)\\ \Delta y' &= -\frac{2N_p r_p}{\gamma}\frac{y}{(x+d)^2+y^2} \\ &= -\frac{2N_p r_p}{\gamma d}\left[\frac{y}{d}-\frac{2xy}{d^2}+\frac{3x^2y-y^3}{d^3}+\cdots\right] , \qquad (5)\end{aligned}$$

where d is the horizontal separation between $p\overline{p}$ beams.

For a small amplitude betatron oscillation, the tune shifts are given by

$$\Delta\nu_x = -\frac{\beta_x N_p r_p}{2\pi\gamma d^2}\left[1+\frac{3(A_x^2-2A_y^2)}{4d^2}+\cdots\right] , \qquad (6)$$

$$\Delta\nu_y = -\frac{\beta_y N_p r_p}{2\pi\gamma d^2}\left[-1+\frac{3(A_y^2-2A_x^2)}{4d^2}+\cdots\right] . \qquad (7)$$

The leading term results in the linear tune shift per ring,

$$\Delta\nu_{LR} = \frac{N_b N_p r_p}{\pi\epsilon_N g^2} = \Delta\nu_{HO}\frac{4N_b}{g^2} , \qquad (8)$$

where N_b is the bunch number per beam, an $d = g\sigma$ in average. The horizontal and vertical tunes have opposite signs, "−" for the horizontal tune and "+" for the vertical tune.

The tune spread is contributed by the amplitude dependent terms, mainly from the octupole term, given by

$$\delta\nu_x = -\frac{3N_b N_p r_p}{2\pi\epsilon_N g^4}(\alpha_x-2\alpha_y) = -\Delta\nu_{LR}\frac{3(\alpha_x-2\alpha_y)}{g^2} . \qquad (9)$$

The vertical tune spread $\delta\nu_y$ is the same as $\delta\nu_x$ with x and y interchanged.

[Numerical values] A 2×2 TeV $p\overline{p}$ collider [2]:

p: $\Delta\nu_{HO} = 0.0037$, $N_b = 108$, $g = 10$, $\alpha_x = \alpha_y = 1$,

$$\Delta\nu_{LR} = 0.0158 , \quad \delta\nu_x = \delta\nu_y = -0.0005 .$$

$\overline{p}$: $\Delta\nu_{HO} = 0.0097$, $N_b = 108$, $g = 10$, $\alpha_x = \alpha_y = 1$,

$$\Delta\nu_{LR} = 0.0419 , \quad \delta\nu_x = \delta\nu_y = -0.0013 .$$

III. Stability Limits of Beam Motions

For a collider with p sections of IR's, the stability limitation due to the head-on collision is given by [3]

$$\xi = \frac{\cos(2\pi/p) - \cos[\pi(2m+l)/p]}{4\pi \sin(2\pi/p)} , \tag{10}$$

where $\xi = \frac{N_p r_p}{4\pi \epsilon_N}$ is the linear tune shift factor, and m is the mode number, $m = 0, \pm 1, \pm 2, \cdots$, and $l = 0, 1$. The orbit distortion due to the beam-beam interaction has contributed a factor of $1/2$.

In the case of the 2×2 TeV collider, there are two IR's, i.e., $p = 2$. The stabilities should also take the long range interaction into account. Since there are N_b encounters within one section, one obtains $\xi^* = \xi \frac{2N_b}{g^2}$ from Eq. (9). The stability limits for different seperations between $p\bar{p}$ beams are shown in Fig. 1, where the first curve denotes the limit for $d = 10\sigma$ and the second one for $d = 20\sigma$, and the dashed line includes only the head-on collision. Below the curves, the beam motion is stable, otherwise unstable.

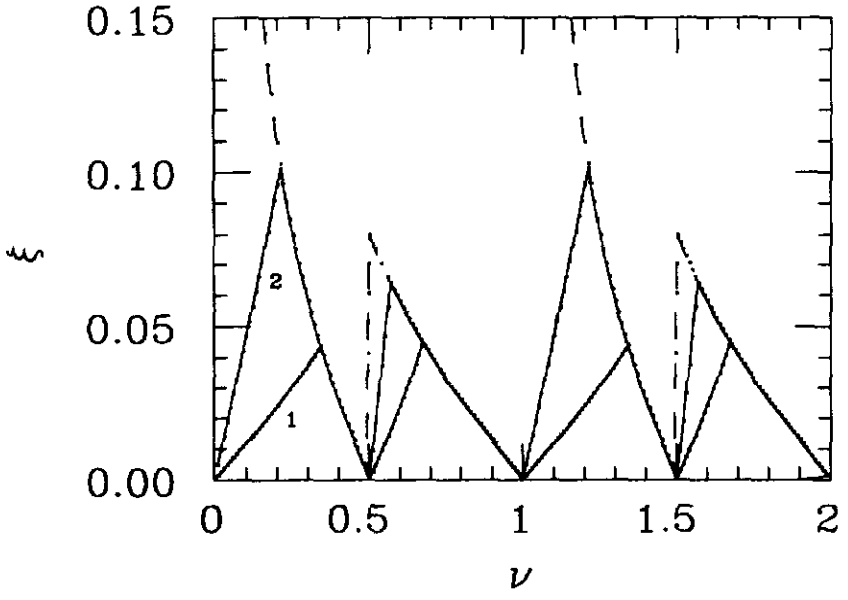

Figure 1: Stability limits for different beam separations: the $1st$ curve is for $d = 10\sigma$, the $2nd$ curve for $d = 20\sigma$, and the dashed line for the head-on collision only.

[References]

1. SSC Central Design Group, "Conceptual Design of the Superconducting Super Collider", 1986

2. Parameters are available from this workshop

3. A. Piwinski, Proc. VIII Int. Conf. High Energy Accel. CERN, p. 357 (1971)

Fermi National Accelerator Laboratory

Analytic Solutions for Phase Trombone Modules

D. Li, L. Wang and S.Y. Lee

Indiana University Cyclotron Facility
2401 Milo B. Sampson Lane, Bloomington, Indiana 47408

Operated by Universities Research Association Inc. under Contract No. DE-AC02-76CHO3000 with the United States Department of Energy

Analytic Solutions for Phase Trombone Modules

Derun Li, L. Wang and S.Y. Lee
Indiana University Cyclotron Facility
2401 Milo B. Sampson Lane, Bloomington, IN 47408

Abstract

Analytic solutions for phase trombones in arc and straight sections are attempted. Solutions for a linearized deviations of quadrupole strength in thin lens approximation are obtained and discussed. Examples for phase advance $\mu = 90^0$ and $\mu = 76^0$ of FODO cells are used to demonstrate the applicability of the method.

1 Introduction

In the lattice deign of a circular accelerator or a storage ring, the concept of using standard modules has been playing an important role in simplifying the machine design and reducing the machine cost. FODO cell, which has been widely employed by many accelerators, is a typical example. For storage rings with tunable betatron functions in insertion region (IR), a novel concept of using phase trombone was advanced during the SSC design to absorb necessary tune shifts in β function tuning. This is important to maintain the relative phase of the FODO cells in the arc, where many correction packages are sensitive to their relative betatron phases. This note discusses an analytic solution in thin lens approximation.

A possible phase trombone shown in Figure 1, was discussed in this workshop [1]. It consists of five FODO like cells in arc section with adjustable quadrupole strengths. (see also Figure 2 in Appendix B for a possible phase trombone in straight section). With this flexibility, it can be used to adjust the betatron phases (or tunes equivalently) leaving other outside lattice parameters intact by varying only quadrupole strengths in the phase trombone.

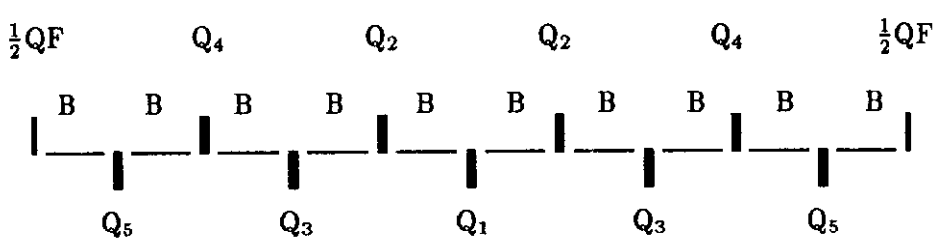

Figure 1 Layout of a phase trombone module in arc section

In order to see explicitly how each quadrupole strength depends on the required phase adjustments and how much the phases one can adjust, it is worth working out the analytic solutions for phase trombone modules. Of course, numerical solutions can be easily obtained

by running many lattice design codes. Nevertheless a simple handy analytic solution is helpful in conceptual lattice design.

2 Matrix Representation of Phase Trombone Modules

Mathematically, phase trombone in an arc section (see Appendix B for the discussions on phase trombone in straight section) can be expressed as [2],

$$\{\frac{1}{2}\mathrm{QF}, \mathrm{B}, \mathrm{Q5}, \mathrm{B}, \mathrm{Q4}, \mathrm{B}, \mathrm{Q3}, \mathrm{B}, \mathrm{Q2}, \mathrm{B}, \mathrm{Q1}, \mathrm{B}, \mathrm{Q2}, \mathrm{B}, \mathrm{Q3}, \mathrm{B}, \mathrm{Q4}, \mathrm{B}, \mathrm{Q5}, \mathrm{B}, \frac{1}{2}\mathrm{QF}\},$$

where $\frac{1}{2}$QF,B and Q_i are respectively the transfer matrix for a half focusing quadrupole, a bending magnet and quadrupole i, i = 1,2,3,4,5. In thin lens approximation, they are given by

$$\frac{1}{2}\mathrm{QF} = \begin{pmatrix} 1 & 0 & 0 \\ \frac{-1}{2f} & 1 & 0 \\ 0 & 0 & 1 \end{pmatrix}, \quad B = \begin{pmatrix} 1 & L & \frac{L\theta}{2} \\ 0 & 1 & \theta \\ 0 & 0 & 1 \end{pmatrix}, \quad \mathrm{Q}_i = \begin{pmatrix} 1 & 0 & 0 \\ \frac{1}{\pm f_i} & 1 & 0 \\ 0 & 0 & 1 \end{pmatrix}, \tag{1}$$

where L, θ and f are respectively the half length, bending angle and focal length of a regular FODO cell. f_i is the focal length of the quadrupole Q_i with $i = 1,2,3,4,5$. To match the betatron and dispersion functions at the ends of the module in both planes, the following constraints must be imposed at the center of the module,

$$\alpha_x = 0, \quad \alpha_y = 0 \quad \text{and} \quad D'(s) = 0, \tag{2}$$

where $\alpha_{x,y} = \frac{1}{2}\beta'_{x,y}(s)$ with $\beta(s)_{x,y}$ as the betatron amplitude function and $D(s)$ is the dispersion function in x plane. The above constraints can be satisfied equivalently by imposing the whole transfer matrix of the phase trombone, M to obey the following equation,

$$M = \begin{pmatrix} m_{11} & m_{12} & m_{13} \\ m_{21} & m_{22} & m_{23} \\ m_{31} & m_{32} & m_{33} \end{pmatrix}_{x,y} = \begin{pmatrix} \cos\phi_{x,y} & \beta_{\mathrm{F,D}}\sin\phi_{x,y} & D_{\mathrm{F,D}}(1-\cos\phi_{x,y}) \\ -\frac{1}{\beta_{\mathrm{F,D}}}\sin\phi_{x,y} & \cos\phi_{x,y} & \frac{D_{\mathrm{F,D}}}{\beta_{\mathrm{F,D}}}\sin\phi_{x,y} \\ 0 & 0 & 1 \end{pmatrix} \tag{3}$$

with the initial conditions as,

$$\begin{aligned} &\beta_x = \beta_{\mathrm{F}} = \frac{2L(1+\sin\frac{\mu}{2})}{\sin\mu}, \qquad \beta_y = \beta_{\mathrm{D}} = \frac{2L(1-\sin\frac{\mu}{2})}{\sin\mu}, \\ &D_x = D_{\mathrm{F}} = \frac{L\theta(1+\frac{1}{2}\sin\frac{\mu}{2})}{\sin^2\frac{\mu}{2}}, \quad D'_x = D'_y = D_y = 0, \\ &\alpha_x = 0 \quad \text{and} \quad \alpha_y = 0, \end{aligned} \tag{4}$$

where $\phi_{x,y} = 5\mu + \Delta\mu_{x,y}$ is the total phase advance of the module in (x, y) planes with μ as the phase advance of a regular FODO cell. To find the relations between f_i and $\phi_{x,y}$, one has to work out the elements m_{ij} of the transfer matrix, which is given by the following matrix multiplications,

$$M = \frac{1}{2}\mathrm{QF}\cdot\mathrm{B}\cdot\mathrm{Q5}\cdot\mathrm{B}\cdot\mathrm{Q4}\cdot\mathrm{B}\cdot\mathrm{Q3}\cdot\mathrm{B}\cdot\mathrm{Q2}\cdot\mathrm{B}\cdot\mathrm{Q1}\cdot\mathrm{B}\cdot\mathrm{Q2}\cdot\mathrm{B}\cdot\mathrm{Q3}\cdot\mathrm{B}\cdot\mathrm{Q4}\cdot\mathrm{B}\cdot\mathrm{Q5}\cdot\mathrm{B}\cdot\frac{1}{2}\mathrm{QF}.$$

Analytic expressions for the above transfer matrix elements m_{ij} have been acquired [3].

3 Equations For Phase Trombone Modules

Relating the transfer matrix elements m_{ij} to Eq. (3), a set of equations, which consist of five equations with five adjustable parameters, are established,

$$\begin{cases} m_{11x} - \cos\phi_x = 0 & m_{12x} + \beta_{\rm F}^2 m_{21x} = 0 \\ m_{11y} - \cos\phi_y = 0 & m_{12y} + \beta_{\rm D}^2 m_{21y} = 0 \\ m_{23x} + D_{\rm F} m_{21x} = 0. \end{cases} \tag{5}$$

If solutions for the above equations exist, one can always adjust the phases to desired values with matched betatron and dispersion functions at each end of the module. However, to find the general analytic solutions for Eq. (5) is difficult.

4 Linearized Approximation

With certain conditions, the matrix elements, therefore the equations for f_i, $i = 1,2,3,4,5$ can be greatly simplified. If we assume that each quadrupole strength can be adjusted in the proximity of a nominal FODO cell value f, the focal lengths for quadrupoles in phase trombone then can be written in the form of

$$f_i = f(1 + \frac{\Delta f_i}{f}), \quad i = 1,2,3,4,5, \tag{6}$$

with $\frac{\Delta f_i}{f} << 1$. In this case, a linear approximation, which means only the first order terms of $\Delta f_i/f$ are considered, should represent the system well. Substituting Eq. (6) back into Eq. (5), expanding and keeping the first order terms of $\Delta f_i/f$ only, five linear equations are obtained with the unknowns as $\Delta f_i/f$, $i = 1,2,3,4,5$. These equations can be solved analytically. Their solutions are listed in Appendix A.

For example, a solution for a betatron phase advance of a regular FODO cell $\mu = 90^0$ is given by

$$\begin{cases} \frac{\Delta f_1}{f} = -0.3997 \sin\Delta\mu_x - 0.1721 \sin\Delta\mu_y, \\ \frac{\Delta f_2}{f} = -0.1600 \sin\Delta\mu_x - 0.02746 \sin\Delta\mu_y, \\ \frac{\Delta f_3}{f} = -0.01831 \sin\Delta\mu_x - 0.1067 \sin\Delta\mu_y, \\ \frac{\Delta f_4}{f} = -0.05335 \sin\Delta\mu_x - 0.009153 \sin\Delta\mu_y, \\ \frac{\Delta f_5}{f} = 0.1815 \sin\Delta\mu_x - 0.02063 \sin\Delta\mu_y, \end{cases} \tag{7}$$

where $\phi_x = \frac{5}{2}\pi + \Delta\mu_x$ and $\phi_y = \frac{5}{2}\pi + \Delta\mu_y$ with $\Delta\mu_x$ and $\Delta\mu_y$ are the intended phase shifts.

Note that the linearized solution is independent of θ and cell length. The shifts in focal lengths depend linearly on $\cos\Delta\mu_x$ and $\cos\Delta\mu_y$. It turns out that Q1 requires the largest tunable strength for the betatron phase adjustments of the phase trombone in arc section. By confining $\Delta f_i/f$ within $\pm 10\%$, Eq. (7) give good estimates of how much phases one can adjust. To find the maximum ranges of the phase adjustments corresponding to the $\pm 10\%$ variations of $\Delta f_i/f$, rough calculations are made by considering the most sensitive quadrupoles only. It shows that the phase adjustment ranges are $\Delta\phi_x = |\Delta\mu_x^+ - \Delta\mu_x^-| \approx 30^0$,

$\Delta\phi_y = |\Delta\mu_y^+ - \Delta\mu_y^-| \approx 70^0$ for phase trombone in arc section at $\mu = 90^0$, where $\Delta\mu_{x,y}^+$ and $\Delta\mu_{x,y}^-$ are respectively x and y plane phase shifts corresponding to +10% and −10% variations of $(\Delta f_i/f)_{\max}$. Numerical calculations performed by varying $\Delta\mu_x$ with fixed $\Delta\mu_y$ or *vice versa* confirmed above estimates [3] .

5 Conclusion

Analytic solutions for phase trombone modules have been obtained in linear approximation. The adjustable ranges of the betatron phases within ±10% variations of $\Delta f_i/f$ estimated are,

$$\Delta\phi_x \approx 30^0, \quad \Delta\phi_y \approx 70^0 \qquad \text{for arc section with } \mu = 90^0$$

References

[1] Al. Garren and S.Y. Lee, *Discussion Notes on Phase Trombone module*, In the meeting of *Future Hadron Facilities Workshop*, Bloomington, Indiana (July 6 – 10, 1994)

[2] S.Y. Lee, *Lecture Notes on Accelerator Physics*

[3] L. Wang, *Matrix Elements for a phase trombone in an arc section*; D. Li, *Solutions for phase trombone in a straight section*, Internal Technical Notes of IUCF Accelerator Group.

Appendix A: Solutions For Phase Trombone in Arc Section

In linear approximation, the relative quadrupole strength changes $\Delta f_i/f$, $i = 1,2,3,4,5$ for phase trombone module at arc section have been solved analytically. They are given by,

$$\begin{aligned}
\frac{\Delta f_1}{f} &= \{-96f^{16} - 44f^{15}L + 1336f^{14}L^2 + 630f^{13}L^3 - 4148f^{12}L^4 - 2120f^{11}L^5 + 5684f^{10}L^6 \\
&\quad + 3020f^9L^7 - 4110f^8L^8 - 2120f^7L^9 + 1668f^6L^{10} + 772f^5L^{11} - 378f^4L^{12} - 140f^3L^{13} \\
&\quad + 44f^2L^{14} + 10fL^{15} - 2L^{16} + (96f^{16} + 34f^{15}L - 137f^{14}L^2 - 54f^{13}L^3 + 52f^{12}L^4 \\
&\quad + 10f^{11}L^5 - 5f^{10}L^6 + f^9L^7)\cos\phi_x + (10f^{15}L + f^{14}L^2 - 26f^{13}L^3 - 4f^{12}L^4 + 10f^{11}L^5 \\
&\quad + f^{10}L^6 - f^9L^7)\cos\phi_y]\} \times \{4(4f - L)L^5(-2f + L)(10f^9 + 5f^8L - 40f^7L^2 - 20f^6L^3 \\
&\quad + 42f^5L^4 + 21f^4L^5 - 16f^3L^6 - 8f^2L^7 + 2fL^8 + L^9)\}^{-1} \\
\frac{\Delta f_2}{f} &= \{(f^4 - 4f^2L^2 + L^4)[-4f^{10} + 50f^8L^2 - 100f^6L^4 + 70f^4L^6 - 20f^2L^8 + 2L^{10} + (2f^{10} \\
&\quad + f^9L)\cos\phi_x + (2f^{10} - f^9L)\cos\phi_y]\} \times \{8L^4(-20f^{10} + 85f^8L^2 - 104f^6L^4 + 53f^4L^6 \\
&\quad - 12f^2L^8 + L^{10})\}^{-1} \\
\frac{\Delta f_3}{f} &= \{f[-64f^{14} + 8f^{13}L + 864f^{12}L^2 - 124f^{11}L^3 - 2404f^{10}L^4 + 500f^9L^5 + 2770f^8L^6 \\
&\quad - 740f^7L^7 - 1540f^6L^8 + 460f^5L^9 + 422f^4L^{10} - 124f^3L^{11} - 52f^2L^{12} + 12fL^{13} + 2L^{14} \\
&\quad + (64f^{14} - 12f^{13}L - 62f^{12}L^2 + 20f^{11}L^3 + 4f^{10}L^4 + f^9L^5)\cos\phi_x + (4f^{13}L - 2f^{12}L^2 \\
&\quad + 4f^{11}L^3 - f^9L^5)\cos\phi_y]\} \times \{8(2f - L)(4f - L)L^5(5f^8 - 20f^6L^2 + 21f^4L^4 - 8f^2L^6 + L^8)\}^{-1}
\end{aligned}$$

$$
\begin{aligned}
\frac{\Delta f_4}{f} &= \{f^4[-4f^{10}+50f^8L^2-100f^6L^4+70f^4L^6-20f^2L^8+2L^{10}+(2f^{10}+f^9L)\cos\phi_x \\
&\quad +(2f^{10}-f^9L)cos\phi_y]\}\times\{8L^4(20f^{10}-85f^8L^2+104f^6L^4-53f^4L^6+12f^2L^8-L^{10})\}^{-1} \\
\frac{\Delta f_5}{f} &= \{f^5[32f^{11}+4f^{10}L-400f^9L^2-50f^8L^3+800f^7L^4+100f^6L^5-560f^5L^6-70f^4L^7 \\
&\quad +160f^3L^8+20f^2L^9-16fL^{10}-2L^{11}-(32f^{11}+6f^{10}L+f^9L^2)\cos\phi_x+(2f^{10}L \\
&\quad +f^9L^2)\cos\phi_y]\}\times\{8(4f-L)L^5(20f^{10}-85f^8L^2+104f^6L^4-53f^4L^6+12f^2L^8-L^{10})\}^{-1}
\end{aligned}
$$

Appendix B:
Solutions For Phase Trombone in a Straight Section

Figure 2 is the layout of a phase trombone in straight section, where QD denotes a defocusing quadrupole.

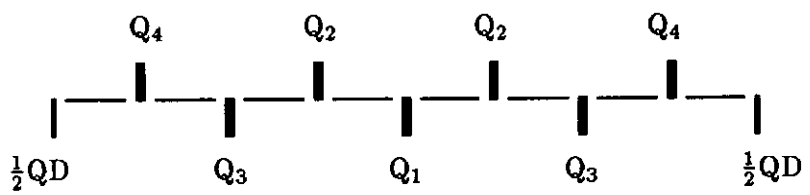

Figure 2 Layout of a phase trombone in straight section

Similar as for the phase trombone in arc section case, in thin lens and linear approximation, the changes of each quadrupole strength can be solved analytically from the following equations,

$$
\begin{cases}
m_{11x}-\cos\phi_x=0 & m_{12x}+\beta_{\rm F}^2 m_{21x}=0 \\
m_{11y}-\cos\phi_y=0 & m_{12y}+\beta_{\rm D}^2 m_{21y}=0\,.
\end{cases}
$$

Where m_{ij} are the transfer matrix elements, which are given by the following matrix multiplications,

$$
M_{\rm spt}=\frac{1}{2}{\rm QD}\cdot{\rm B}\cdot{\rm Q}_4\cdot{\rm B}\cdot{\rm Q}_3\cdot{\rm B}\cdot{\rm Q}_2\cdot{\rm B}\cdot{\rm Q}_1\cdot{\rm B}\cdot{\rm Q}_2\cdot{\rm B}\cdot{\rm Q}_3\cdot{\rm B}\cdot{\rm Q}_4\cdot{\rm B}\cdot\frac{1}{2}{\rm QD}
$$

Note here that B is the transfer matrix of a drift space, not a bending magnet, with its length equal to L, the half length of the regular FODO cell. Their solutions are given by,

$$
\begin{aligned}
\frac{\Delta f_1}{f} &= \{4f^8-32f^6L^2+40f^4L^4-16f^2L^6+2L^8-2f^8\cos(\phi_x)+f^7L\cos(\phi_x)-2f^8\cos(\phi_y) \\
&\quad -f^7L\cos(\phi_y)\}\{4L^4(8f^4-6f^2L^2+L^4)\}^{-1} \\
\frac{\Delta f_2}{f} &= \{(-f^4+4f^2L^2-L^4)(-4f^8+32f^6L^2-40f^4L^4+16f^2L^6-2L^8+2f^8\cos(\phi_x) \\
&\quad +f^7L\cos(\phi_x)+2f^8\cos(\phi_y)-f^7L\cos(\phi_y))\}\{8(2f-L)L^4(2f^2-L^2)(4f^5+2f^4L \\
&\quad -8f^3L^2-4f^2L^3+2fL^4+L^5)\}^{-1} \\
\frac{\Delta f_3}{f} &= \{-4f^{12}+32f^{10}L^2-40f^8L^4+16f^6L^6-2f^4L^8+2f^{12}\cos(\phi_x)-f^{11}L\cos(\phi_x) \\
&\quad +2f^{12}\cos(\phi_y)+f^{11}L\cos(\phi_y)\}\{4(2f-L)L^4(2f+L)(2f^2-L^2)(2f^4-4f^2L^2+L^4)\}^{-1} \\
\frac{\Delta f_4}{f} &= \{f^4(-4f^8+32f^6L^2-40f^4L^4+16f^2L^6-2L^8+2f^8\cos(\phi_x)+f^7L\cos(\phi_x)+2f^8\cos(\phi_y) \\
&\quad -f^7L\cos(\phi_y))\}\{8(2f-L)L^4(2f^2-L^2)(4f^5+2f^4L-8f^3L^2-4f^2L^3+2fL^4+L^5)\}^{-1}
\end{aligned}
$$

Solution for the drift space length not equal to L has also been obtained [3].

For example, when the $\mu = 76^0$, equally simple solution forms are obtained,

$$\begin{cases} \frac{\Delta f_1}{f} = -0.06956\,(\cos\phi_x - \cos 4\mu) - 0.2924\,(\cos\phi_y - \cos 4\mu), \\ \frac{\Delta f_2}{f} = -0.2290\,(\cos\phi_x - \cos 4\mu) - 0.05448\,(\cos\phi_y - \cos 4\mu), \\ \frac{\Delta f_3}{f} = -0.03939\,(\cos\phi_x - \cos 4\mu) - 0.1615\,(\cos\phi_y - \cos 4\mu), \\ \frac{\Delta f_4}{f} = -0.08280\,(\cos\phi_x - \cos 4\mu) - 0.01970\,(\cos\phi_y - \cos 4\mu). \end{cases}$$

The obtained phase adjustment range corresponding to $\pm 10\%$ variations of $\Delta f_i/f$ are,

$$\Delta\phi_x \approx 50^0, \quad \Delta\phi_y \approx 40^0.$$

Fermi National Accelerator Laboratory

Chromatic Correction of RHIC When One or Two Insertions is at $\beta^* = 0.5$ m

W. Scandale

CERN
Geneva, Switzerland

S. Tepikian

Brookhaven National Laboratory
Upton, Long Island, New York 11973

Operated by Universities Research Association Inc. under Contract No. DE-AC02-76CHO3000 with the United States Department of Energy

Chromatic Correction Of RHIC when One or Two Insertions is at $\beta^* = 0.5$ m*

W. Scandale and S. Tepikian
CERN BNL

The experimental insertion of RHIC can be tuned to $\beta^* = 0.5m$ with the appropriate gradients of the insertion quadrupoles as shown Fig. 1. Under these conditions, proton beams with nominal emittance of 24 $\pi mm\text{-}mrad$ can still be accommodated in the inner triplet of $\beta^* = 0.5m$. However, the off momentum orbit functions are quite sizably distorted while the detuning with the relative momentum becomes large. Figures 2 and 3 show the behavior of the tunes as a functions of the relative momentum with one or two experimental insertions set to $\beta^* = 0.5m$.

A way to reduce the off momentum perturbation of the orbit functions is to introduce six families of chromatic sextupoles according to the following scheme[1]:

Outer Arc	SF	SD + ε_1 SD - ε_1
Inner Arc	SF - ε_2 SF + ε_2	SD

where in the outer arc a perturbation is added to the defocussing sextupoles and on the inner arc a perturbation is introduced on the focussing sextupoles. This is well suited to reduce the maximum sextupole excitations. As a result of the chromatic detuning of RHIC becomes reasonably smooth as shown in Fig. 3 and 4 for one or two insertions with $\beta^* = 0.5m$.

To limit the sextupole excitation to below 100*Amps*, it is suggest to use only one $\beta^* = 0.5m$ insertion for proton -proton collisions. The use of it for ions will be limited due to the larger emittances growths caused by intrabeam scattering.

No attempt was made to correct the chromatic effects of the insertion with a local correction scheme to avoid large sextupole excitations. There are many studies that need to be done including tracking to better understand this correction scheme.

References

[1] Conceptual Design of the Relativistic Heavy Ion Collider, May 1989, BNL-52195

*Work performed under the auspices of the U.S. Department of Energy.

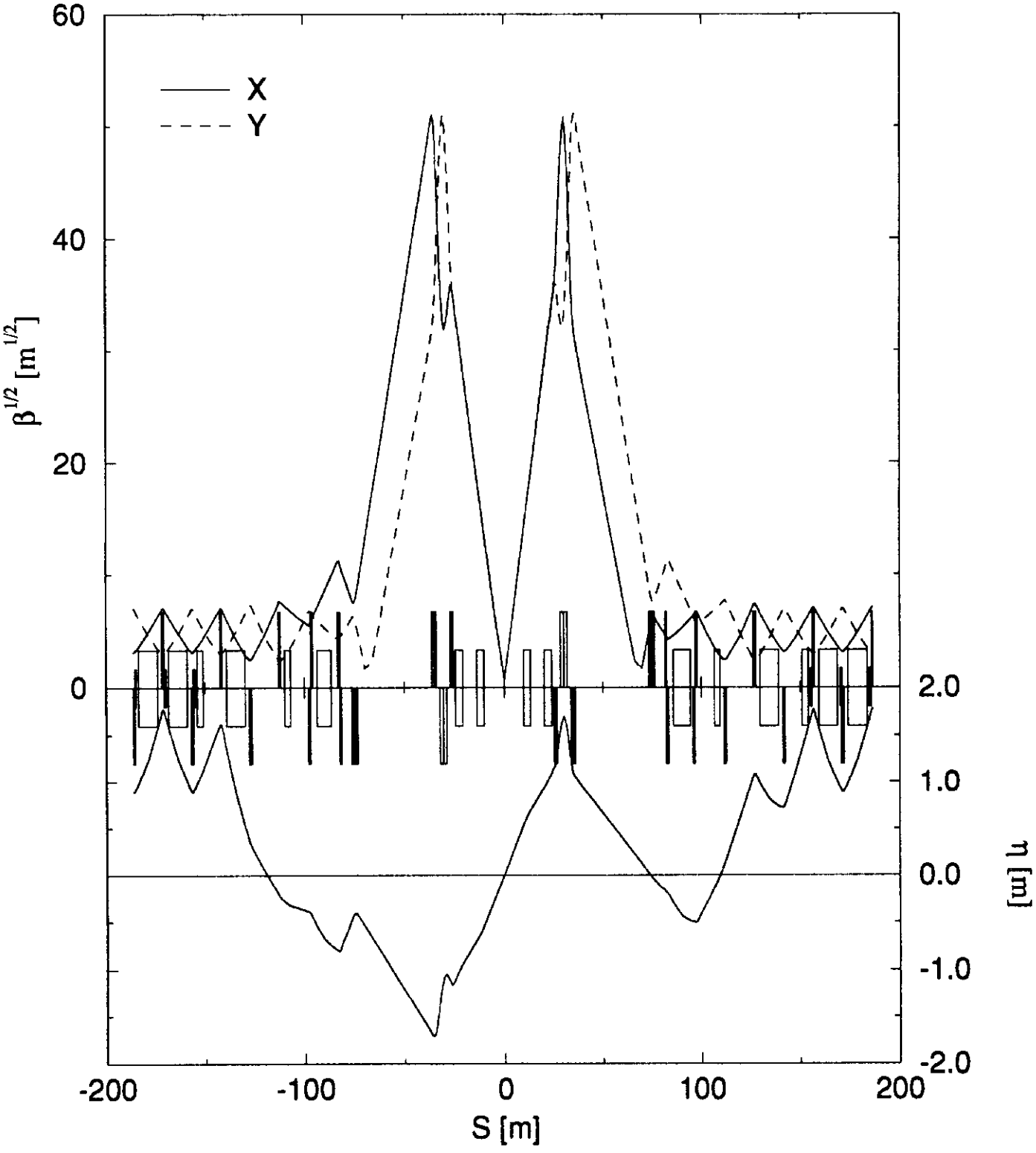

Figure 1. The beta and dispersion functions of a RHIC insertion at $\beta^* = 0.5$ m.

Two Families of Sextupoles.

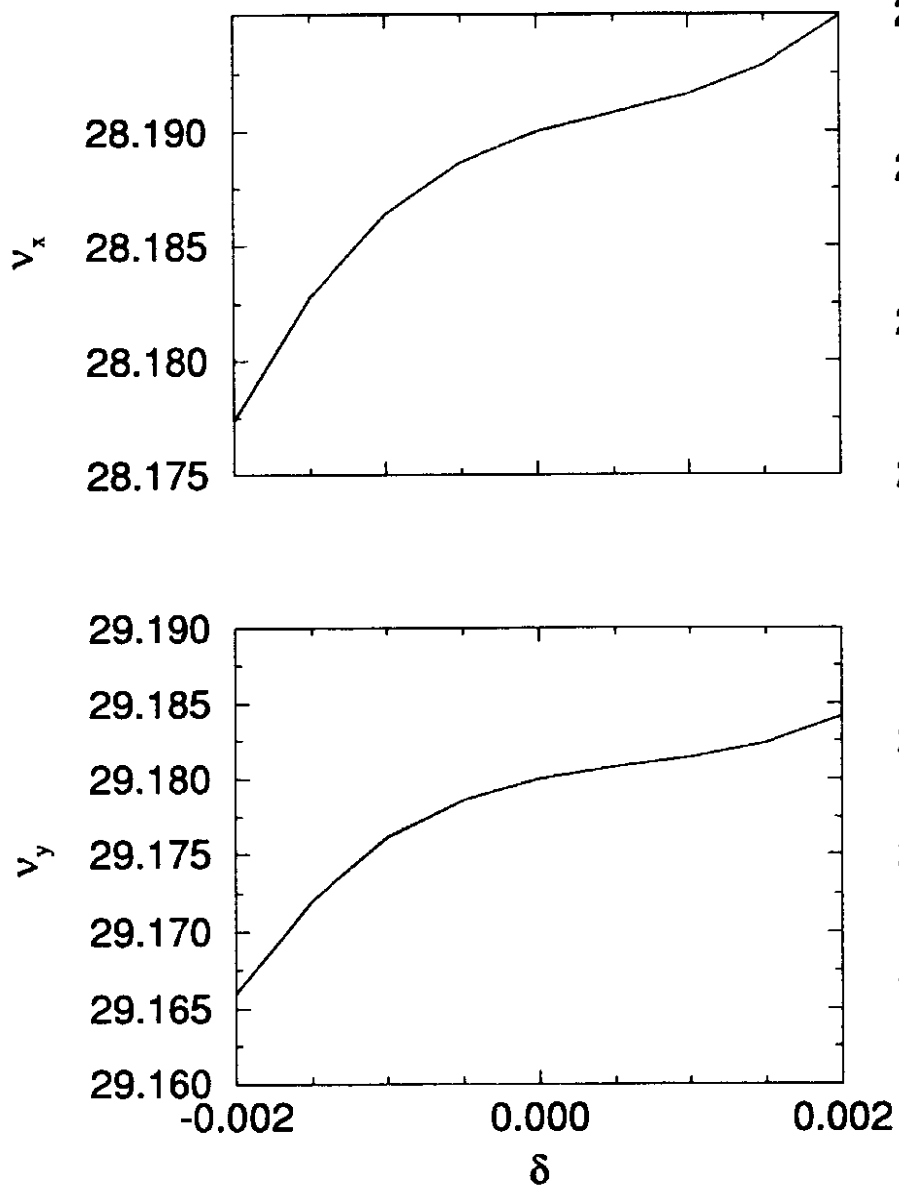

Figure 2 One insertion at $\beta^* = 0.5\text{m}$

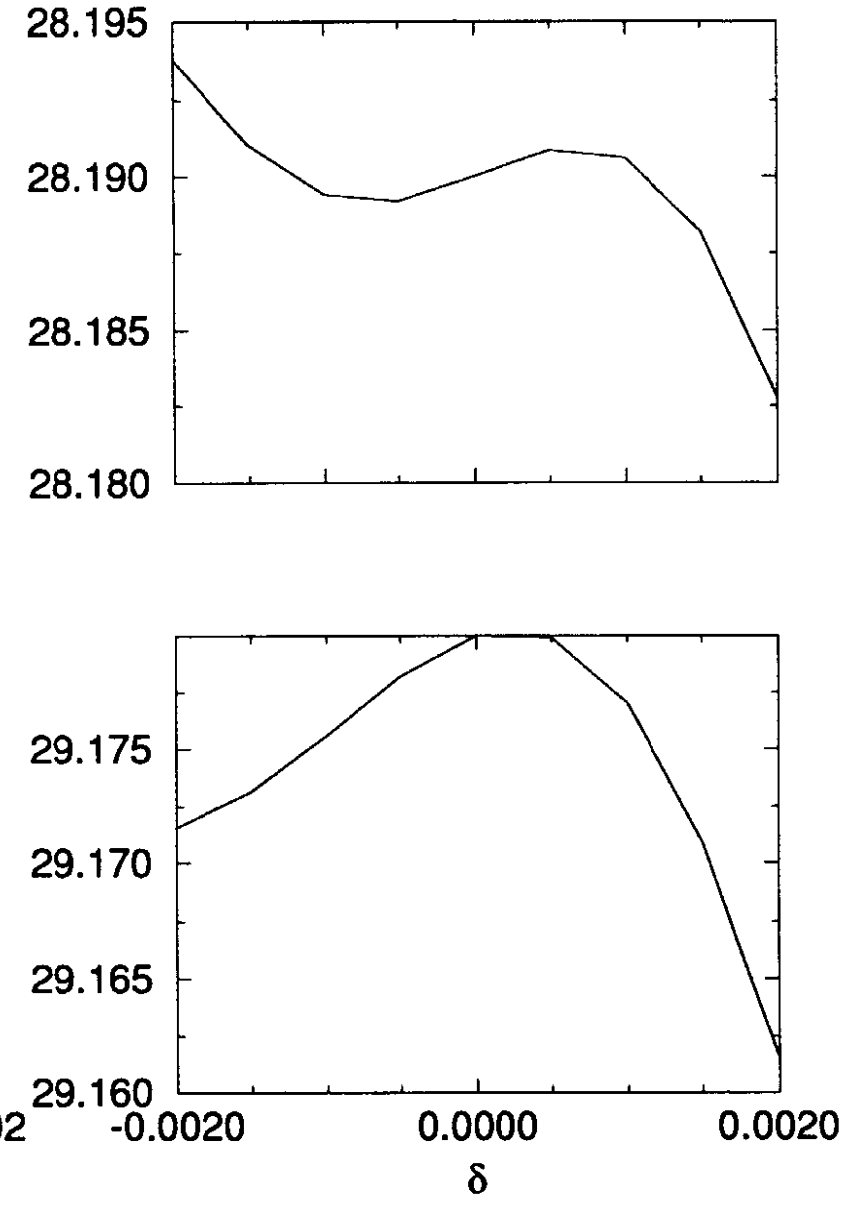

Figure 3 Two insertions at $\beta^* = 0.5\text{m}$

Six Families of Sextupoles

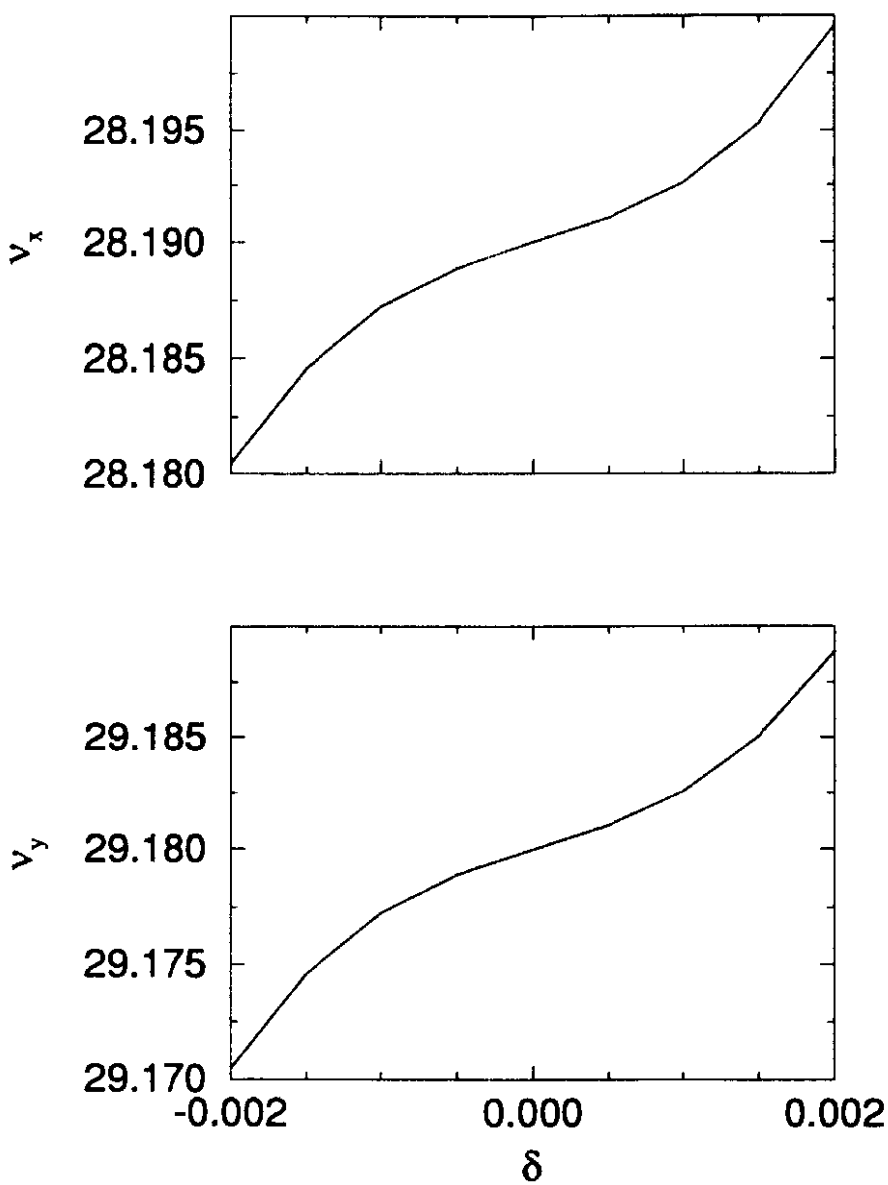

Figure 4 One insertion at $\beta^* = 0.5\text{m}$

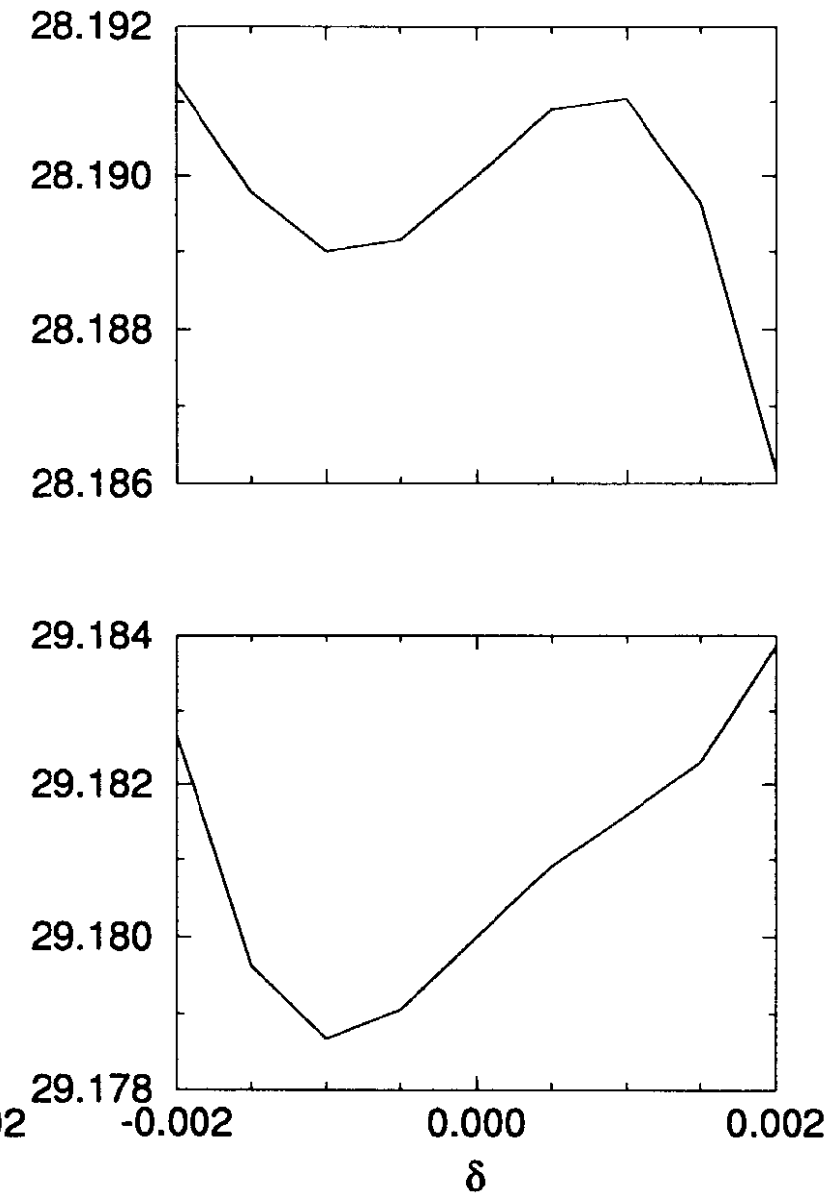

Figure 5 Two insertions at $\beta^* = 0.5\text{m}$

Workshop Registrants

Name	Affiliation
Dan Amidei	Univ. of Michigan
Vinod Bharadwaj	Fermilab
Frank Bieniosek	Fermilab
David Caussyn	Univ. of Michigan
Alex Chao	SLAC
Gerry Chapman	SSCLab
Mike Church	Fermilab
Mark Coles	SSCLab
Pat Colestock	Fermilab
Yaroslav Derbenev	Univ. of Michigan
Gerry Dugan	SSCLab
Bill Foster	Fermilab
Jim Griffin	
Samar Guharay	Univ. of Maryland
Mike Harrison	Brookhaven National Lab
Steve Holmes	Fermilab
Yunxiang Huang	SSCLab
Gerry Jackson	Fermilab
Roland Johnson	Department of Energy
John Johnstone	Fermilab
Moyses Kuchnir	Fermilab
S.Y. Lee	Indiana Univ.
Derun Li	Indiana Univ.
Jianyang Liu	Indiana Univ.
Derek Lowenstein	Brookhaven National Lab
Jim MacLachlan	Fermilab
John Marriner	Fermilab
Mike McAshan	
Peter McIntyre	Texas A&M Univ.
Rainer Meinke	SSCLab
Stanley Mendelsohn	Princeton Univ.
Sergei Nagartsev	Indiana Univ.
Steve Peggs	Brookhaven National Lab
Tom Peterson	Fermilab
Miolrad Popovic	Fermilab
Claus Rode	CEBAF
Walter Scandale	CERN
Bob Schermer	
Jicong Shi	Univ. of Houston
Robert Siemann	SLAC
Greg Snitchler	American Superconductor
Mike Syphers	Brookhaven National Lab
Richard Talman	Cornell Univ.
Steven Tepikian	Brookhaven National Lab
Jay Theilacker	Fermilab
John Tompkins	Fermilab
William Turner	Lawrence Berkeley Lab
Lian Wang	Indiana Univ.
Steve Werkema	Fermilab
K.C. Wu	Brookhaven National Lab
Richard York	Michigan State Univ.